2013

New Insights into the Spinal Recurrent Inhibitory Pathway Normally and After Motoneuron Regeneration

Ahmed Zayed Obeidat
Wright State University

NEW INSIGHTS INTO THE SPINAL RECURRENT INHIBITORY PATHWAY NORMALLY AND AFTER MOTONEURON REGENERATION

A dissertation submitted in partial fulfillment of the requirements for the degree of Doctor of Philosophy

By

AHMED ZAYED OBEIDAT

M.D., Jordan University of Science and Technology, 2008

2013
Wright State University

Wright State University

Graduate School

May 17, 2013

I HEREBY RECOMMEND THAT THE DISSERTATION PREPARED UNDER MY SUPERVISION BY Ahmed Zayed Obeidat ENTITLED New Insights into the Spinal Recurrent Inhibitory Pathway Normally and after Motoneuron Regeneration BE ACCEPTED IN PARTIAL FULFILLMENT OF THE REQUIREMENTS FOR THE DEGREE OF Doctor of Philosophy.

_____

Timothy Cope, Ph.D.
Dissertation Director

_____

Gerald Alter, Ph.D.
Director, Biomedical Sciences Ph.D. Program

_____

William Ayres, Ph.D.
Interim Dean, Graduate School

Committee on
Final Examination

_____
Timothy Cope, Ph.D.

_____
Francisco Alvarez Leefmans, M.D., Ph.D.

_____
Steven Berberich, Ph.D.

_____
Sherif Elbasiouny, Ph.D., PE, PEng.

_____
David Ladle, Ph.D.

_____
Mark Rich, M.D., Ph.D.

Abstract

Obeidat, Ahmed Zayed M.D., Ph.D. Biomedical Sciences Ph.D. program, Wright State University, 2013, New Insights into the spinal recurrent inhibitory pathway normally and after motoneuron regeneration

Despite more than seven decades of intensive research, uncertainty is the hallmark of spinal recurrent inhibition. The simplest possible structure that is formed between the α-motoneuron and its inhibitory interneurons has been the subject of long lasting scientific debate. To date, there is no consensus on the functional significance of this circuit. Even the simplest assumption of a negative feedback loop does not hold true.

The current work used the technique of *in vivo* intracellular recording from the adult rat α-motoneurons to study the normal function and the plasticity after nerve injury and regeneration of this simple, yet intricate spinal circuit.

The long lasting notion that inhibition must adversely affect neuronal firing rates has been challenged and the counterintuitive finding that recurrent inhibition can increase firing rate under certain circumstances is reported for the first time. In addition, recurrent inhibition was found to strongly affect action potential spike timing and was found to prolong the duration of repetitive firing of α-motoneurons. Furthermore, the circuit behavior at different frequencies has been examined and novel findings are reported.

The circuit adaptation to peripheral nerve injury and successful regeneration was studied. Results showed that peripheral nerve regeneration failed to restore the structure and

function of this central circuit. In conclusion, the current thesis calls for a reevaluation of the concept that recurrent inhibition must suppress α-motoneuron firing and suggests that inhibition in general plays more of a role in modulating firing behavior. Finally, another example of permanent central nervous system dysfunction despite successful peripheral recovery is reported and perhaps adds to the permanent functional deficits that remain in victims of peripheral nerve injury.

TABLE OF CONTENTS

LIST OF FIGURES

LIST OF TABLES

ACKNOWLEDGMENT

Several beloved mentors, teachers, colleagues, friends and family have contributed to the success of this dissertation. First and foremost, I would like to thank my advisor, Dr. Timothy Cope. He has been a great mentor, teacher, and an exceptional friend. I owe him my gratitude and I truly appreciate everything he has done to me since I first joined his laboratory.

Next, I would like to thank all my committee members for all the support, comments, feedback and guidance up until the final examination. Their input into my dissertation was invaluable, their sincere reviews and comments have highly improved my scientific thinking and writing. I owe them my gratitude and I truly appreciate their time and input into my scientific career.

I would like to especially thank Paul Nardelli and Lori Goss for their continuous support and for teaching me laboratory skills needed to successfully achieve my dissertation work.

I owe special gratitude to the biomedical sciences Ph.D. program at Wright State directed by Dr. Gerald Alter and to Jordan University of Science and Technology, especially Dr. Said Al-khatib who originally introduced me to Wright State University. The great support received from WSU and JUST has been so generous and was truly vital to my success.

DEDICATION

I dedicate this doctoral dissertation to my parents: Jamilah and Zayed who fully devoted their lives to help us achieve our dreams and to my wife: Nadia who dedicated the past years of her life in supporting me to succeed while taking great care of our beloved sons: Zayed and Bassel

Chapter 1: General Background

The spinal cord is the structure that links higher cortical areas to the biomechanical locomotive apparatus. In other words, it is the structure that mediates the command to movement through the well-studied and highly complex final common pathway (Burke 2007). The spinal cord itself has gained wide interest mainly from physiologists. For example, it was referred to by Sir Charles Sherrington as "the better point of attack physiologically" for examining the sensorimotor system as opposed to the cortex where he started his own scientific career (Liddell 1952). In fact, animals lacking their cerebral cortex (decerebrates) can produce meaningful movements (Whelan 1996). So, the spinal cord is fully equipped with simple yet intricate machineries necessary for vital motor behavior. For example, the rapid execution of the withdrawal reflex is intrinsic to the spinal cord (Clarac 2005). Built-in spinal circuits are modulated by descending inputs; however, it seems that their functions are primarily driven locally.

One great example of this type of organization is the well-known and heavily studied spinal recurrent inhibition, also known as Renshaw inhibition after Dr. Birdsey Renshaw who first described this circuit (Renshaw 1941; Renshaw 1946). This spinal circuit (Figure 1.1) is principally formed between α-motoneurons (α-MNs) and a group of inhibitory interneurons, named Renshaw cells (Eccles, Fatt et al. 1954). The circuit is a recurrent circuit and is the first feedback system to be discovered within the mammalian central nervous system (CNS) (Katz and Pierrot-Deseilligny 1999). Other recurrent

inhibitory circuits were later described in several regions such as the cerebellum, thalamus, auditory cortex, hippocampus, respiratory networks and olfactory bulb (Windhorst 1996). So it seems that recurrent circuits are common and important features of the CNS organization.

The current work had three main aims: First, to investigate the effects of recurrent inhibition on α-MN firing behavior; Second, to examine the circuit frequency dynamics and their functional significance; and finally, to explore the circuit adaptation to selective peripheral nerve injury and regeneration.

Spinal recurrent inhibition

In 1941, Renshaw demonstrated that antidromic impulses traveling along motoneuron axons result in a long lasting inhibition (with short central latency) of homonymous and synergistic motoneurons; he also proposed that this effect is mediated via the motoneuron axon collaterals (Renshaw 1941; Renshaw 1946). Later, Sir John Eccles and others continued to study this inhibition in detail using intra and extra-cellular electrophysiological methods. In their 1954 paper, Eccles and colleagues proposed to honor those “inhibitory” interneurons with the distinguishing title of “Renshaw cells” (Eccles, Fatt et al. 1954). Therefore, in this thesis, the terms Renshaw cell and Renshaw inhibition will be used to address this important circuit.

Figure 1.1. ***Renshaw cell firing is locked to the motoneuron.*** Unless modulated by other synaptic sources (spinal and supra-spinal), recurrent inhibition results in an obligatory self-regulation of the activity of α-MNs. As the motoneuron excite the Renshaw cell(s), the latter fire back and "inhibit" the α-MN, apparently very simple but in reality extremely tricky.

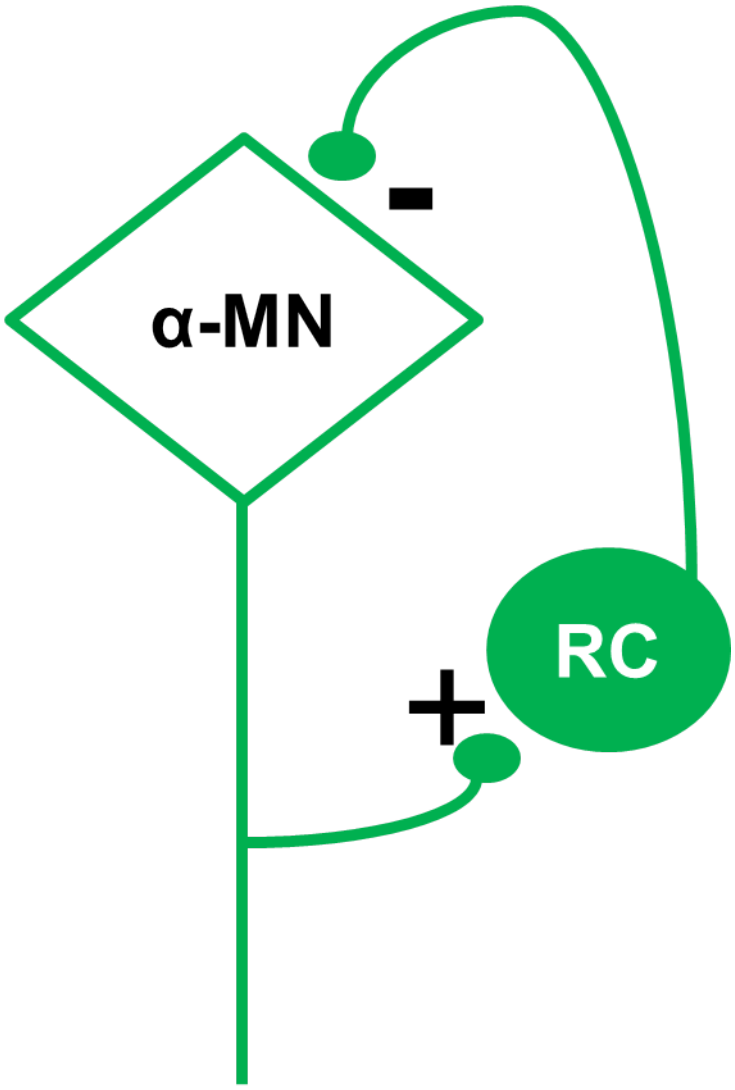
α-MN
RC
To Skeletal muscle

So, the circuit is operated via two chemical synapses, the first of which (site no. 1 in Figure 1.2) is cholinergic, i.e. releases acetylcholine onto nicotinic ACh receptors. In immature animals (Mentis, Alvarez et al. 2005; Nishimaru, Restrepo et al. 2005; Lamotte d'Incamps and Ascher 2008), glutamate is also co-released at this synapse. However, in the adult animal, there is yet no definitive evidence for their co-release (Liu, Bannatyne et al. 2009). The second synapse (site no. 2 in Figure 1.2) is confirmed in the adult cat to release both glycine and GABA (Cullheim and Kellerth 1981). The two inhibitory neurotransmitters then act on postsynaptic receptors causing inward anionic current in the α-MN (hyperpolarization of the target α-MN).

Despite the above described structural simplicity, further simplified here by ignoring descending projections, many issues about the operation and the function of this circuit remain unresolved. For example, one of the earliest question raised by Renshaw himself (Renshaw 1946) was about the functional significance of the characteristic high frequency (up to 1500 Hz) repetitive firing of the Renshaw cell in response to a single impulse in the α-MN. This unique feature is reflected as “ripples” on the rising phase of the recurrent inhibitory post synaptic potential (RIPSP) intracellularly recorded from α-MNs (see Figure 1.3). To date, there still no specific answer regarding the functional significance of this distinctive behavior. Specific aim 2 in the current thesis (Chapter 4) will provide some insight into possible functional significance of this behavior.

Figure 1.2. ***The basic structure of spinal recurrent inhibition***. Activity in the α-motoneuron constitutes the primary drive for the circuit operation. For each impulse arriving at site 1, Renshaw cells respond by a repetitive train of action potentials (shown records are original and obtained via intracellular impalement of a Renshaw cell or α-MNs in the adult rat).

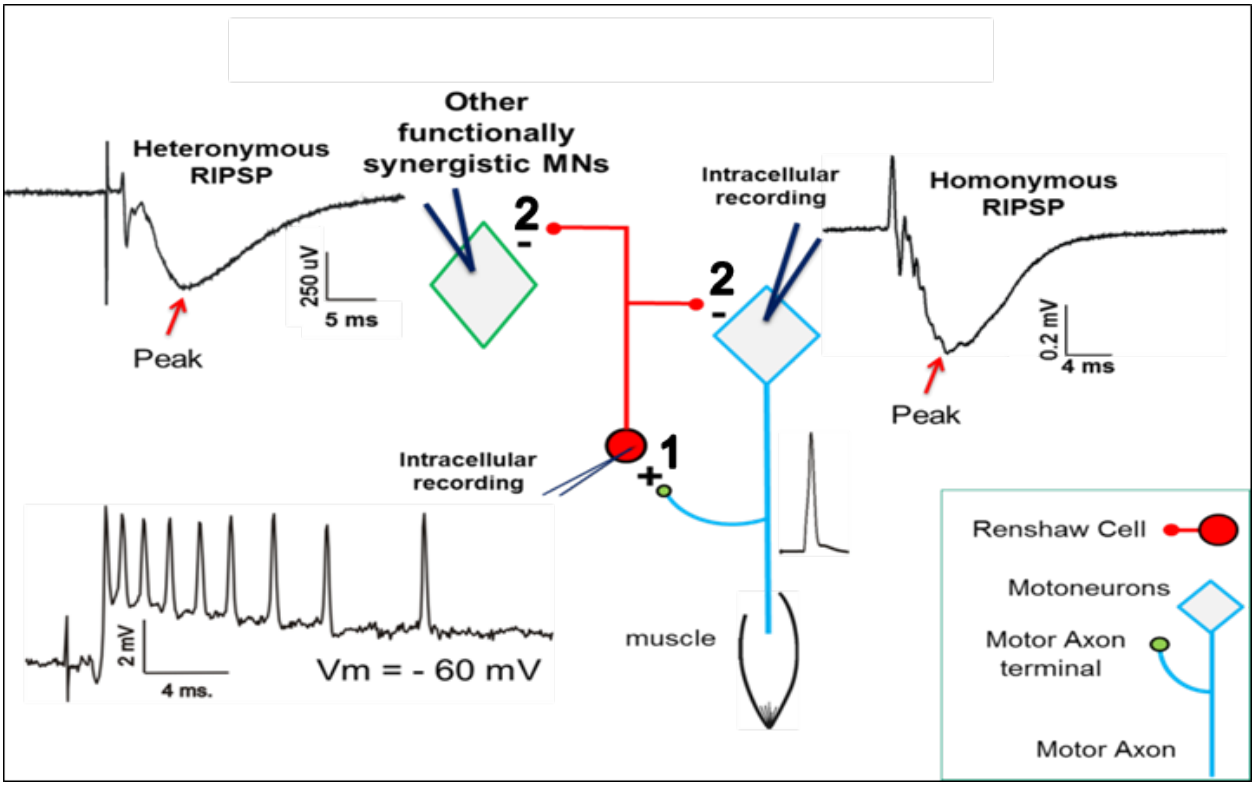
Heteronymous RIPSP
Peak
250 uV
5 ms
Other functionally synergistic MNs
2
-
Intracellular recording
2
-
Homonymous RIPSP
0.2 mV
4 ms
Peak
Intracellular recording
1
+
2 mV
4 ms.
Vm = - 60 mV
muscle
Renshaw Cell
Motoneurons
Motor Axon terminal
Motor Axon

Figure 1.3. ***Ripples***. The characteristic reflection of repetitive firing behavior of Renshaw cells on the rising phase of the RIPSP. Data obtained in-vivo from the adult anesthetized rat, Ripples (arrows).

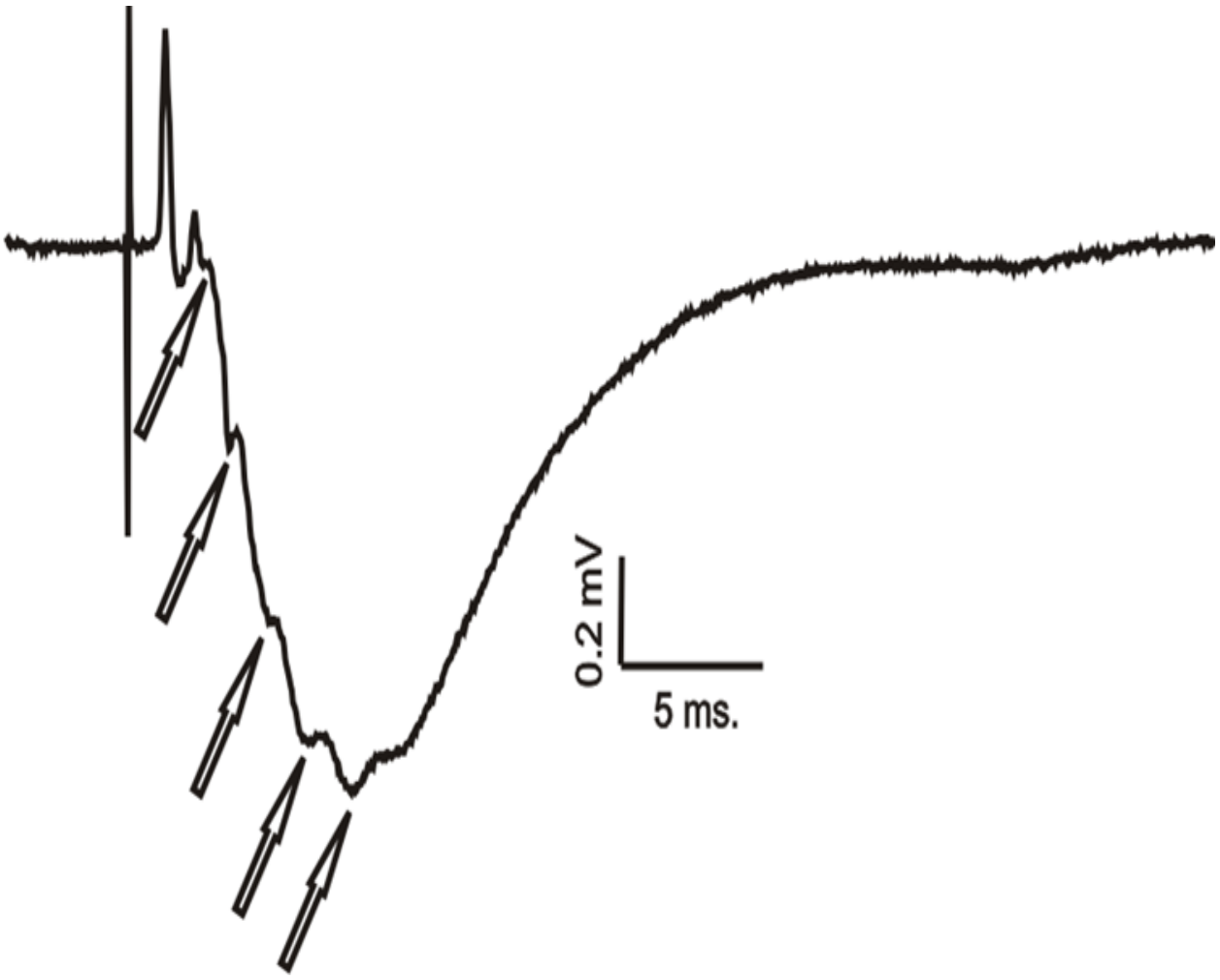
0.2 mV
5 ms.

The magnitude of the recurrent inhibitory potentials

In quiescent animal preparations, Renshaw inhibition is usually recorded from α-MNs at or near their resting membrane potential (Vm). This can underestimate the magnitude of RIPSPs because RIPSP reversal potential (Eccles, Fatt et al. 1954; Coombs, Eccles et al. 1955) is so close to the resting Vm of α-MNs which ranges from -55 to -80 mV (Eccles, Fatt et al. 1954; Coombs, Eccles et al. 1955; McCurdy and Hamm 1994a). Consequently, it is expected to observe smaller values for RIPSP peak amplitudes (maximum of few millivolts). This led some authors to argue or even to estimate that the effect of the current mediated by Renshaw inhibition on α-MN firing would be minimal (Lindsay and Binder 1991). Other lines of evidence argue against this conclusion. For example, if Renshaw inhibition occurs mainly during α-MN firing, then functioning RIPSPs are expected to be larger than those measured at resting Vm. This is simply because the Vm of α-MN during firing is depolarized and is farther away from the RIPSP reversal potential (Fetz and Gustafsson 1983). Furthermore, in most quiescent animal preparations, RIPSPs are antidromically evoked by electrical stimulation of one or a few motor nerves which might not be the case in behaving animals where in addition to homonymous effect, many other functionally synergistic pools are active and are expected to supply additional Renshaw inhibition (McCurdy and Hamm 1994a). Many studies have actually demonstrated a measurable effect for Renshaw inhibition on α-MN firing rate (Granit, Haase et al. 1960; Granit and Rutledge 1960; Granit and Renkin 1961;

Cleveland, Kuschmierz et al. 1981; Hultborn, Denton et al. 2003). These studies are summarized in the next section.

Effect of Renshaw inhibition on α-MN firing

The earliest proposed function for Renshaw cells is inhibition of α-MN firing as originally proposed in (Eccles, Fatt et al. 1954). The anatomical structure of the circuit itself has strongly suggested a general suppressor function on α-MNs and led investigators to assume that Renshaw inhibition is most likely a simple negative feedback loop, reviewed in (Windhorst 1996). The currently accepted view is that Renshaw inhibition can reduce α-MN firing rate. However, the magnitude of this effect varied widely from one study to another. For example, some studies suggested minimal effects (Lindsay and Binder 1991) while others reported strong effects (Cleveland, Kuschmierz et al. 1981) or even complete cessation of α-MN firing after activation of Renshaw inhibition (Granit and Rutledge 1960). Most of the reduced animal work was done in the feline preparation, and almost all investigators used faster rates of axon stimulation (50 to more than 100 pps) in contrast to the actual range of α-MN repetitive firing in the cat which is 10-40 pps (Granit and Renkin 1961; Hultborn, Denton et al. 2003). The reason being that at lower frequencies, Renshaw inhibition was not as effective in reducing the discharge rate of α-MNs in decerebrate cats (Granit and Renkin 1961). In fact, Cleveland and colleagues (Cleveland, Kuschmierz et al. 1981) studied the change in firing rates of four α-MNs (driven by suprathreshold intracellular current injection) in response to static

antidromic activation of Renshaw inhibition, and found the same qualitative results as reported previously by the Granit group. However, it is important to mention that they observed stronger effects than those reported by the Granit group who instead used synaptic activation of α-MNs (Granit and Renkin 1961). In striking contrast, Hultborn and colleagues showed that in α-MNs driven to fire synaptically, Renshaw inhibition is more effective in suppressing α-MN firing in comparison to α-MNs driven to fire by intracellular current injection. They attributed their findings to the effect Renshaw inhibition has on persistent inward currents (PICs) which are likely active in α-MNs driven synaptically but not in those driven by current injection. The reason being that Renshaw cell synapses distribute on the dendrites similar to PIC current (Fyffe 1991; Hultborn, Denton et al. 2003). Of note, most studies mentioned were implemented in the decerebrate cat where PICs are active compared to anesthetized preparations (Guertin and Hounsgaard 1999). It can be seen from Figures 3 and 4 in (Hultborn, Denton et al. 2003) that RIPSP are very long (several hundreds of milliseconds) and are activated at very high tetanic (functionally less relevant) rates (100 pps in a decerebrate cat), so a possibility of summation of multiple RIPSPs cannot be excluded. Surprisingly, none of previous animal studies has examined RIPSP parameters during repetitive firing, i.e. RIPSP amplitude and/or time course. Both of which could be responsible for quantitative differences observed across different studies or within each study. So, it appears that the current knowledge about the effect of Renshaw inhibition on α-MN firing is inconclusive and still holds some ambiguity.

Adopting a novel approach in the analysis of Renshaw inhibition on α-MN firing might clarify some of the current debate. First, we propose to replace the term "limitation of discharge rate" by "modulation of firing behavior" because firing rate is only one part of the beauty and complexity of action potential voyage through the final common pathway. Chapter 3 in this thesis will examine the effects of Renshaw inhibition on α-MN firing behavior. Briefly, it is possible that Renshaw inhibition can affect firing pattern, variance, duration, and spike timing in addition to rate itself. Also, the timing of the RIPSP in relation to the firing train of action potentials has not been thoroughly examined in animal studies. Here, RIPSP timing of arrival during repetitive firing, RIPSP size and RIPSP time course, all will be considered in the analysis of the effect on firing modulation.

The next section will briefly discuss some insights into the timing of inhibition followed by a discussion of other recurrent circuits within the CNS.

Timing of Renshaw inhibition and motoneuron firing behavior

With such a circuit where inhibition is locked to α-MN firing (Figures 1.1 and 1.2), it appears that one can predict at least a few possibilities for RIPSP timing in relation to α-MN firing. The estimation is based on the assumption that Renshaw inhibition is primarily driven by α-MN recurrent axon collaterals while descending inputs are only playing a modulatory role (Windhorst 1996). If this assumption holds true, then RIPSPs generated in α-MNs should have fixed timing that roughly corresponds to a central

disynaptic delay. Another prerequisite would be that synchronous stimulation of motor axons is relevant to Renshaw cell function. The latter was addressed by Cleveland and colleagues who showed that responses of Renshaw cells to individual inputs (by stimulating the functional minimum of motor fibers) were similar to those obtained following synchronous activation of multiple α-MNs, see Figure 4 in (Cleveland, Kuschmierz et al. 1981). Therefore, they concluded that the input-output characteristics of synchronously activated Renshaw cells are qualitatively similar to Renshaw cells stimulated by the functional minimum of motoneurons.

Several studies have examined the effect of recurrent inhibition on human motor unit discharge rate. In fact, measuring Renshaw inhibition in human subjects depends on the assumption that the inhibition hyperpolarizes the membrane potential and delays the occurrence of the next spike, i.e. can prolong the inter-spike interval (ISI), (Katz and Pierrot-Deseilligny 1999). Interestingly, in an attempt to examine the effect of Renshaw inhibition on human motor unit firing rates, Kudina and Pantseva (1988) reported that the timing of arrival of the inhibitory volley during the ISI is critical. They reported that if inhibition arrives at the end of the ISI, firing rate is reduced (Kudina and Pantseva 1988; Miles, Le et al. 1989). This was in contrast to inhibition arriving at the beginning of ISI, i.e. at the onset of the afterhyperpolarizing potential (AHP), which failed to reduce firing rate under the same experimental conditions. The explanation for this discrepancy was based on the assumption that the size of the antidromically evoked IPSPs are large near the end of the ISI (Vm is more depolarized) and are minimal or not even present if

arrived early during the ISI (Vm is already hyperpolarized by the AHP). The latter work concluded that Renshaw inhibition might not decrease the discharge rate of homonymous α-MNs because within the same motor pool, inhibition is highly expected to arrive early within the ISI, i.e. at the onset of the AHP. In contrast, one other group reported results that did not fully agree with Kudina and Pantseva. In a pathologically deafferented patient, recurrent inhibition arriving early during the ISI was more effective in rate reduction than inhibition arriving at the end of the ISI (Mattei, Schmied et al. 2003). The latter study was based on a single observation obtained under a pathological condition and therefore, might not represent the circuit behavior under healthy condition.

The current study is designed to investigate the controversy arising from the human literature. Chapter 4 will address the effect of Renshaw inhibition on α-MN firing rate. In addition, other effects of Renshaw inhibition on α-MN firing will be studied and compared with findings from other inhibitory systems within the central nervous system (CNS). The next section will briefly describe some other inhibitory pathways that are distributed across the CNS.

Other inhibitory pathways within the CNS

In 1996, Windhorst started his comprehensive review on the role of Renshaw inhibition by referring to other recurrent circuits within the CNS (Windhorst 1996). Using this approach, he wanted to emphasize that recurrent circuits (whether excitatory

or inhibitory) might actually be serving similar general functions, but at different CNS locations.

As the case for Renshaw inhibition, several investigators have examined the functions of inhibitory circuits across the CNS, mainly on neuronal firing behavior. For example, in two recent reports (Bengtsson, Ekerot et al. 2011; Person and Raman 2011), researchers examined the cerebellar circuit formed by Purkinje cells (PCs, inhibitory), and deep cerebellar nuclear neurons (DCN, target neurons). In both studies, synchronous activation of PCs was required to achieve large IPSPs. The first study (Bengtsson, Ekerot et al. 2011) described the phenomenon of rebound excitation following strong inhibition of DCN neurons in vivo (IPSP amplitudes of 15 -20 mV). The second study (Person and Raman 2011) demonstrated that DCN neurons time-lock their spikes to synchronous PC inputs. Moreover, they reported a strong relation between the degrees of synchrony between PC and DCN neuronal firing rates, i.e. faster firing rates of DCN neurons are seen with higher degrees of synchrony (Person and Raman 2011).

Similar phase-locking of target neurons to inhibition was reported in the hippocampus (Cobb, Buhl et al. 1995), olfactory bulb (Desmaisons, Vincent et al. 1999), and auditory cortex (Wehr and Zador 2003). The demonstration of the robust effect of inhibition on spike timing in different areas within the CNS suggests that inhibition in general might not primarily affect firing rate but rather have a modulatory effect on the firing behavior,

especially spike timing. Therefore, we hypothesized that Renshaw inhibition effects on α-MN spike timing are strong.

Input-output behavior of Renshaw inhibition

Renshaw cells are known to fire repetitively in response to single impulses arriving at the α-MN – Renshaw cell synapse (Figure 1.2) and (Renshaw 1946; Eccles, Fatt et al. 1954). Later, it was observed that this repetitive firing behavior is not fixed and can change according to the frequency of the motor input to Renshaw cells (Haase 1963). This phenomenon, named by Haase as "transformation", is characterized by the shortening of the Renshaw cell firing duration in response to increasing the frequency of the peripheral axon stimulation, i.e. increasing the frequency of antidromic stimulation. In their 1961 paper, Granit and Renkin stated that the transformation observed by Haase (cited as a personal communication) indicates that the characteristic repetitive discharge of Renshaw cells observed at lower frequencies of peripheral stimulation is nothing but an experimental artifact (Granit and Renkin 1961). However, to date, whenever Renshaw cells are described, their repetitive firing behavior is frequently pointed out. Therefore, further investigations are needed to establish whether this unique behavior is simply an artifact of stimulation or rather a functionally significant phenomenon. The second specific aim of this thesis (Chapter 4) was to examine this phenomenon in correlation to frequency dynamics of the RIPSPs. Moreover, experiments to establish the functional significance of this "transformation" were implemented.

Brief and general background about the normal function of inhibition was provided above. Next, I will briefly describe some of the previous work done to investigate the plasticity of central spinal cord circuits, including Renshaw inhibition, after peripheral nerve injury.

Central spinal circuits and peripheral nerve injury

Traumatic and non-traumatic injuries to peripheral nerves constitute a common clinical problem. Even after standard surgery of severed nerves, 90% of patients do not regain normal motor coordination and 40% have difficulty achieving gross manual activity (Robinson 2000). Experimentally, reinnervated muscles showed dramatic failure in their ability to respond to stretch (Cope, Bonasera et al. 1994). This was proved later to be at least in-part due to disorganization of central synaptic connections (Alvarez, Titus-Mitchell et al. 2011; Bullinger, Nardelli et al. 2011). In the case of the sensory system it is possible for regenerated sensory fibers to connect with inappropriate peripheral targets (e.g. muscle spindle vs. Golgi tendon organ), and this can contribute to observed central deficits in connectivity that remain after nerve regeneration. On the other hand, regenerated motor axons are more successful in re-innervating their appropriate target, i.e. extrafusal muscle fibers. They are known to successfully reestablish functional relationship within the motor unit (Cope and Clark 1993). The response of the circuit of Renshaw inhibition to peripheral axotomy followed by ligation (i.e. prevention of regeneration) has been studied before (Havton and Kellerth 1984; Havton and Kellerth

1990a; Havton and Kellerth 1990b). These authors showed that in a feline preparation, the function of Renshaw inhibition (initially lost after injury) undergoes full recovery at 12 weeks post injury which was in disagreement with anatomical findings suggesting gradual and permanent loss of central recurrent collaterals originating from injured motor axons (Havton and Kellerth 1990b). So, the functional recovery of recurrent inhibition was attained despite failure of motor axon regeneration either peripherally or centrally. Potential explanations were proposed and will be discussed further (Chapter 5).

The extent by which successful regeneration of the injured motor axon branch in the peripheral nerve can restore the central branches is unknown. One would expect that successful peripheral re-connections might restore central ones. If this is the case, then one would expect even better functional recovery with nerve regeneration than what was observed in the setting of nerve ligation. In addition, one might wonder about the relevance of nerve ligation experiments to the clinical setting where most nerves (if not all) undergo some degree of regeneration, either natural (i.e. highly non-specific) or assisted (i.e. mostly specific). So, specific aim 3 in this thesis was designed to investigate the extent of recovery of Renshaw inhibition (both morphology and function) after selective peripheral nerve injury and successful regeneration (Chapter 5).

Summary of major questions addressed by the current work

Since its discovery (Renshaw 1941; Renshaw 1946), Renshaw inhibition has been a source of scientific debate (Windhorst 1996). Renshaw himself raised several questions about his discovery, many of which are still pending definitive answers. For example, in 1946 Renshaw inquired about the functional significance of the characteristic repetitive response of Renshaw cells to inputs from α-MNs (Renshaw 1946). Also, Renshaw and many others raised several questions about the functional significance of this type of inhibition (Renshaw 1946; Eccles 1954; Windhorst 1996).

One important question is the functional significance of Renshaw inhibition. Current understanding is thoroughly reviewed in (Windhorst 1996) and is further addressed by many human and simulation studies (Kudina and Pantseva 1988; Miles, Le et al. 1989; Piotrkiewicz, Kudina et al. 2004; Uchiyama and Windhorst 2007; Iles 2008; Lamy, Iglesias et al. 2008). One of the earliest and seemingly straight forward functions of Renshaw inhibition is limitation and stabilization of α-MN firing rates (Granit and Rutledge 1960; Granit and Renkin 1961; Noga, Shefchyk et al. 1987; Pratt and Jordan 1987; Hamm 1990). As mentioned above, and especially in human studies, there is a lack of consensus on the magnitude of the effect on firing rate and / or even the nature of the effect itself (Kudina and Pantseva 1988; Miles, Le et al. 1989). Here, I would like to refer to an interesting argument raised by Windhorst in 1996: *"For the sole purpose of reducing or limiting an output, it would be a waste to use an additional, potentially*

energy-expensive negative feedback system; this would be like driving a car by continually pushing the accelerator and simultaneously activating the brake!"
(Windhorst 1996, p. 528)

The latter argument failed to gain much popularity and studies to date assume and continue to report that Renshaw inhibition adversely affects α-MN discharge rates (Hultborn, Denton et al. 2003). Specific aim 1 in this thesis re-examined this seemingly straight forward function in a novel way (Chapter 3). Briefly, Renshaw inhibition failed to reduce α-MN firing rates under the experimental conditions used in this thesis. Surprisingly, inhibition was shown to even increase α-MN firing rate under certain circumstances. In addition, Renshaw inhibition was shown to strongly modulate spike timing of α-MNs.

Specific aim 2 in this thesis examined the intriguing frequency dynamics of Renshaw cells (increase input → decrease output). The "transformation" of Renshaw cell firing, first described by Haase in 1963, was confirmed. In addition, frequency dynamics of RIPSP amplitude and time course were explored. In addition, the functional significance of Renshaw cell transformation and RIPSP time course frequency dynamics were investigated.

Finally, specific aim 3 in this thesis followed on the well-known work done in the laboratories of Timothy Cope, Francisco Alvarez and others where the CNS is found to experience some degree of adaptation in response to peripheral nerve injury. In fact, in

some central circuits, permanent dysfunction remains despite successful reinnervation in the periphery (Cope, Bonasera et al. 1994; Navarro, Vivo et al. 2007; Alvarez, Titus-Mitchell et al. 2011; Bullinger, Nardelli et al. 2011). Due to the fact that motor axon regeneration is highly successful in re-connecting to its appropriate peripheral targets, i.e. extrafusal muscle fibers (Cope and Clark 1993), it is likely that motor axon regeneration is sufficient to restore the motoneuron central projections, i.e. axon collaterals.

In contrast to previous findings where the motor nerve was prevented from regeneration, it is highly expected that both structure and function will be restored after nerve regeneration. Thus, collaborative experiments described in the current thesis were designed to specifically examine the degree of structural and functional recovery of the recurrent pathway. Surprisingly, despite successful peripheral nerve regeneration, permanent structural and functional deficits remained (Chapter 5).

Chapter 2: General Methods

Animals

In all experiments, adult female wistar rats were used (240-500 g, Charles Rivers Laboratories, Wilmington, MA). Rats were used to stay in line with other reports that examined the central plasticity of other synaptic circuits after nerve injury and regeneration (Bullinger, Nardelli et al. 2011). All rats were housed within Wright State University LAR facility. Food and water was available ad libitum, and rats were given wooden chew sticks to encourage activity. All rats underwent terminal experiments to collect electrophyiological data.

Terminal experiments

Anesthesia

Anesthesia was induced by isoflurane (5% in 100% O_2, inhalation in induction chamber) and maintained by isoflurane (1-2.5% in 100% O_2, through nasal cone at the beginning, then through an endotracheal tube). The level of anesthesia was judged effective by testing the withdrawal reflex and by monitoring respiratory rate <60 breath per minute. In addition, pulse rate, blood O_2 saturation, expired CO_2 end tidal volume, and temperature

were monitored. These vital signs were maintained within normal limits through the adjustment of isoflurane concentration, adjustment of heat (radiant and water-pad) and administration of subcutaneous fluids (Ringer-lactate solution). Withdrawal reflexes were frequently tested to ensure they remained suppressed during the experiment.

Surgical Preparation

After anesthesia was induced, the anterior biceps – semimembranosus (ABSM), medial gastrocnemius (MG), lateral gastrocnemius and soleus (LGS) nerves were isolated in the left hindlimb. Standard surgical procedures were used to dissect the spinal cord for intracellular recording from motoneurons (Seburn and Cope 1998). In brief, the lumbar spinal cord (T10-S1) was exposed dorsally by dissecting the covering layers, performing a laminectomy (for bone removal) and removing meningeal layers (dura and arachnoid). Then, the rat was fixed in a recording frame for continuous stability. Skin flaps were used to form pouches that were filled with warm mineral oil. The aim was to cover the exposed tissue and prevent drying. All ipsilateral dorsal roots were severed and reflected away from the cord before starting the recording session.

Recording Preparation

All three muscle nerves were placed on monopolar stimulating hook electrodes for stimulation and antidromic identification of impaled motoneurons. Peripheral nerve stimulation strength was set at 2.5 times the threshold for visible muscle contraction.

Data collection

Motoneurons were impaled as glass microelecrodes filled with 2M potassium acetate (1.2 mm OD, 6-11 MΩ resistance, World Precision Instruments) advanced through the spinal cord using a micromanipulator. Cells were identified as either MG, LGS or ABSM motoneurons when the stimulation of one of the mentioned peripheral nerves resulted in antidromic action potential spike. Upon identification, the antidromic action potential was recorded, and its amplitude was measured. Only those cells whose membrane potential was stable and action potential amplitude was meaured at +60 mV or larger were included for further analysis. The motoneuron's intrinsic electrical properties (rheobase current, afterhyperpolarization (AHP) half decay time and peak amplitude) were recorded. In addition, homonymous (submaximal peripheral stimulation for the antidromic action potential) and/or heteronymous (supramaximal peripheral nerve stimulation) recurrent inhibitory post synaptic potentials (RIPSPs) were recorded from one or up to three sources depending on the stability of the recorded cell. RIPSPs were evoked by antidromic stimulation of individual nerves at 20 Hz (pulse duration = 40 microseconds), the reason for using this frequency is described later (Chapter 4). In some motoneurons, intracellular, constant suprathreshold current injection was done to drive repetitive firing during which Renshaw inhibition was simultaneously activated in some trials (Chapter 3).

Data analysis

Specific methods are presented in each chapter. In general, in all α-MNs recorded, the presence or absence of a recurrent synaptic potential in response to homonymous and/or heteronymous motor pool stimulation was determined. RIPSP amplitude and time course were measured. In some experiments (Chapter 4), RIPSPs were recorded after stimulating the peripheral nerve at multiple frequencies (2, 10, 20, and 30 Hz). In general, inhibitory synaptic potentials were collected and averaged over many sweeps ranging from 50 to 1000 . Figure 2.1 presents one example of a RIPSP showing the measurements obtained and used for comparison in the different experiments described in the current thesis.

Statistical analysis

See specific method sections in each chapter below. In general, for continuous variables, independent Student t-tests or factorial two way ANOVA were used for pair-wise comparison of the means. Bonferroni post hoc analysis was done to correct for multiple tests when needed. Percentages were compared using the two-tailed Fisher Exact test. In many experiments (Chapters 3 and 4), each motoneuron served as its own internal control, i.e. normalization of results within each motoneruon was frequently implemented. Significance was set at $p<0.05$. Statistical help was obtained through Wright State statistical center, specifically Bev Grunden.

Figure 2.1. ***RIPSP with electrophysioogical measurements***. An illustration of one example of a RIPSP recorded intracellularly. Note the different electrophysiological measurements analyzed.

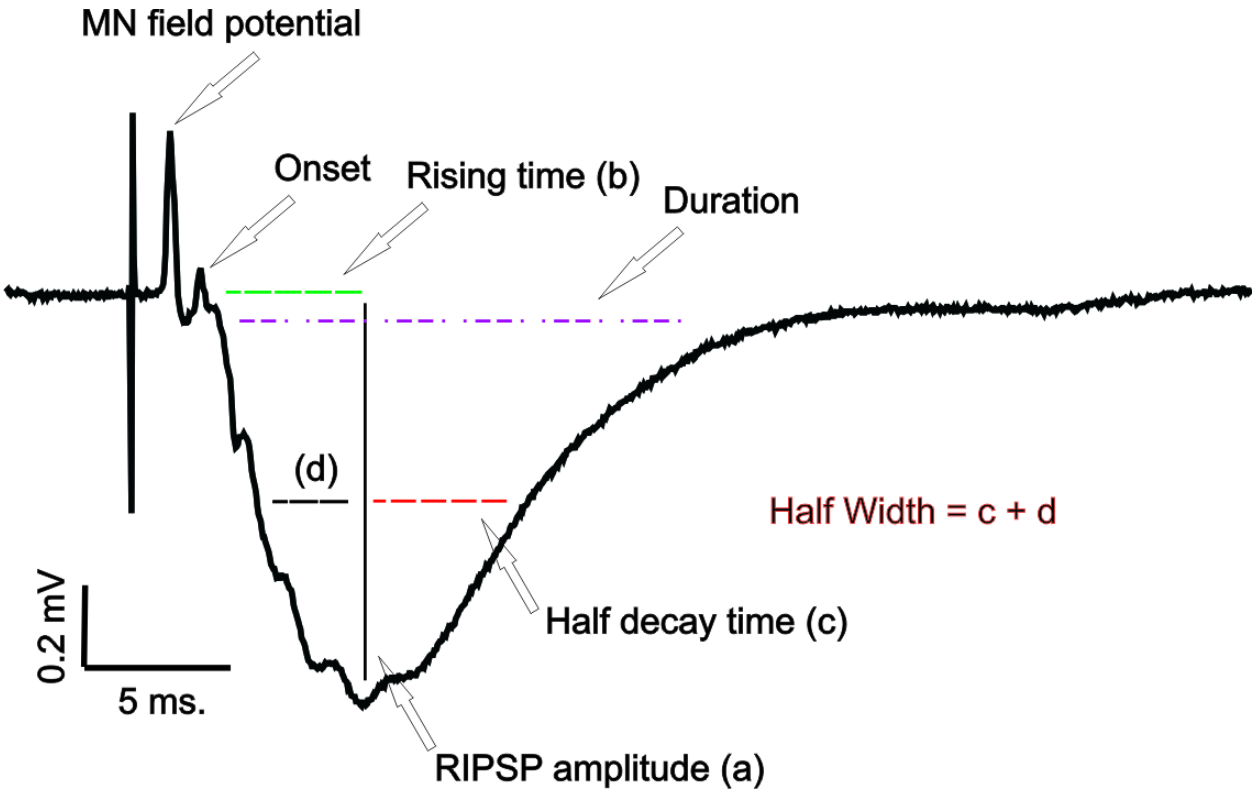
MN field potential
Onset
Rising time (b)
Duration
(d)
Half Width = c + d
Half decay time (c)
0.2 mV
5 ms.
RIPSP amplitude (a)

Chapter 3: Modulation of Motoneuron Firing Behavior via the Recurrent Pathway

Introduction

The unique anatomical structure of recurrent inhibition has led many investigators to propose a primary effect on motoneuron firing, for review see (Windhorst 1996). One of the earliest assumptions was that Renshaw inhibition is nothing but a simple negative feedback loop with generalized suppressor effects on the speed of motoneuron firing (Eccles, Fatt et al. 1954; Holmgren and Merton 1954). To date, the primary effect of Renshaw inhibition on motoneuron firing remains uncertain.

Firing Rate versus Spike Timing

Motoneurons in most motoneuron pools exert disynaptic inhibitory effects on one another via Renshaw interneurons (recurrent inhibition; Renshaw 1941; 1946). One of the earliest proposed roles of recurrent inhibition is the limitation of motoneuron firing rates (Windhorst 1996). This effect was demonstrated in several studies (Granit, Haase et al. 1960; Granit and Rutledge 1960; Granit and Renkin 1961; Cleveland, Kuschmierz et al. 1981; Noga, Shefchyk et al. 1987; Pratt and Jordan 1987; Lindsay and Binder 1991; Hultborn, Denton et al. 2003). However, the magnitude of the effect varies widely from small < 2 pulses per second (Lindsey and Binder 1991) to large effects or even to a complete cessation of motoneuron firing (Granit and Rutledge 1960).

Despite all the work cited above, limitation of firing rate may not be the only or even the primary effect of recurrent inhibition on motoneuron firing. Perhaps recurrent inhibition plays a more complex role in firing modulation. In fact, Windhorst in his thorough review on the functional significance of recurrent inhibition argues for a problem with this earlier theory (Renshaw inhibition as a negative feedback loop). His justification is based on the energy cost of operating this circuit for the sole purpose of limiting motoneuron discharge rates, he wrote in reference to earlier theories: “This would be like driving a car by continually pushing the accelerator and simultaneously activating the brake” (Windhorst 1996).

Because of the fixed timing of Renshaw interneuron discharge to motoneuron firing, we expect that recurrent inhibition might phase-lock the activity of the motoneuron. In fact, this has been shown for several inhibitory systems within the CNS (e.g. the hippocampus (Cobb, Buhl et al. 1995), auditory cortex (Wehr and Zador 2003), cerebellum (Bengtsson, Ekerot et al. 2011; Person and Raman 2011) and olfactory bulb (Desmaisons, Vincent et al. 1999). In two recent papers, it was shown that the deep nuclear cells of the cerebellum are phase-locked by synchronous inhibition (Bengtsson, Ekerot et al. 2011; Person and Raman 2011). A possible mechanism for phase-locking is shifting of spikes away from the peak of inhibitory post synaptic potential (IPSP) to the IPSP decay phase (Fetz and Gustafsson 1983).

This timing effect, if demonstrated for spinal recurrent inhibition, will have potential importance and direct relevance to function. For example, Davey and others demonstrated a rhythmic pattern for human motor unit discharge that was prominent only in motoneuron pools known to receive recurrent inhibition (Davey, Ellaway et al. 1993); therefore, they proposed that the observed rhythmicity may involve recurrent inhibition. In addition, Mattei and colleagues were able to increase the degree of synchrony of human motor unit discharge via pharmacological augmentation of recurrent inhibition (Mattei, Schmied et al. 2003). So, if established, the effect of firing rate modulation by Renshaw cell rather than simple limitation may be most relevant to motor control.

M**otoneuron firing rate modulation**

Work done in the anesthetized and / or decerebrate cat preparation, *in vivo*, has consistently shown that recurrent inhibition, activated at frequencies much higher than the motoneuron firing rate, can reduce the discharge rate of motoneurons (Granit and Rutledge 1960; Granit and Renkin 1961; Cleveland, Kuschmierz et al. 1981; Pratt and Jordan 1987; Hultborn, Denton et al. 2003). On the other hand, if lower frequencies were used, or the antidromic electrical shock was triggered off the motoneuron action potential spike, then the reduction in motoneuron discharge rate was unclear (Granit and Rutledge 1960; Granit and Renkin 1961). Therefore, a decision to stimulate at higher frequencies was taken in all subsequent studies and the notion that recurrent inhibition must reduce motoneuron discharge rate was adopted (Cleveland, Kuschmierz et al. 1981; Hultborn,

Denton et al. 2003). Now, the question of whether tetanic or rather slower rates of recurrent inhibition activation are more relevant to behavior requires deeper analysis.

Renshaw cells receive their primary input from motoneurons (Figures 1.1 and 1.2). Unless suppressed by descending inputs, it is compulsory for Renshaw cells to fire every single time they are excited by the motoneuron via the motoneuron – Renshaw cell synapse. This results in RIPSPs in target α-MNs. The central latency for these synaptic events follows that of a disynaptic pathway > 1 msec. (Eccles, Eccles et al. 1961). In fact the mean ± SD for central latency of homonymous RIPSPs in this thesis was 1.37 ± 0.54 msec. (n=70). With such a central latency, RIPSPs are expected to modulate motoneuron firing through the interaction with the afterhyperpolarizing potential aka the afterhyperpolarization (AHP).

One of the major determinants of motoneuron firing rate is the AHP (Kernell 1965; Stauffer, McDonagh et al. 2007). AHP duration varies between different types of α-MNs and between different species. For example, motoneurons of the slow type are characterized by longer AHPs while those of the faster type are typically characterized by shorter AHPs (Eccles, Eccles et al. 1958; Kudina and Alexeeva 1992). Although AHP duration correlates well with repetitive firing in quiescent cat preparations (Kernell 1965), human motor units don't demonstrate such a correlation, i.e. the minimal firing rate of human motor units does not correlate with AHP duration (Kudina and Alexeeva 1992). The latter authors proposed that other mechanisms might come into play during

repetitive firing of motoneurons. So, human studies together with other reports, recently reviewed in (Stauffer, McDonagh et al. 2007) suggest that the AHP can be shaped by active synaptic conductances. Indeed, Renshaw inhibition is one strong candidate. Remember that the timing of the RIPSPs is perfectly suited to arrive at the beginning of the AHP. Moreover, the duration of the RIPSP is shorter than the typical duration of AHP regardless of the α-MN type. In the rat the mean duration for normal RIPSPs collected for the experiments described in this thesis was 23 ± 6 msec. (n=166). This is important since the typical duration for AHPs measured in rat MG α-MNs range between 30 – 116 msec (Bakels and Kernell 1993). So, one would expect that RIPSPs might actually shape AHPs to become faster and larger. In fact, it was shown that in patients with generalized epilepsy and paroxysmal dyskinesia, a mutation of the α-subunit of Calcium-sensitive potassium channels (BK) results in larger and faster repolarization (AHP). This change was proposed to be responsible for the observed neuronal hyperexcitability seen in these patients (Du, Bautista et al. 2005). Therefore, if the RIPSP aligns with AHP to make it deeper and perhaps faster, then one might expect inhibition to actually increase or at least not to decrease motoneuron firing rate.

In fact, one study, done in humans, examined the timing of recurrent inhibition (Kudina and Pantseva 1988). In their work, Kudina and Pantseva showed that recurrent inhibition is not effective in reducing firing rates of motor units if it arrives at the beginning of the inter-spike-interval (ISI), i.e. at the beginning of the AHP. In order to explain their findings, they suggested that the membrane potential of the α-MN at the beginning of the

ISI is already in a state of hyperpolarization, thus recurrent inhibition is expected to be small and will have negligible effect. Consistent with previous cat work showing adverse effects on motoneuron firing, Kudina and Pantseva demonstrated a prolongation of ISI if the inhibitory volley arrived near the end of the ISI. However, in their post stimulus time histograms (PSTHs), an inhibition "silent period" was followed by a significant increase in firing probability that was accompanied with shortening of ISIs. They proposed that this secondary effect originates from excitation in cutaneous afferents. In general, work done in human subjects is based on the assumption that the inhibitory volley observed is recurrent inhibition, i.e. there is no certainty that the observed effects are only due to recurrent inhibition. In addition, Kudina and Pantseva proposed that any active α-MN will fail to exert effective recurrent inhibition on itself since the inhibitory volley will always arrive at the beginning of the ISI, i.e. will not cause additional hyperpolarization in the membrane potential.

Interestingly, Mattei and colleagues found that in a deafferented patient (through a disease involving large sensory afferents for 21 years), Renshaw inhibition was most effective in delaying the spike if it arrives early during the ISI, and not near the end of ISI (Mattei, Schmied et al. 2003). This is in striking contrast to what Kudina and Pantseva previously observed. In partial agreement with other groups, Mattei and colleagues observed consistent shorting of ISIs that followed the one with the IPSP (up to 5 ISIs). In fact, they refer to it as the most consistent and the strongest finding in their patient (Mattei, Schmied et al. 2003). Because their patient was deafferented, they stated with

confidence that the apparent increase in excitation cannot be accounted for by peripheral reflexes originating from the skin or the tendon organ as interpreted before (Kudina and Pantseva 1988; Miles, Le et al. 1989). Instead, they proposed that central mechanisms such as recurrent facilitation that is preceded by inhibition (McCurdy and Hamm 1994a) might be responsible for the observed shorting of ISIs following the initial inhibition. The current work was designed to examine multiple hypotheses in acutely deafferented adult rats, *in vivo*: First, RIPSPs arriving early during the ISI can augment the hyperpolarization produced by AHP. Second, timing of arrival of RIPSPs modulates firing rate differently. Third, the effect of recurrent inhibition on spike timing is stronger than the effect on firing rate and finally, the rebound increase in firing observed in human subjects is secondary to recurrent inhibition.

Modulation of spike frequency adaptation: a novel role for Renshaw inhibition

The α-MN or better known as the final common pathway to movement has the ability to fire repetitively in response to constant intracellular current injection (Granit, Kernell et al. 1963a; Granit, Kernell et al. 1963b; Brownstone 2006). From a behavioral perspective, this fits well with earlier descriptions of movement as expression of prolonged tetani, p.149 in (Fulton 1926). One issue encountered during repetitive firing experiments is the slowing of firing rate over time before complete cessation (despite continuous and constant intracellular suprathreshold current injection), known as spike frequency adaptation (SFA). It is divided into three phases: initial SFA (occurs over the

first few spikes), early SFA (over the first hundreds of milliseconds) and late SFA (over seconds to minutes), see (Brownstone 2006; Button, Kalmar et al. 2007). Soon after its description, SFA was investigated, reviewed in (Brownstone 2006). In a series of investigations of SFA during experimentally induced fictive locomotion, Brownstone and colleagues failed to detect SFA in the cat α-MNs (Brownstone, Jordan et al. 1992; Brownstone, Krawitz et al. 2011). The novelty of their findings resulted in a recent debate of whether SFA, frequently observed in quiescent preparations, is a natural phenomenon or simply an experimental artifact, (Brownstone 2012;Wilanowski and Piotrkiewicz 2012).

Wilanowski and Piotrkiewicz argue that SFA is not an experimental artifact but rather a natural phenomenon also observed in human motor units (Person and Kudina 1972; Bigland-Ritchie, Johansson et al. 1983). Interestingly, SFA is observed more frequently and it is much faster in motoneurons innervating fast muscle fibers than those innervating slow ones (Kernell and Monster 1982; Spielmann, Laouris et al. 1993; Wilanowski and Piotrkiewicz 2012). This is quite interesting because slow motoneurons are known to receive larger amount of Renshaw inhibition compared to faster ones (Eccles, Eccles et al. 1961; Friedman, Sypert et al. 1981). In their illustrations, Spielmann and colleagues actually showed minimal to no SFA in slow motor units (Spielmann, Laouris et al. 1993). During motor behaviors such as locomotion, α-MN intrinsic properties can be modulated (Stauffer, McDonagh et al. 2007; Brownstone, Krawitz et al. 2011). Synaptic conductances, both excitatory and inhibitory are known to shape the ultimate output of

the motoneuron (Stauffer, McDonagh et al. 2007). In their discussion, Brownstone and colleagues proposed that Na^+ channel de-inactivation might be responsible for the observed reversal of late SFA (Brownstone, Krawitz et al. 2011).

The current work was designed to test the hypothesis that Renshaw synaptic inhibition can modulate spike frequency adaptation by facilitating Na^+ channel de-inactivation. This was based on the intriguing antiparallel distribution of SFA and recurrent inhibition across different types of motoneurons.

Methods

Animals

A total of 9 adult female Wistar rats (240 – 260g; Charles River Laboratories, Wilmington, MA) were included in this part of the thesis. All procedures were approved by the Wright State University Laboratory Animal Care and Use Committee (LACUC). All surgeries were terminal.

Surgery

After anesthesia was induced, the ABSM, MG, and LGS nerves were isolated in the left hindlimb. Standard surgical procedures were used to dissect the spinal cord for prepartion for recording motoneruon bioelectric signals (Seburn and Cope 1998). In brief, the lumbar spinal cord (T10-S1) was exposed dorsally by dissecting the layers including laminectomy (for bone removal) and removeal of meningeal layers (dura and arachinoid). Then. the rat was fixed in a recording frame for continuos stability. Skin flaps were used to form pouches that were filled with warm mineral oil. The aim was to cover the exposed tissues and prevent their drying. All ipsilateral dorsal roots were acutely severed and reflected away from the cord before starting the reording session.

Data collection

Motoneurons were impaled by borosilicate glass microelectrodes (1.2-mm OD, 7- to 10-MΩ DC resistance, 2 M K-acetate) advanced through the spinal cord with a micromanipulator system (Transvertex Microdrive). Motoneurons were antidromically identified by the electrical stimulation of their peripheral nerve (current strength 2.5× muscle contraction threshold, pulse duration 40 μs) and were assessed as adequately impaled if they showed membrane potential stability and action potential spike amplitude of >60 mV. The study of Renshaw inhibition effect on repetitive firing of α-MNs was completed only when sustained, repetitive response to suprathreshold long current step injections was attained. After impalement, Rheobase current, intracellularly evoked AHPs, recurrent inhibitory post synaptic potentials (RIPSPs) at resting and depolarized membrane potential were recorded. All records were stored for off-line analysis.

In 11 α-MNs, repetitive firing was driven by suprathreshold continuous current injection through the glass micropipette. Trials of repetitive firing with and without superimposed Renshaw inhibition were compared. RIPSPs were simultaneously and antidromically activated via supra-maximal electrical stimulation of the heteronymous nerves and/or submaximal stimulation of the homonymous nerve (to avoid contamination with the antidromic spike). Renshaw inhibition was activated at 20Hz regardless of the firing rate of motoneuron. The reason is explained in (Chapter 4). The application of the electrical stimulus of the peripheral nerve at random moments relative to the motoneuron discharge

enabled the examination of the effect of different timings of arrival of the RIPSP during the inter-spike-interval (ISI) on motoneuron firing rate.

Data Analysis

Spike Timing (phase locking)

Peristimulus time histograms (PSTHs) were derived from α-MN responses to current injection. Spike count index, or K is the peak bin count (1 msec. bin size) divided by the mean background bin count (Sears and Stagg 1976). This parameter was used to quantify the magnitude of RIPSP effects across cells. Mean background bin count was calculated from 1 msec. bins that were not affected by the RIPSP. If the peak spike count crossed the mean + (2) SD of background spike count, then the effect of RIPSPS on spike timing was considered statistically significant. Also if the decrease in the spike count at the peak of the RIPSP crossed the mean – (2) SD of background spike count, then the effect was considered statistically significant.

Firing Rate and RIPSP Timing

In each α-MN recorded, repetitive firing was induced by suprathreshold current injection through the glass micropipette. Recurrent inhibition was antidromically activated by electrical stimulation of the peripheral nerve(s) at 20 pps. This allowed random RIPSP occurrence during firing. A specific script was written in *spike II* computer program to selectively pick spikes based on their lag from the peripheral electrical shock i.e. their

timing in relation to RIPSP. Qualitatively, three effects in relation to the ISI were analyzed. First, In-Phase: ISIs where the RIPSP arrived early during the AHP. In this case, all electrical shocks occurred within 0 - 3 msec. before the spike allowing enough time for synaptic delay ≈ 2 msec., then, the following ISI was measured by subtracting the time of the spike from the time of the following spike (Figure 3.1).

Second, out-of-phase: ISIs in which the RIPSP arrived at a relatively later time during the ISI. In this case, all electrical shocks occurred within 8 msec. from the action potential spike and 5 msec. from the preceding spike (Figure 3.1). The time of all spikes that followed a stimulus artifact arriving within the defined period were printed and the ISI interval was calculated by subtracting the time of the preceding spike from the time of the actual spike picked by the program. Third, the rebound ISI was considered as the ISI that immediately followed the out-of-phase ISI (Figure 3.1). Finally, the mean firing rate for the two control trials surrounding the one with superimposed Renshaw inhibition was calculated and adopted as the mean control firing rate.

In addition, peristimulus frequencygrams (PSFs) which plot firing rate as a function of time from RIPSP onset were derived from the data and used to illustrate firing behavior in some cells.

Repetitive firing duration

In each α-MN, the total firing duration of trials with and without superimposed recurrent inhibition were calculated and compared. In 4 out of 11 α-MNs, simulated IPSPs were

injected into the α-MN directly via the glass micropipette and were triggered off the action potential spikes.

Figure 3.1.***Method used to label inter-spike-intervals***. The stimulus for in-phase RIPSP has to arrive within 3 msec. from the spike, the following ISI is picked as the modulated interval. The stimulus for out-of-phase RIPSP has to arrive within the out-of-phase ISI, 8 msec. and 5 msec. were taken as a safety margin. In one motoneuron the mean ISI was ≈ 13 msec. so in that particular cell, the 5 msec. margin was decreased to 3 and the 8 msec. margin was decreased to 6. Rebound ISI: immediately followed out-of-phase ISI.

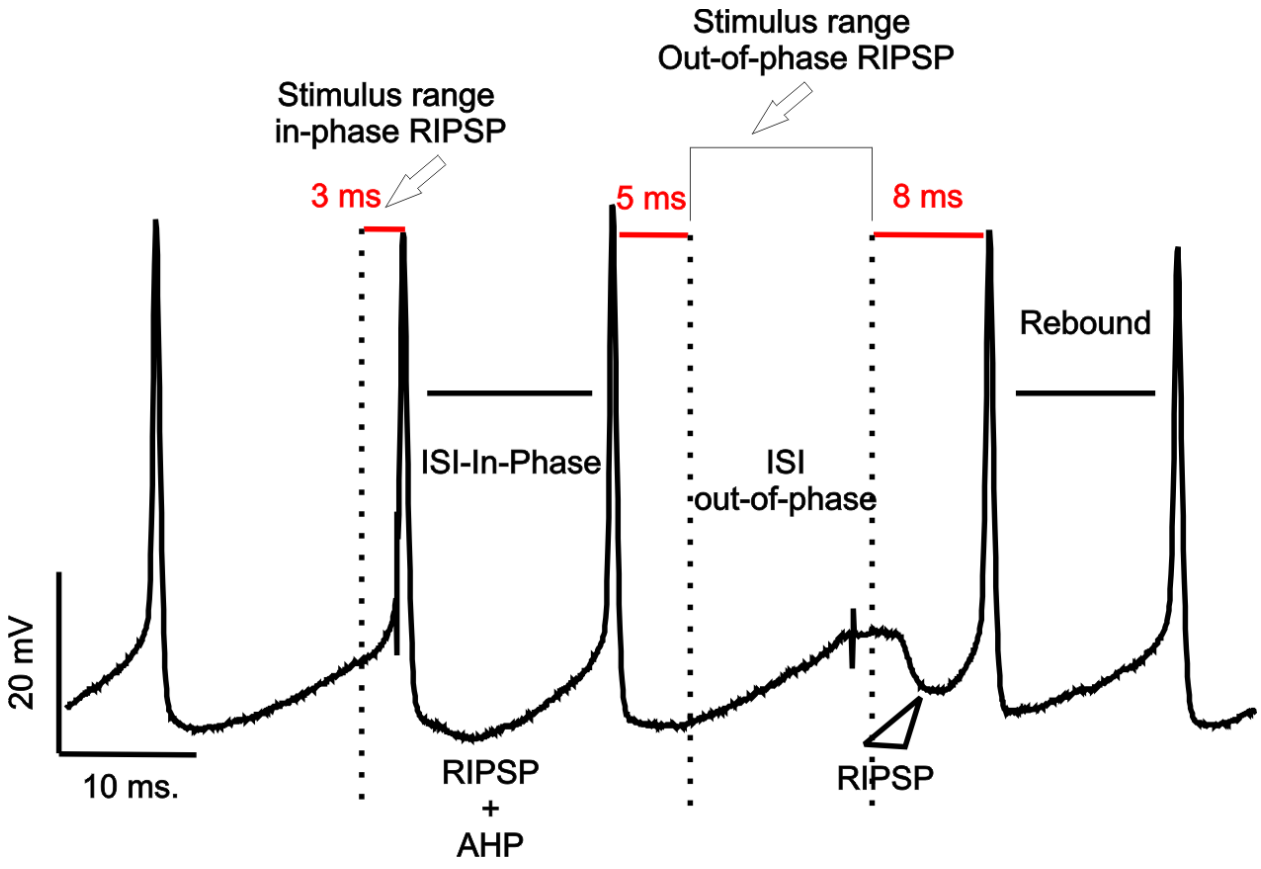
Stimulus range
Out-of-phase RIPSP
Stimulus range
in-phase RIPSP
3 ms
5 ms
8 ms
Rebound
ISI-In-Phase
ISI
out-of-phase
20 mV
10 ms.
RIPSP
+
AHP
RIPSP

Results

Renshaw inhibition augments the hyperpolarization caused by the AHP

The uncertainty raised by human studies showing no effect on firing rate when Renshaw inhibition arrived at the beginning of ISI led to the following simple experiment. Here, AHPs evoked by intracellular suprathreshold current injection, i.e. only the impaled motoneuron is firing, were compared in each motoneuron with AHPs that followed the antidromic spike, i.e. all motoneurons within the homonymous motor pool were active and supplying additional Renshaw inhibition (Figure 3.2). In each cell, both AHPs (electrically and antidromically evoked) were compared in amplitude (given that they were measured at the exact resting membrane potential). Results are presented in (Table 3.1). There was a 47% increase in the mean amplitude of the AHP that can only be contributed by the additional recurrent inhibition supplied by the other motoneurons in the same pool. Although some autogenic recurrent inhibition (from the same motoneuron) is expected in the electrical AHP, it is shown to be minimal Mean = 12.7 μV (Van Keulen 1981) and it is also present in the antidromic AHP records. Thus it won't minimize the absolute AHP difference measured in each cell. Moreover, faster rates for rise and decay were observed. Thus one can conclude that RIPSPs caused larger and faster hyperpolarization when co-operated with the AHP.

Figure 3.2**. *Electrically evoked versus antidromically evoked AHP*.** Panel (a) illustrates the method to record antidromically evoked AHPs, labeled blue in the lower panel. Panel (b) illustrates the method to record electrically evoked AHP, labeled black in the lower panel.

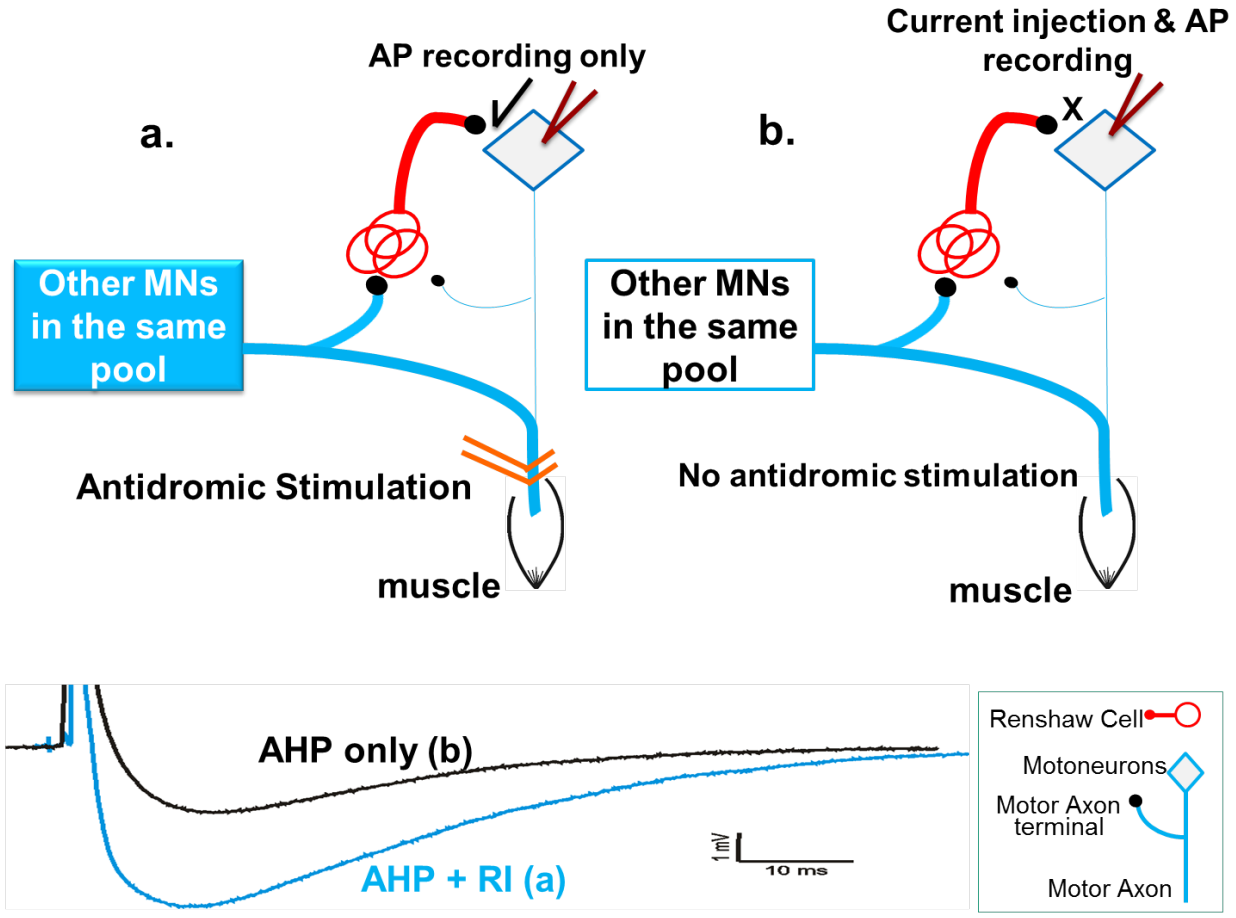
a.
AP recording only
Other MNs in the same pool
Antidromic Stimulation
muscle
b.
Current injection & AP recording
X
Other MNs in the same pool
No antidromic stimulation
muscle
AHP only (b)
AHP + RI (a)
1mV
10 ms
Renshaw Cell
Motoneurons
Motor Axon terminal
Motor Axon

Table 3.1**.** ***Electrical and antidromic AHPs show different amplitudes and kinetics*****.** Antidromically evoked AHPs were significantly larger and faster (In each case, electrically evoked AHPs served as an internal control for antidromically evoked AHPs). AHP maximal amplitude, rate of rise, and rate of half decay were all significantly different between the two groups. Independent Student t- test was used. In each cell, resting Vm was the same for both cases. Data were compiled from 65 motoneurons.

	Antidromic AHP **Mean ± SD**	**Electrical AHP** **Mean ± SD**	***P value***
Peak Amplitude **(mV)**	2.2 ± 1.5	1.5 ± 1.1	< 0.007
Resting Vm **(mV)**	-62 ± 8	-62 ± 8	1
Rate of Rise **(mV/ms)**	0.4 ± 0.22	0.26 ± 0.15	< 0.0001
Rate of half decay **(mV/ms)**	0.072 ± 0.04	0.052 ± 0.028	< 0.002

Renshaw inhibition in relation to spike timing during repetitive firing

Here, RIPSPs were antidromically evoked at 20 Hz during repetitive firing of α-MNs. This caused random arrival of the RIPSP during the ISI, see also methods used in (Kudina and Pantseva 1988). Figure 3.1 displays different timings of arrival of RIPSPs in relation to the ISI.

As can be seen in (Figures 3.3 and 3.4), Renshaw inhibition affected action potential spike timing depending on the time of arrival with respect to the ISI. Figure 3.4 shows two consecutive repetitive firing trials in the same motoneuron and under similar conditions except that in the second trial, Renshaw inhibition was antidromically activated at 20 Hz. The effect of the RIPSP on the firing train was robust. Firing frequency variance increased despite undetectable change in the mean discharge rate. This increased the amount of noise in the system and resulted in a distinct firing rhythm, see discussion. The operating RIPSP at the end of the firing trial and under the same level of depolarization was averaged and is shown below the firing train. Similar firing rhythm was seen in another α-MN (Figure 3.4). Here, an interesting change in the firing rhythm was observed as the motoneuron firing rate was decreasing. Interestingly, as the firing rate approached one multiplication of 20, “a transformation” in the firing rhythm was observed (at 80 and 60 Hz). This novel observation suggests that Renshaw inhibition has the potential to shape α-MN firing. In fact, phase-locking to RIPSPs was demonstrated in all 11 motoneurons recorded from the 9 rats included in this study. Post stimulus time

histograms (PSTHs) for spike counts were calculated for repetitive firing trials that were assumed to be modulated by Renshaw inhibition. Several examples are shown below and one control PSTH is also shown for comparison (Figures 3.5 and 3.6). Phase-locking of α-MN firing to Renshaw cell inhibition is shown (Figure 3.5). In panel a, the histogram shows a clear structure in comparison with panel b which was obtained from a control trial in the same α-MN, i.e. without Renshaw inhibition. The latter showed low variability in the spike discharge rates. The measurements used to measure the effect of RIPSP on spike timing are shown in (Figure 3.5a). First, the mean background firing rate was calculated, bin size = 1 millisecond (Cope, Fetz et al. 1987). One line (black) was drawn to represent the mean spike count for background firing. Then, two other lines (red) were drawn to represent 2 standard deviations from the mean. The peak firing was considered significant only if it crossed the mean + 2SD. The gap or the decrease in firing probability caused by the RIPSP was considered significant only if it fell below the lower red line, i.e. crossed the mean - 2SD. In all motoneurons, both effects were statistically significant.

To further quantify the effects, spike count index, K (Sears and Stagg 1976) was calculated for each PSTH. K represents the strength of phase-locking. It represents the ratio of the peak counts in the histogram to the mean counts in a region away from the area of interest (not affected by the RIPSP). Interestingly, K value significantly correlated with the RIPSP peak amplitude (Figure 3.7), $R^2=0.69$, $P<0.05$.

The appearance of a secondary (or rarely a tertiary) peak in the PSTHs was observed frequently in our data set. This is in agreement with PSTHs derived from human subjects where a secondary excitation was frequently observed and still there exist no consensus on its origin (Kudina and Pantseva 1988; Miles, Le et al. 1989; Mattei, Schmied et al. 2003). Figure 3.8 shows one example of a PSTH with a sharp secondary peak. Two action potential spikes taken from the same firing train were superimposed on the PSTH to illustrate the mechanism responsible for the secondary peak. The first peak corresponded to higher probability of firing during the decay of the IPSP as described in (Fetz and Gustafsson 1983). One novel finding here is the mechanism responsible for the secondary peak. Interestingly, rebound spikes exactly matched the timing of the secondary peak and were held responsible for its appearance (Figure 3.8). So, the RIPSP (latency = 3 msec.) was directly responsible for spike accumulation in first peak and indirectly responsible for the second peak.

Finally, in 3 out of the 11 α-MNs included in this study, we observed a period of spike discharge that exactly matched the frequency of RIPSP stimulation, i.e. 20Hz. Indicated by a red Circle in (Figure 3.9a). This was not due to contamination with antidromic spikes since the peripheral stimulus was either heteronymous or submaximal homonymous. Interestingly, each RIPSP was followed by an action potential spike, see (Figure 3.9b). In the PSTH calculated for those spikes, perfect phase-locking can be observed (Figure 3.9c). The PSTH showed a primary peak and very minimal, if any, background firing. Analysis of all motoneurons showing this behavior revealed that

Renshaw inhibition was driving the motoneuron to fire instead of turning it off as one would assume. This behavior is quite interesting given the existing notion that Renshaw inhibition can silence α-MN firing.

Renshaw cell and motoneuron discharge rate

In nine motoneurons, the discharge rates with and without superimposed Renshaw inhibition were measured. Renshaw inhibition was antidromically activated at 20Hz. The mean firing rate was not slower than the mean control discharge (Figure 3.10). In fact, it was frequently faster. Further analysis of each trial with Renshaw inhibition was done based on the timing of the RIPSP in relation to the ISI (Figure 3.1). If the RIPSP arrived early during the ISI, i.e. aligned with AHP, then it was referred to as in-phase. This was important to reproduce the human work described above where early arriving inhibitory volley was shown to have minimal effects on motor units firing rate (Kudina and Pantseva 1988). On the other hand, if the RIPSP arrived late during the ISI, then it was referred to as out-of-phase. This was always followed by rebound increase in firing that was also quantified in each cell. In general, in-phase RIPSPs (Figure 3.10) tended to either increase the discharge rate (if the RIPSP was large enough) or to produce no change (if RIPSP was relatively small or control firing rate was already high). Out-of-Phase RIPSPs (Figure 3.10) tended to decrease firing rates or in some motoneurons tended to produce no change (if the RIPSP was relatively small) or rarely produced a modest increase. Rebound firing (Figure 3.10) produced the most consistent results where

it increased firing almost in every α-MN. When out-of-phase and rebound firing were averaged and plotted against the control discharge rate, an interesting trend for higher rates was seen. This was consistent with the observation that the mean firing rate for most trials with Renshaw inhibition was faster than controls. So, the main finding here was that Renshaw inhibition failed to decrease α-MN discharge rate but also tended to increase α-MN firing rates.

Subsequently, the effect on instantaneous firing rate was further quantified by compiling a peristimulus frequencygram (PSF), which plots firing rate as a function of time from RISPS onset. Figure 3.11a and 3.11b show two PSFs obtained from two α-MNs. Here, recurrent inhibition clearly resulted in two opposite effects, a decrease that was immediately followed by a rebound increase in rate. This dual effect was consistently seen across cells but varied in magnitude. Figure 3.12 shows an example where the RIPSP actually increased α-MN firing rate, in general, and when aligned with AHP. The RIPSP in Figure 3.12 had maximum amplitude of 6.8 mV. This was the largest RIPSP recorded in the current thesis work and had a strong counterintuitive effect on α-MN firing rate, especially when arrived early during the ISI (in-phase).

Figure 3.3. ***Renshaw inhibition caused splitting in the motoneuron discharge pattern.*** An illustration of two consecutive repetitive firing trials in the same motoneuron. The same amount of current (16 nA) was injected in both trials. The same Vm (-57 mV) was measured in both trials. The only difference was the presence or absence of Renshaw inhibition. Mean firing rate was similar regardless of the added inhibition to the 2nd trial. The operating RIPSP is shown on a different scale. RIPSP increased the firing rate variance and resulted in a distinct dual splitting in firing rate (out of phase and rebound)

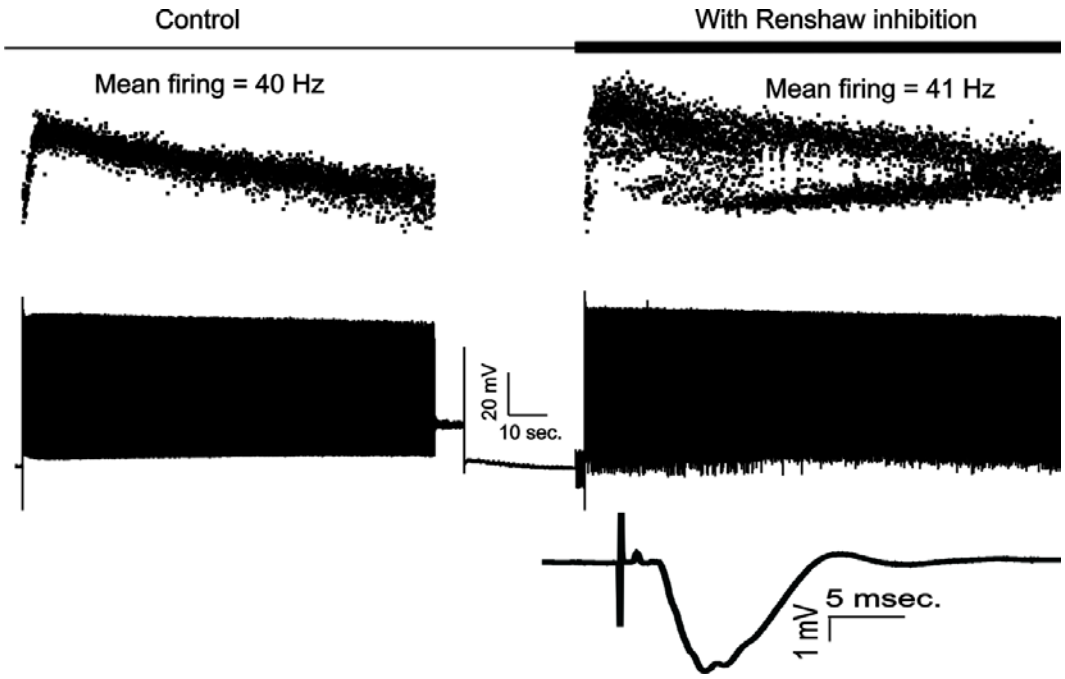
Control
With Renshaw inhibition
Mean firing = 40 Hz
Mean firing = 41 Hz
20 mV
10 sec.
1 mV
5 msec.

Figure 3.4. ***The double bubble phenomenon*.** In 4 out of 11 α-MNs, this kind of firing behavior was observed when Renshaw inhibition was activated during motoneuron repetitive firing. Here, the motoneuron discharge rate was decreasing from around 85 Hz to 57 Hz (SFA). During the deceleration of the discharge rate, a transformation of the effect of the RIPSP was seen. At multiples of 20 (red and blue arrows), the discharge pattern changed from a bubble like (splitting into three distinct spike groups: control, out-of-phase and rebound) into a less distinct pattern.

Injected current 20nA, mean firing rate = 71 Hz. The operating RIPSP is shown on a different scale below.

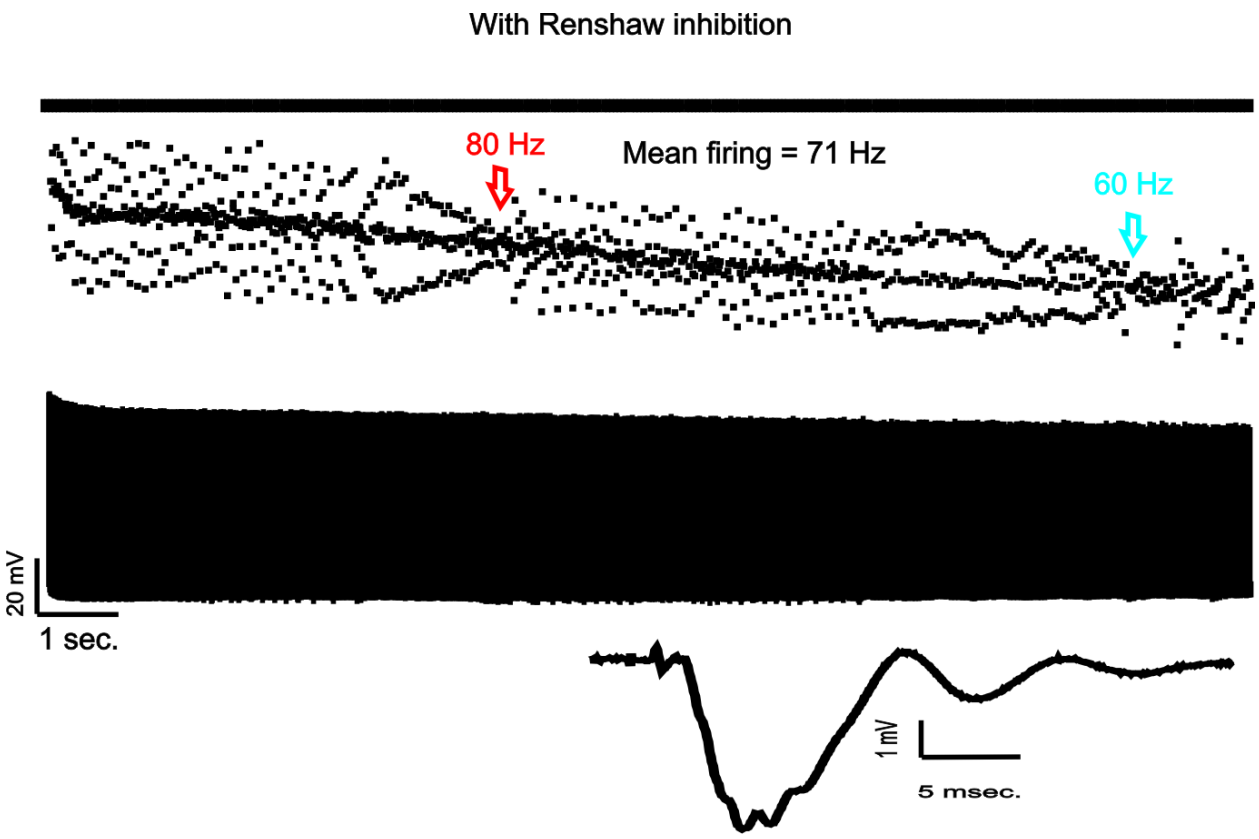
With Renshaw inhibition
80 Hz
Mean firing = 71 Hz
60 Hz
20 mV
1 sec.
1 mV
5 msec.

Figure 3.5***. Post stimulus time histograms for control and modulated firing trials.***

Two PSTHs obtained from a ABSM motoneuron during repetitive firing. Abscissa: time in milliseconds from the electrical stimulus applied to the peripheral nerve (50 msec. long). Ordinate: spike count, bin size = 1 msec. In this PSTH (a) and all subsequent PSTHs, the mean background spike count was calculated (mean value is shown as a black dotted line). Two standard deviations were calculated in both directions from the mean (red dotted lines). The peak spike count was considered statistically significant if it crossed the upper red line. And the drop in firing probability was considered significant if it crossed the lower red line. Panel (b) shows the lack of structure in a PSTH obtained from the same motoneuron but without the activation of Renshaw inhibition. In this PSTH and all subsequent ones, spike count index (K) was calculated by taking the ratio of the peak spike count and the mean background spike count. K = 5.5 for this PSTH and the change in both the peak count and the drop in firing probability were >2SD of the mean background firing probability.

a

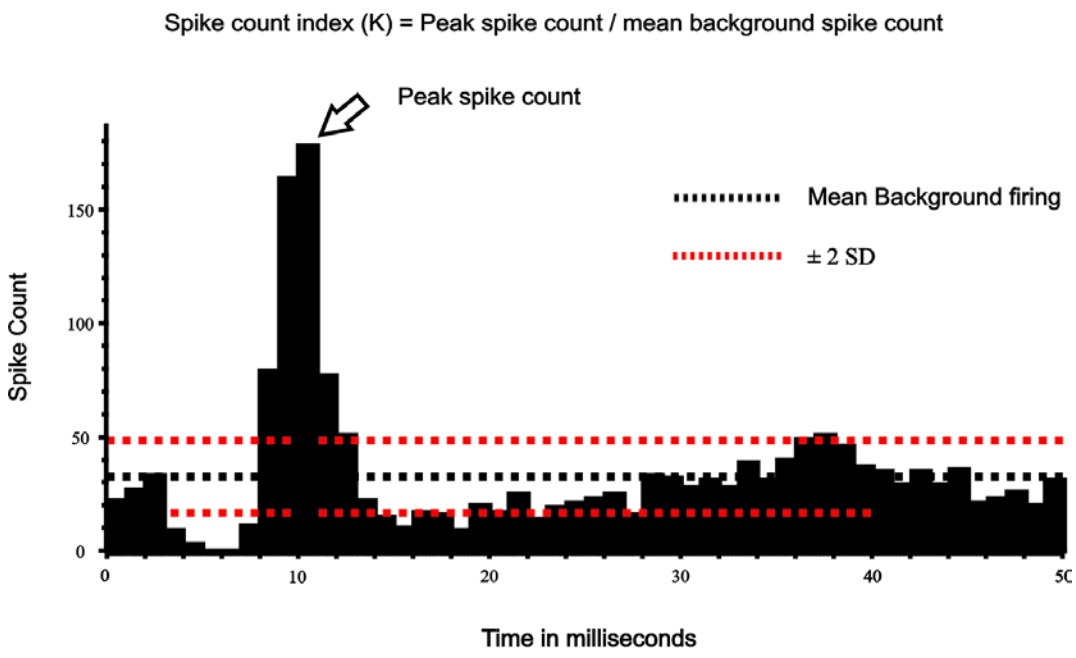
Spike count index (K) = Peak spike count / mean background spike count
Peak spike count
Mean Background firing
± 2 SD
Spike Count
150
100
50
0
0
10
20
30
40
Time in milliseconds

b

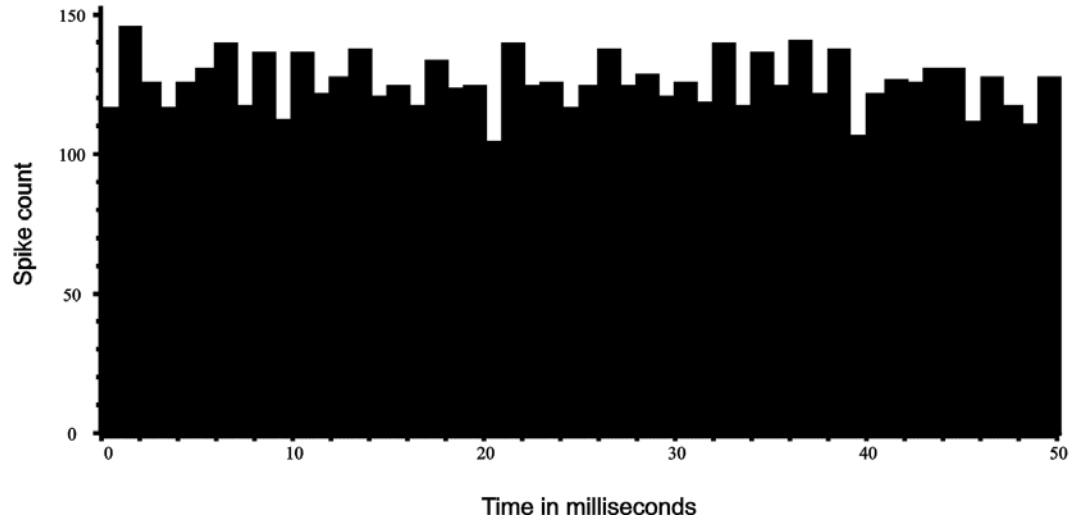
Spike count
150
100
50
0
0
10
20
30
40
50
Time in milliseconds

Figure 3.6***. Several examples of PSTHs shaped by Renshaw inhibition.*** Panels (a) and (b) show PSTHs with higher value for K while (c) and (d) show smaller K value. This was because in the former, the operating RIPSPs, had larger maximal amplitudes than those operating in (c) and (d). In all the increase in firing probability (the peak) and the decrease in firing probability (the gap) crossed the lines for 2 SD. Thus were significant.

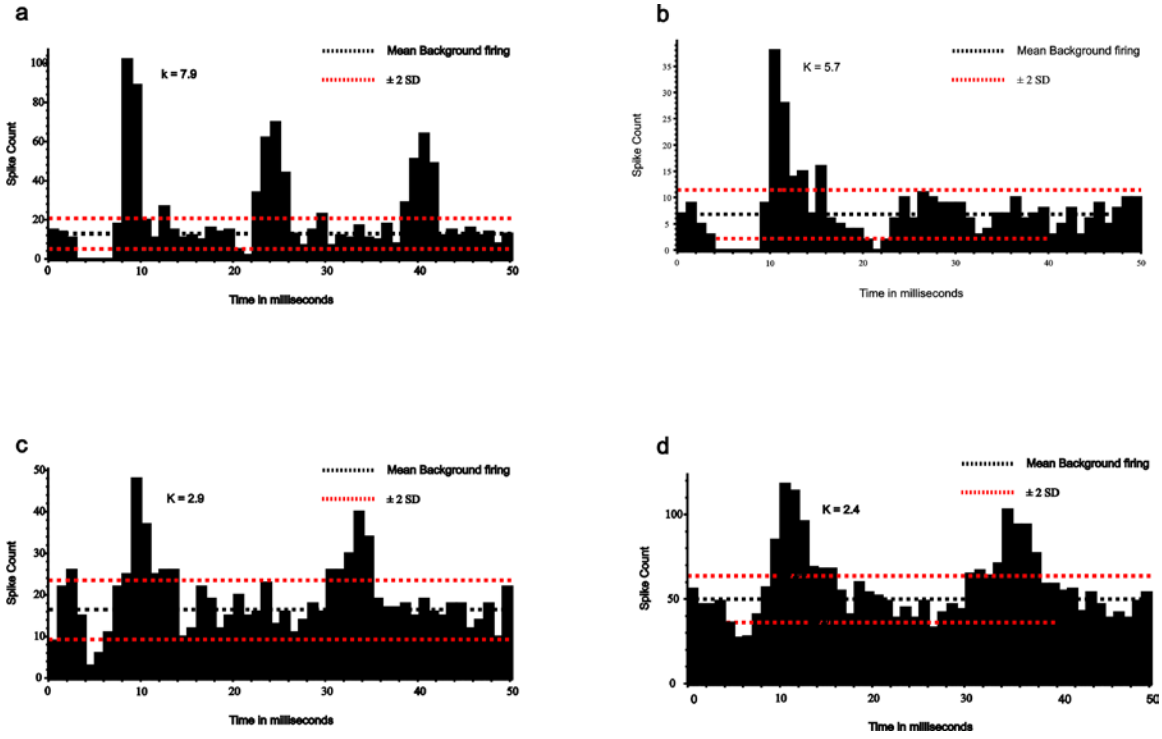
a
Mean Background firing
± 2 SD
k = 7.9
Spike Count
Time in milliseconds
b
Mean Background firing
± 2 SD
K = 5.7
Spike Count
Time in milliseconds
c
Mean Background firing
± 2 SD
K = 2.9
Spike Count
Time in milliseconds
d
Mean Background firing
± 2 SD
K = 2.4
Spike Count
Time in milliseconds

Figure 3.7**. *Spike count index correlates with RIPSP amplitude.***A significant correlation between the maximum amplitude of the operating RIPSP and the K value was detected. RIPSP amplitude measured in mV, data shown for all 11 cells recorded.

Mean for K, 4.3 ± 2.45 (range: 1.96 – 9.2).

Mean for RIPSP amplitude, 2.77 ± 2 mV (range: 0.45 – 6.8)

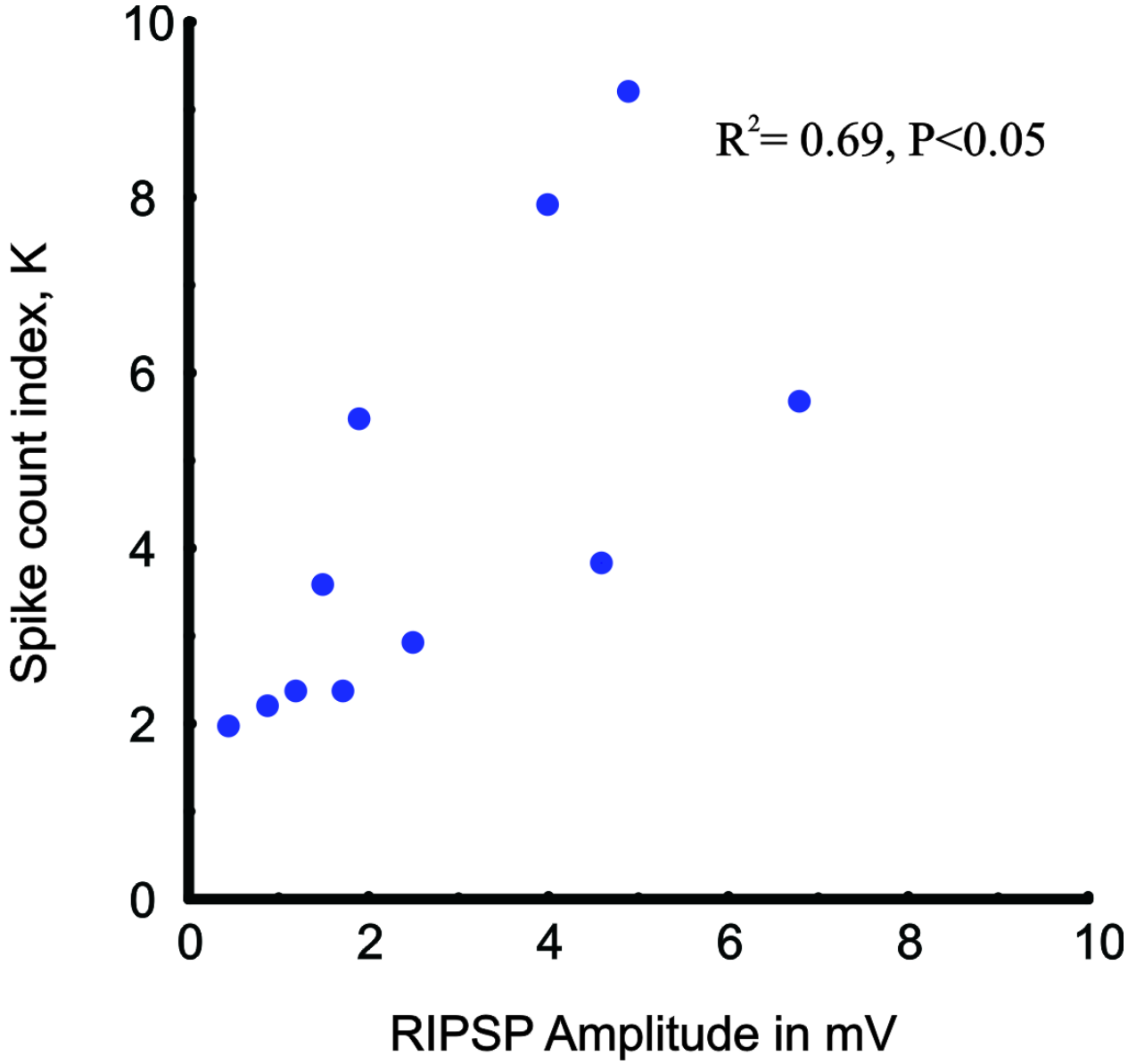
10
8
6
4
2
0
0
2
4
6
8
10
Spike count index, K
RIPSP Amplitude in mV
R^2= 0.69, P<0.05

Figure 3.8***. The secondary peak is due to rebound firing*.** One PSTH calculated from an MG motoneuron. Two distinct peaks appeared in this PSTH. The first was due to accumulation of spikes at the decay of the RIPSP, see superimposed firing trace. The gap in firing is due to the hyperpolarization caused by the peak of the RIPSP (amplified below for details). The second peak was proved to be the result of the rebound firing as defined in this thesis (Figure 3.2). Perfect alignment is seen for action potential derived from the same firing trial from which the PSTH was calculated. Time scale for the PSTH, the action potential train, and the RIPSP was the same.

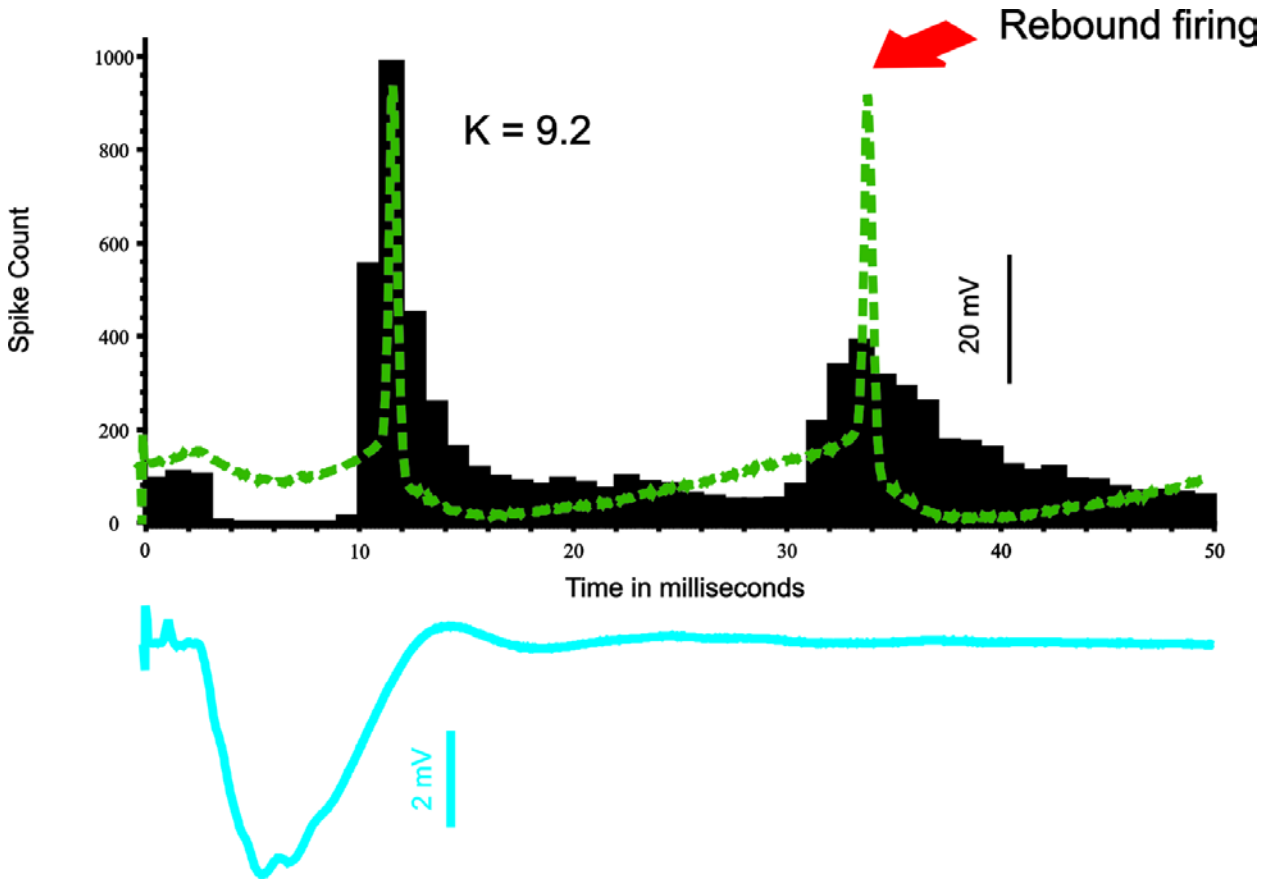
Rebound firing
K = 9.2
Spike Count
1000
800
600
400
200
0
0
10
20
30
40
50
Time in milliseconds
20 mV
2 mV

Figure 3.9**. *Renshaw inhibition can help to maintain firing in the motoneuron***. Here, the discharge rate of the motoneuron decreased over time (220 seconds), instead of complete cessation of firing, the circled area in the instantaneous firing channel appeared. Firing was exactly at 20 Hz, 16 nA current was still on. A small area of the spike train is enlarged in (b), every RIPSP is followed by AP spike, i.e. motoneuron firing was driven by the RIPSPs. (c) Shows PSTH for the circled area, K value was very high because background count was minimal, i.e. almost perfect phase-locking.

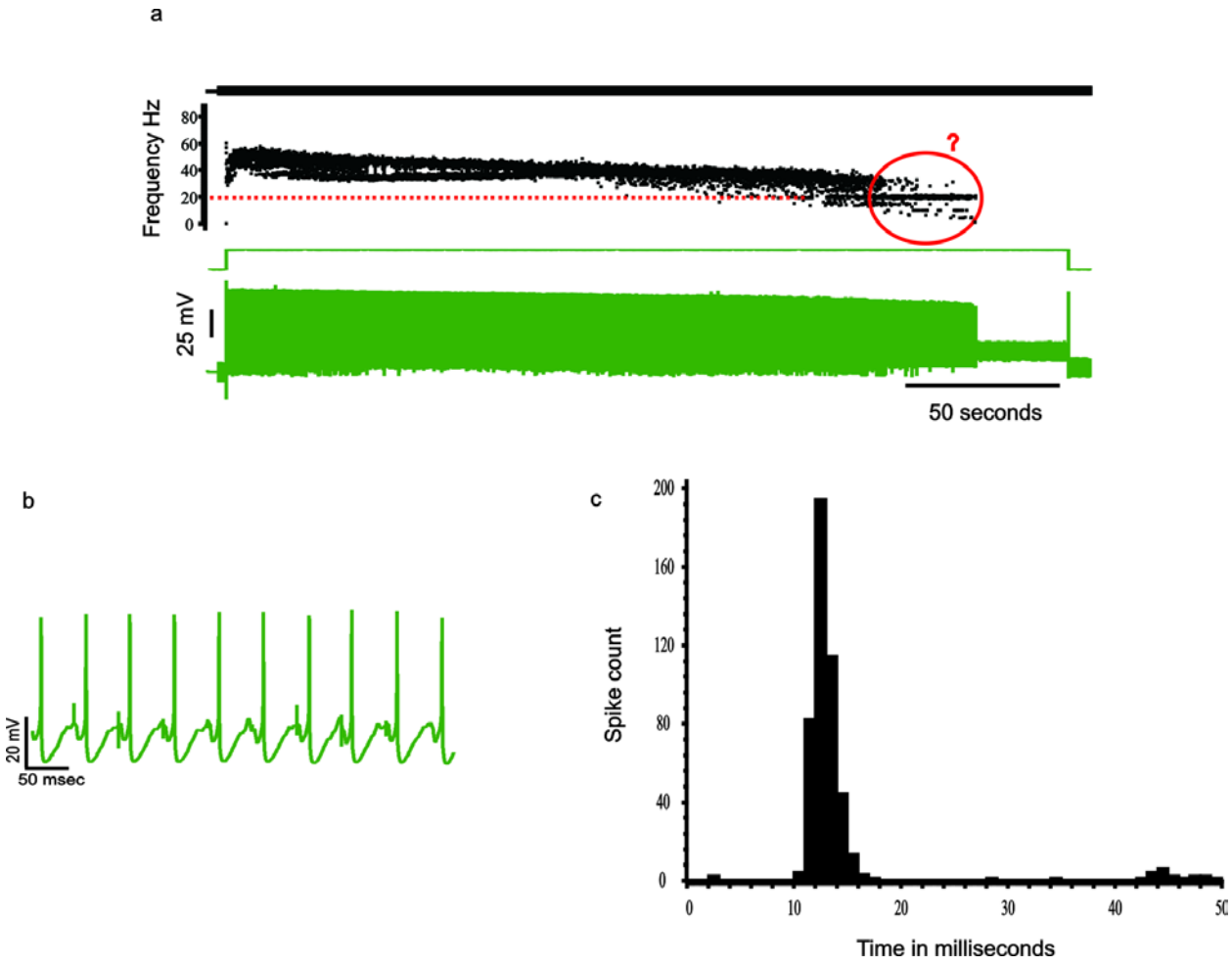
a
Frequency Hz
80
60
40
20
0
?
25 mV
50 seconds
b
20 mV
50 msec
c
Spike count
200
160
120
80
40
0
0
10
20
30
40
Time in milliseconds

Figure 3.10. ***The effect of Renshaw inhibition on motoneuron discharge rate.*** Here the modulation of firing rate caused by Renshaw inhibition is quantified from nine motoneurons. Each motoneuron is labeled by a unique symbol. Abscissa: Control firing rate; Ordinate: modulated firing rate. Firing rate was measure in Hz or impulse per second.

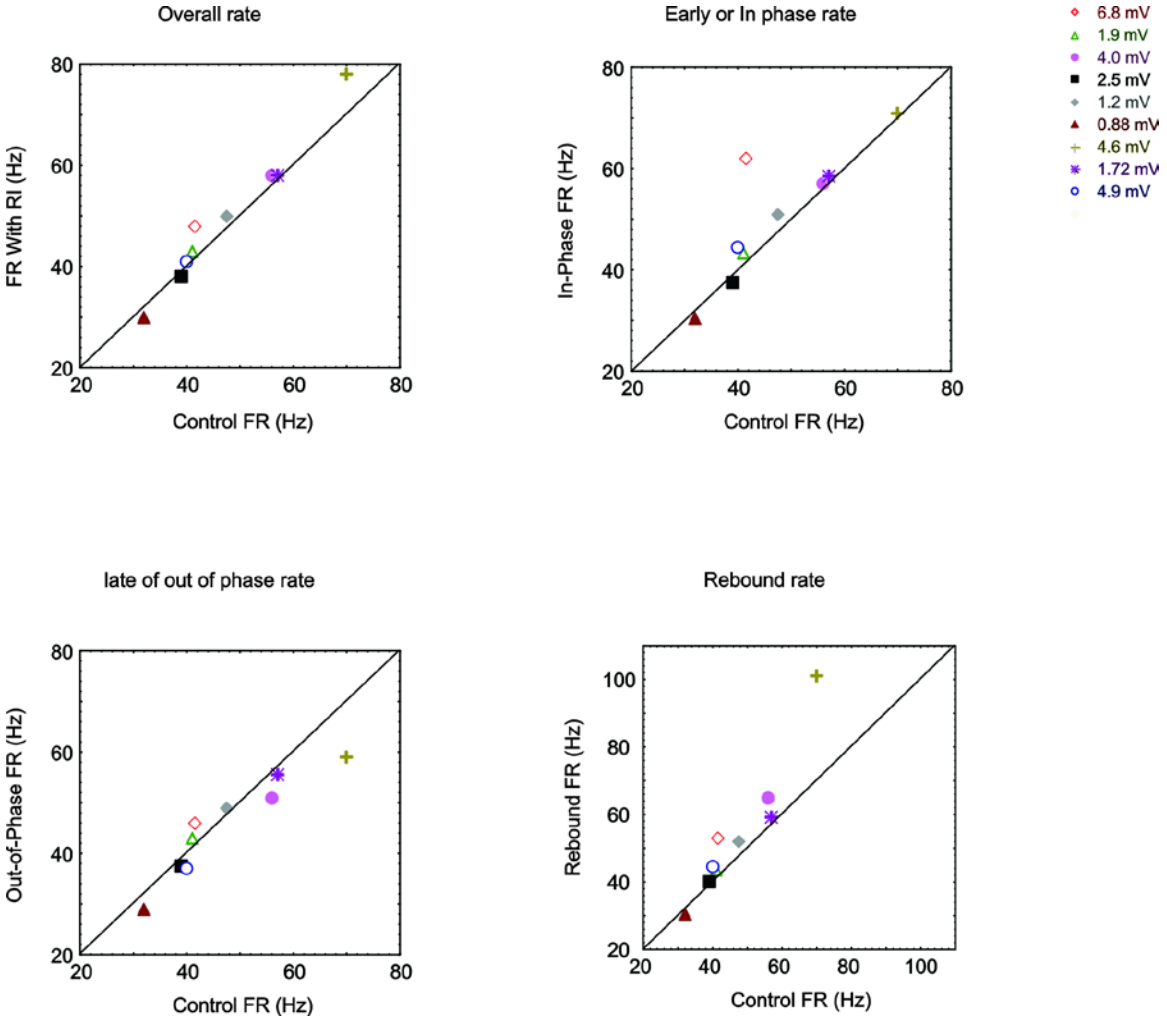
Overall rate
FR With RI (Hz)
Control FR (Hz)
Early or In phase rate
In-Phase FR (Hz)
Control FR (Hz)
6.8 mV
1.9 mV
4.0 mV
2.5 mV
1.2 mV
0.88 mV
4.6 mV
1.72 mV
4.9 mV
late of out of phase rate
Out-of-Phase FR (Hz)
Control FR (Hz)
Rebound rate
Rebound FR (Hz)
Control FR (Hz)

Figure 3.11**. *Distinct clustering for action potential spikes.*** Post stimulus frequency-grams were obtained from all motoneurons. Here two representative examples obtained from the same motoneuron in trials with different discharge rates are shown. A clear distinction between out-of-phase (red circle) and rebound firing (blue circle) is seen. Rebound spikes immediately compensated and in some cases over-compensated for the decrease in firing rate caused by the arrival of the RIPSP late in the ISI. Abscissa: Lag in milliseconds from the time of the peripheral electrical shock to the peripheral nerve (time 0). Ordinate: firing frequency in Hz.

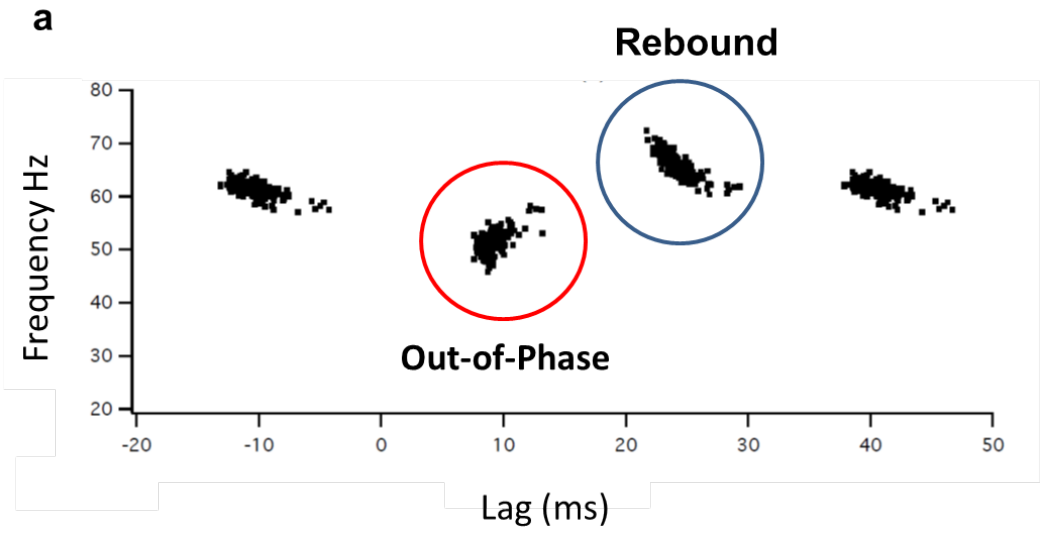
a
Rebound
Out-of-Phase
Frequency Hz
Lag (ms)
80
70
60
50
40
30
20
-20
-10
0
10
20
30
40
50

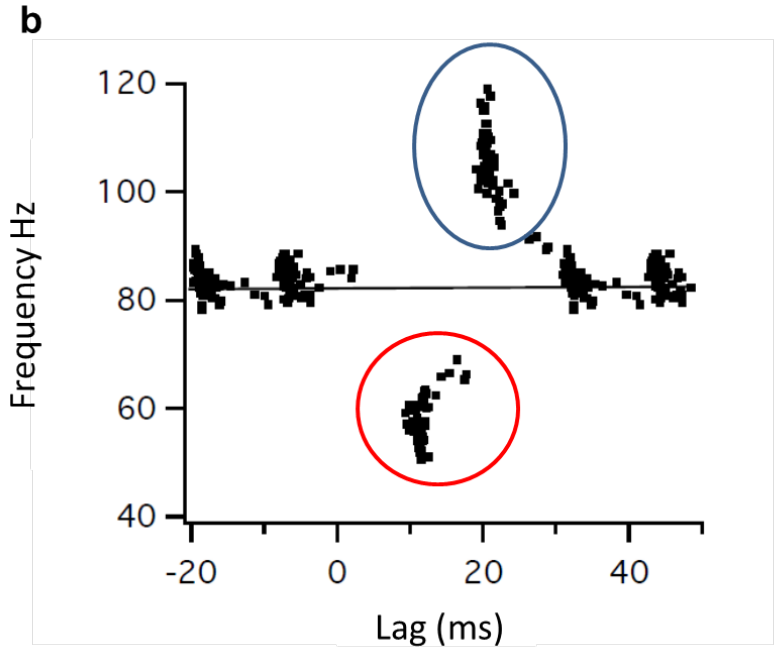
b
Frequency Hz
Lag (ms)
120
100
80
60
40
-20
0
20
40

Figure 3.12***. Renshaw inhibition can increase motoneuron discharge rate.*** One ABSM motoneuron (Rheo = 9, RIPSP = 6.8 mV). Here, the RIPSP actually increased firing rate. (a) Illustration of a repetitive firing train with superimposed Renshaw inhibition. (b) One enlarged area showing the interaction between RIPSPs and ISIs. Blue arrow: In-Phase effect (here significantly shortened the ISI), red arrows: Out-of-Phase (here significantly increased the ISI), green arrows: rebound (strongly compensated by causing the next ISI to become shorter). (c) Enlarged areas from red boxes in (a) showing the consistent effect of the RIPSP in-phase modulation regardless of whether taken at the beginning or later in the repetitive firing train. (d) Enlarged AHPs, one from control (black) and one with superimposed RIPSP (blue). In-Phase interaction resulted in a larger and a faster hyperpolarization.

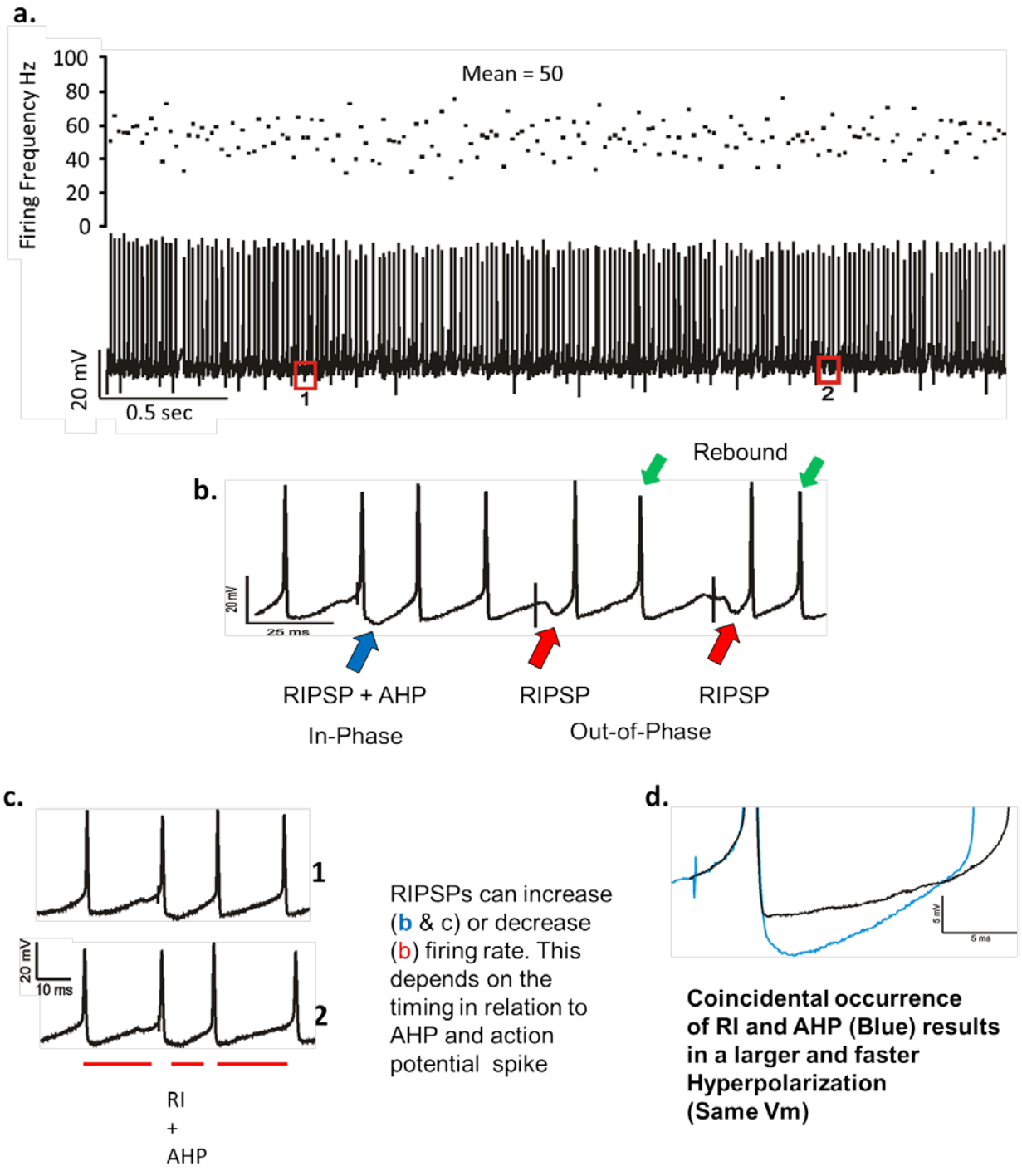
a.
Firing Frequency Hz
100
80
60
40
20
0
Mean = 50
20 mV
0.5 sec
1
2
b.
Rebound
20 mV
25 ms
RIPSP + AHP
In-Phase
RIPSP
RIPSP
Out-of-Phase
c.
1
20 mV
10 ms
2
RI
+
AHP
RIPSPs can increase (b & c) or decrease (b) firing rate. This depends on the timing in relation to AHP and action potential spike
d.
5 mV
5 ms
Coincidental occurrence of RI and AHP (Blue) results in a larger and faster Hyperpolarization (Same Vm)

Renshaw inhibition and spike frequency adaptation

In 5 out of 11 motoneurons, the RIPSP size was > 3 mV. In those, the repetitive firing train modulated by Renshaw inhibition lasted longer than surrounding control trials, i.e. Renshaw inhibition seemed to delay spike frequency adaptation (SFA). Figure 3.13 shows one example where one RIPSP evoked in MG motoneuron via supra-maximal electrical stimulation of the LGS nerve, effectively delayed SFA.

Next, and in order to control IPSP amplitude and timing (mostly in-phase was desired because of direct relation to human experiments), simulated IPSPs (see Chapter 4 for more details) were triggered off the action potential spikes and were inserted at the beginning of the ISI, i.e. aligned with AHP in four α-MNs. Figure 3.14 shows the effect of simulated IPSPs in each of the four α-MNs.

Figure 3.13***. Naturally evoked RIPSPs delay spike frequency adaptation.*** MG motoneuron (Rheobase = 6). Renshaw inhibition activated at 20 Hz. Repetitive firing lasted for 106, 241, and 135 seconds for trials 1, 2, and 3 respectively. So, more than 100 seconds of firing were added due to superimposed RIPSPs in trial 2.

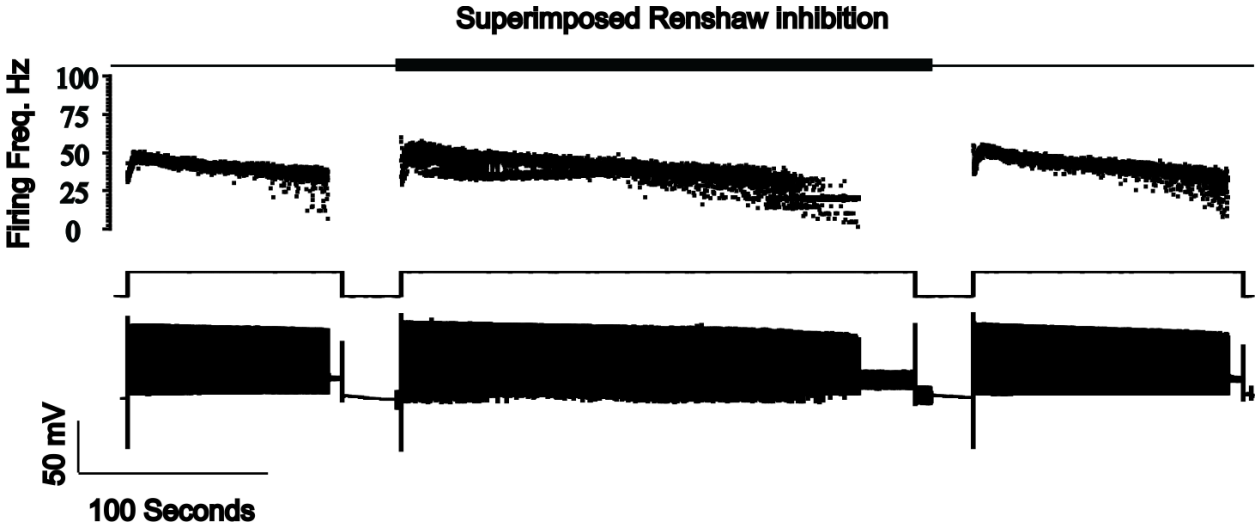
Superimposed Renshaw inhibition
Firing Freq. Hz
100
75
50
25
0
50 mV
100 Seconds

Figure 3.14***. Simulated IPSPs delay spike frequency adaptation.*** Red arrows: Trials with superimposed simulated IPSPs. SFA was fully reversed or delayed in all four motoneurons. In motoneuron (1) the mean control firing duration was 6 ± 1.7 seconds before and 24 ± 2 seconds after adding simulated IPSPs (data shown here for this motoneuron are for 2-second trials only). In motoneuron (2), 16 ± 8 seconds before and 105 ± 10 seconds after. In motoneuron (3), 36.5 ± 13 seconds before and 56 ± 4 seconds after. In motoneuron (4), 10.5 ± 5 seconds before and 44 ± 22 seconds after. All means were calculated from at least two trials in each category and in each motoneuron.

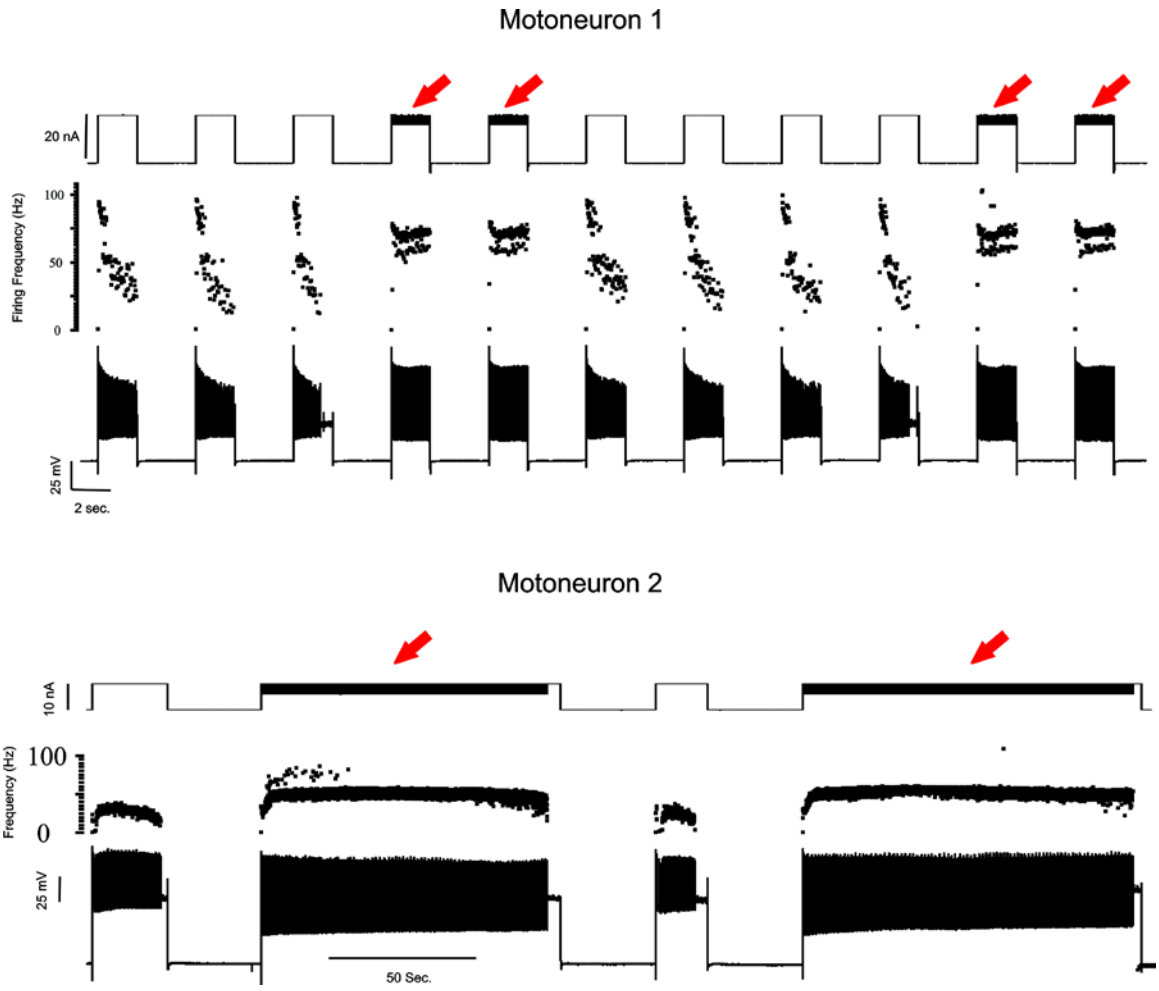
Motoneuron 1
20 nA
Firing Frequency (Hz)
100
50
0
25 mV
2 sec.
Motoneuron 2
10 nA
Frequency (Hz)
100
0
25 mV
50 Sec.

Figure 3.14***. Continued.***

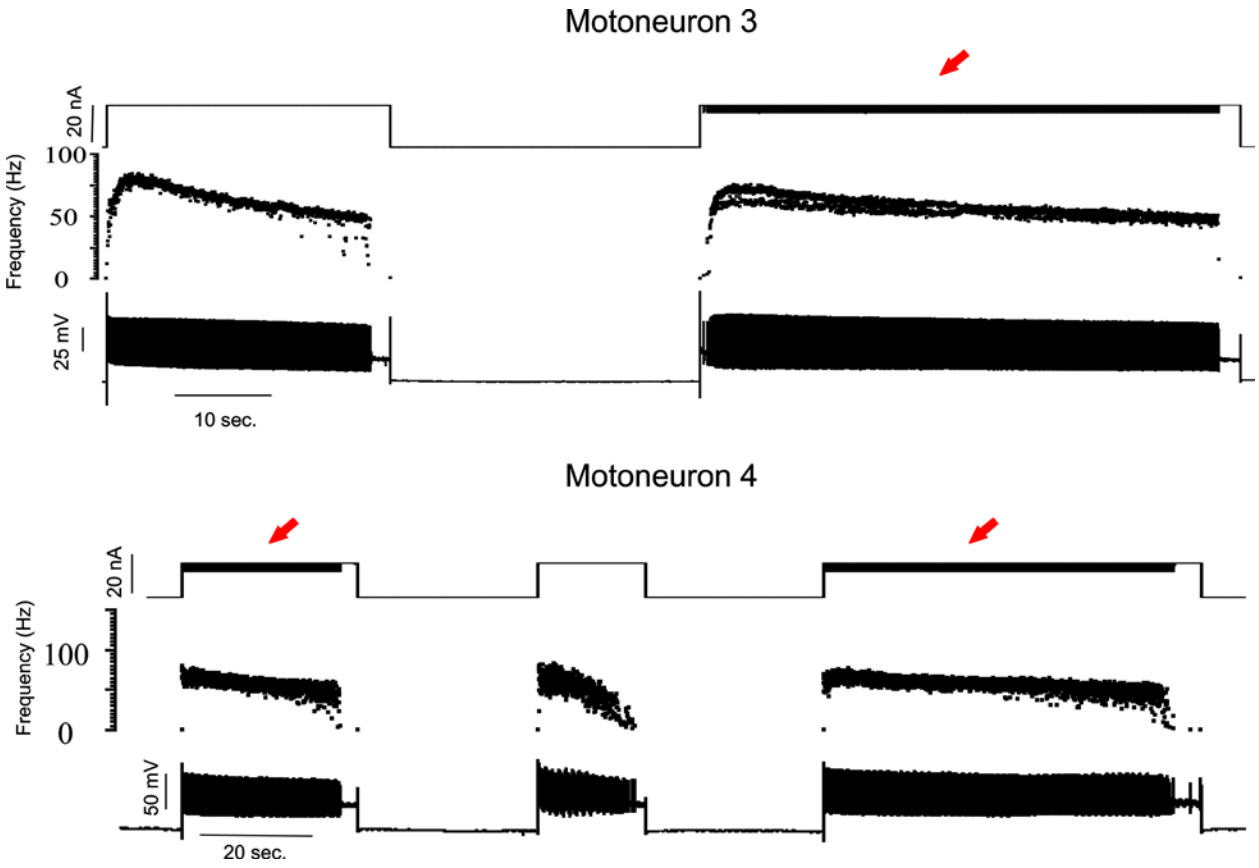

Discussion

The current study employed the technique of *in vivo* intracellular recording to examine the effect(s) of Renshaw inhibition on the modulation of motoneuron firing behavior. The use of the word behavior instead of rate came from the assumption that Renshaw inhibition might have several impacts on motoneuron firing. This assumption was based on the unique structure of this circuit (Figures 1.1 and 1.2). The notion that Renshaw inhibition affects the motoneuron every time it fires, of course unless suppressed by descending inputs, led to three main hypotheses about possible interactions, each is discussed below.

Renshaw inhibition can affect spike timing

Although it was described for many other inhibitory circuits in the nervous system (Cerebellum, auditory cortex, hippocampus, and olfactory bulb), the effect of Renshaw inhibition on motoneuron spike timing was not examined in detail before. Few reports are available and most are accompanied with some degree of uncertainty and opposing views (Kudina and Pantseva 1988; Miles, Le et al. 1989; Davey, Ellaway et al. 1993; Mattei, Schmied et al. 2003; Uchiyama and Windhorst 2007)

The current work performed in the adult rat demonstrated that Renshaw inhibition can indeed affect spike timing. In fact, the magnitude of the effect was so robust that in every single α-MN tested and even when the RIPSP was relatively small, the effect was significant (n = 11). This consistent effect designates a novel function for recurrent

inhibition, i.e. shaping the rhythm of firing. The motoneuron or better called “The final common pathway to movement” is known to possess exceptional abilities that allow for repetitive firing responses to constant or changing inputs, reviewed in (Brownstone 2006). In fact, one would like to think of movement as an expression of repetitive firing or as referred to by John Fulton as an expression of prolonged tetani (P. 149 in Fulton 1926). If we look at the motor behavior in general, one would perceive the great level of complexity and efficiency. This cannot be accounted for by simple trains of unwavering action potentials. Instead, one might look at repetitive firing as a malleable property, and to some degree might resemble the musical notes which move along the lines to produce meaningful and enjoyable sounds.

Our novel illustration of rhythmic firing behaviors in the α-MN when challenged with Renshaw inhibition might indicate that the latter is one member of a team of synaptic inputs that work together to shape the rhythmic output of the final common pathway (Figures 3.3 and 3.4) and might provide some explanation for the observations in human motor units (Davey, Ellaway et al. 1993). In addition, this thesis provided solid evidence that the secondary peak observed in many PSTHs (Figure 3.8) was indeed due to the rebound firing produced by recurrent inhibition and was not due to a peripheral, cutaneous or tendon organ, or supraspinal descending input (Kudina and Pantseva 1988; Miles, Le et al. 1989; Uchiyama and Windhorst 2007) or recurrent facilitation (Mattei, Schmied et al. 2003). The electrophysiological interaction between Renshaw inhibition and spike timing in the adult rat was in great and surprising accord with results obtained

from intact live humans. This similarity is of great importance for advancing the field of recurrent inhibition. First, the great similarity in obtained PSTHs confirmed the validity of the method used to study recurrent inhibition in human subjects (Kudina and Pantseva 1988; Miles, Le et al. 1989; Mattei, Schmied et al. 2003). Second, the current work provided solid interpretation for a long-lasting debate regarding the secondary peak observed in PSTHs obtained from human subjects. Third, in contrast to the work of Mattei and colleagues who measured the interaction between Renshaw inhibition and motoneuron firing in a deafferented patient (Mattei, Schmied et al. 2003), the current work detected a significant correlation between the amplitude of the inhibition and the phase-locking or the strength of effect on spike timing (K) (Figure 3.7). Finally, in contrast to the current notion that Renshaw inhibition might increase the failure of α-MN recruitment during the H-reflex studies in humans (Katz and Pierrot-Deseilligny 1998), RIPSPs in our work were able to actually drive firing in some α-MNs (Figure 3.9). This might suggest an opposite role of rather aiding in α-MN recruitment which might serve as a subject for future investigations.

Renshaw inhibition does not decrease motoneuron firing induced by current injection

Here, we failed to support one of the main proposed functions for Renshaw "inhibition", i.e. limiting motoneuron firing rate. Although we approached the problem in a different way (activating recurrent inhibition at slower rates) compared to other studies performed in animal models (Windhorst 1996), we believe that our method is relevant to what has

been described in human studies (Kudina and Pantseva 1988; Miles, Le et al. 1989; Mattei, Schmied et al. 2003). Due to the fact that Renshaw cell activity is primarily driven by α-MN firing and in a fixed timing delay, it is expected that the RIPSP would arrive very early during the ISI, i.e. at the onset of the AHP. On the other hand, if the RIPSP is initiated by another motor pool that is firing asynchronously to the pool of interest, one might expect the RIPSP to arrive at a different time during the ISI. Therefore, our method accounted for all possibilities and was designed to answer the question of whether different timing of the RIPSP can result in different effects on α-MN firing rate. First, we wanted to know if the RIPSP can add to the hyperpolarization caused by the AHP. This was based on interpretations coming from human studies described above and briefly here: if the recurrent inhibitory volley arrives early enough to align with the AHP, then no effect on firing rate can be observed because the former cannot add further hyperpolarization (Kudina and Pantseva 1988; Miles, Le et al. 1989; Mattei, Schmied et al. 2003). To resolve this issue, a simple study was performed (Figure 3.2 and Table 3.1). Briefly, AHPs with and without superimposed homonymous RIPSPs were compared in amplitude. Results showed that RIPSPs can significantly increase the magnitude and the speed of hyperpolarization. This finding indicated that the RIPSP is able to modify the AHP and can indeed add to the amount of hyperpolarization following the action potential spike.

The method used in the current work was very similar to the one used in the human work (Kudina and Pantseva 1988). However, the current study had the advantage of being able

to control for many variables and actually be certain that the observed effect is only due to Renshaw inhibition (deafferented rats versus intact humans). In addition, we were able to directly examine the interaction between the RIPSP and the ISIs in the α-MN soma itself, and to measure the operating RIPSP.

RIPSP amplitudes varied widely from relatively small ones < 1 mV to large ones > 6 mV. We observed unforeseen results. First, Renshaw inhibition failed to decrease α-MN firing rate. In fact, a common trend to fire faster with superimposed "inhibition" was observed. In general, in-phase inhibition either increased firing rate (novel finding) or produced no change (as observed in human studies). On the other hand, out-of-phase tended to decrease the discharge rates; however, this was always followed by a rebound increase in firing rates affecting mainly the immediate ISI that followed the prolonged one. In some cases, rebound was observed in two consecutive ISIs (Data not shown). In conclusion, Renshaw inhibition failed to decrease α-MN firing rate. Instead, it produced an unpredicted increase in some motoneuron. This is in contrast to previous reports stemming from experiments where tetanic rates ≥ 100 Hz were used for recurrent inhibition activation, most recent (Hultborn, Denton et al. 2003). The main difference aside from species differences between the current thesis and previous cat work is the frequency of Renshaw inhibition activation (20 Hz compared to ≥ 100Hz in previous work). The rate used in the current study is more physiological and allowed the examination of different timing possibilities of the interaction between recurrent inhibition and α-MN firing.

In addition, from a functional perspective and during rapid ballistic actions, Renshaw inhibition might serve to accelerate the firing of slow motor units to further add to the force output instead of the widely accepted notion that was first described by Sir John Eccles and colleague in 1961: *"Since tonic alpha motoneurones are special targets for recurrent inhibition, the intensive motoneuronal discharge subserving rapid movements would inhibit specifically the tonic motoneurones. This action would be functionally desirable, else the slowly contracting and relaxing muscles would impede the rapid movements. Thus recurrent inhibition would have the important function of suppressing all discharges from tonic motoneurons during the rapid movements of running or jumping"*, P. 497 in (Eccles, Eccles et al. 1961). The same concept is also mentioned in a later report (Friedman, Sypert et al. 1981).

Renshaw inhibition delays spike frequency adaptation

Briefly, the concept of spike frequency adaptation was addressed by the current study. Interestingly, it is known that SFA is reversed during fictive locomotion (Brownstone, Jordan et al. 1992; Brownstone, Krawitz et al. 2011). This is in contrast to quiescent preparations where SFA is observed frequently (Brownstone 2006). The mechanism behind the reversal of SFA is still to be discovered. Brownstone and colleagues proposed that Na channels de-inactivation might be responsible for the observed reversal of late SFA (Brownstone, Krawitz et al. 2011). The current thesis aimed to test if Renshaw inhibition has the capacity to modulate SFA. This was proposed because Renshaw inhibition is time-locked to α-MN firing and therefore, it is expected for RIPSPs to arrive

at the onset of the AHP and thus result in a larger and faster hyperpolarization (Figure 3.1). These types of AHP modulations might in fact result in faster de-inactivation of Na channels (Du, Bautista et al. 2005) and thus might also reverse or at least delay SFA. During fictive locomotion, recurrent inhibition is known to be active (McCrea, Pratt et al. 1980; Pratt and Jordan 1987), thus it might be a strong candidate to explain, at least in-part, the observations under fictive locomotion. Here, we showed that antidromically evoked Renshaw inhibition can increase the duration of repetitive firing in motoneurons driven by suprathreshold current injection (Figure 3.13). In addition, another set of experiments were designed to further examine the effect by injecting simulated IPSPs through the glass micropipette into the firing train and specifically at the onset of the AHP. This was done in four motoneurons (Figure 3.14). In all motoneurons, simulated IPSPs successfully prolonged the duration of firing and even reversed SFA completely in one motoneuron when short, 2 second constant pulses, were used. The current findings suggested a novel role for Renshaw inhibition, i.e. modulation of SFA in motoneurons. Therefore, Renshaw inhibition might be one key player, perhaps among others, in the reversal of SFA observed during locomotion.

To summarize, the current set of experiments examined the effect of Renshaw inhibition on motoneuron firing behavior. Obtained results confirmed some of the earlier findings mainly from human experiments. In addition, the secondary peak observed frequently in human derived PSTHs was confirmed and found to be due to recurrent inhibition and specifically due to the rebound firing. In addition, it was shown that RIPSPs can indeed

add to the hyperpolarization caused by the AHP. Moreover, the effect of Renshaw inhibition on spike timing was more robust than the effect on firing rate. Interestingly, Renshaw inhibition was shown to increase firing rate under certain conditions or at least failed to decrease α-MN discharge rate. Finally, it was shown that Renshaw inhibition and simulated IPSPs can modulate SFA and might be responsible for the observed reversal of SFA observed during experimental fictive locomotion.

Chapter 4: Renshaw inhibition is highly specialized to accommodate changes in motoneuron firing frequency

Introduction

In his 1946 paper, Renshaw showed that the activity of the internuncial system (named later as Renshaw cells) is conditioned by preceding activity. He showed that a Renshaw cell response to a second input has slower initial frequency, number of action potentials, and shorter duration of response (Renshaw 1946). His observation led Haase, Ross, Cleveland and the Windhorst research groups to further explore the relation between the frequency of motor nerve or ventral root electrical stimulation and the dynamics of Renshaw cell responses, i.e. input – output frequency dynamics (Haase 1963; Ross, Cleveland et al. 1973; Ross, Cleveland et al. 1976; Cleveland and Ross 1977; Cleveland, Kuschmierz et al. 1981; Ross, Cleveland et al. 1982) (Christakos, Windhorst et al. 1987; Boorman, Windhorst et al. 1994; Windhorst, Boorman et al. 1995). Based on physiological records and mathematical computations, most investigators agreed that in order to understand the function of Renshaw inhibition, one must study the circuit under dynamic conditions and that Renshaw cells and hence Renshaw inhibition respond to all dynamic changes in the α-MN activity. However, the functional significance of the observed frequency dynamics is still unclear and most work except (Boorman, Windhorst et al. 1994) did not refer to the dynamics of the RIPSP measured in the α-MN. Boorman and colleague studied the frequency dynamics of RIPSP amplitude and the slope of the

hyperpolarization. They found that both variables decrease in magnitude in response to increasing stimulus frequency. However, no clear functional significance regarding the observed frequency dynamics was reported.

Renshaw raised in 1946 a question about the functional significance of the repetitive firing behavior of Renshaw cells and its relation to the normal functioning of the spinal cord. To date, there is no definite answer to this interesting question.

In 1961, Granit and Renkin referred to the experimentally observed repetitive discharge of Renshaw cells in response to slower stimuli as an “artifact” (Granit and Renkin 1961). Their argument was based on the fact that Renshaw cell discharge transforms into few or single spikes at higher frequencies, cited in Granit and Renkin as personal communication from Haase and later published in the German language (Haase 1963).

One attempt to correlate the frequency dynamics of Renshaw cells to those of RIPSPs produced in α-MNs reached conclusions that are not fully supported by the data presented. For example, it was concluded that the “transformation” of Renshaw cell discharge is responsible for the smaller amplitude and slope of RIPSPs recorded when a faster rate of antidromic stimulation was used (Boorman, Windhorst et al. 1994). However, one could argue that in their illustrations (their Figures 2, 3, 4 and 6), the decline in RIPSP amplitude and slope wasn’t instant but rather showed an initial increase that peaks around 10 Hz and then started to decline exponentially as the input frequency increases (Boorman, Windhorst et al. 1994). If the transformation described first by

Haase is the basis for the observed quenching in RIPSP amplitude, then why would we see an initial increase in RIPSP amplitude? It is clear that the input: output relation is complex and not yet fully understood. Therefore, one main goal of this thesis was to advance the current level of understanding by direct examination of the frequency dynamics of Renshaw cells and RIPSPs followed by direct testing of the effect of frequency dynamics on α-MN firing behavior.

RIPSP amplitude can easily be altered by changes in α-MN membrane potential (Coombs, Eccles et al. 1955). During α-MN firing, Vm is depolarized and RIPSPs are expected to become larger than those reported experimentally under quiescent conditions. Therefore, one might argue that the decrease in RIPSP amplitude seen at higher frequencies of stimulation might be, at least in-part, compensated for by the increase in anionic (mainly Cl^-) driving force during cell firing (depolarized Vm). This can be expected to minimize the impact of frequency dynamics on RIPSP amplitude.

RIPSP time course is another parameter that is less modifiable by ongoing changes in the α-MN. Moreover, as shown in Fetz and Gustafsson, the time course of IPSPs, in general, is important for α-MN firing behavior. The probability of α-MN firing drops to zero at the peak of the IPSP (which can be either long or short) while followed by an increase in firing probability starting at the decay of the IPSP (Fetz and Gustafsson 1983). Therefore, one would expect that if IPSPs with shorter durations arrived during the ISI, α-MN firing might be accelerated.

Rat α-MNs fire at a wide range of frequencies (Gorassini, Eken et al. 2000). Some tasks require motoneurons to discharge at sustained slow rates (≈30 Hz) while others require brief faster activity (60 – 100 Hz). However, one problem might arise from the innate structure of the circuit of Renshaw inhibition, (Figures 1.1 and 1.2). This inhibitory circuit is uniquely locked to α-MN firing. This structural organization requires that the RIPSP generated in the α-MN has to accommodate changes in α-MN discharge rate by changing its time course, i.e. shorten its duration to avoid possible summation. If this ability was lacking in this system, then RIPSPs with a time course of up to 50 milliseconds (Eccles, Fatt et al. 1954), will certainly decrease α-MN firing probability, and thus hamper firing behavior. For example, if the RIPSP remains prolonged during α-MN firing, then the maximum discharge rate attainable by the α-MN will be 20 – 25 Hz. However, without adjustment of RIPSP duration, α-MNs will be impeded from achieving higher rates required by a variety of motor tasks. So, the current thesis aimed to investigate the possibility that RIPSPs generated in α-MNs have the capacity to adjust to changes in α-MN firing rates.

Although reported to become smaller at higher frequencies when measured at resting Vm (Boorman, Windhorst et al. 1994), RIPSP amplitude necessarily increases during α-MN firing (even at high frequencies). This is an unavoidable consequence of the increase in driving force for anions with Vm depolarization. The only way to prevent the increase in RIPSP amplitude from limiting α-MN firing rate is to decrease RIPSP duration. This relieves the CNS from having to inhibit Renshaw cells every single time the α-MN fires

at a faster rate. In other words, the circuit might adjust automatically to allow faster firing.

Here, we directly examined the recurrent inhibitory pathway *in vivo* using the adult rat. In addition to the re-examination of RIPSP amplitude frequency dynamics, we specifically tested the following hypothesis: RIPSPs are highly dynamic and are capable of changing their time course in accord with changes in α-MN firing rates and Renshaw cell discharge pattern. We went further to examine the effects of simulated IPSPs with different durations on α-MN discharge rates. We showed a tendency for faster α-MN discharge rates with shorter simulated IPSPs.

Methods

Animals

A total of 16 adult female Wistar rats (240 – 260g; Charles River Laboratories, Wilmington, MA) were included in this part of the thesis. All procedures were approved by the Wright State University Laboratory Animal Care and Use Committee (LACUC). All surgeries were terminal.

Surgery

After anesthesia was induced, the ABSM, MG, and LGS nerves were isolated in the left hindlimb. Standard surgical procedures were used to dissect the spinal cord for prepartion for recording motoneruon bioelectric signals (Seburn and Cope 1998). In brief, the lumbar spinal cord (T10-S1) was exposed dorsally by dissecting the layers including laminectomy (for bone removal) and removal of meningeal layers (dura and arachinoid). Then. the rat was fixed in a recording frame for continuos stability. Skin flaps were used to form pouches that were filled with warm mineral oil. The aim was to cover the exposed tissues and prevent their drying. All ipsilateral dorsal roots were acutely severed and reflected away from the cord before starting the reording session.

Electrophysiology

Peripheral nerves were isolated and prepared for electrical stimulation. Motoneuron search and recording were as described above. Upon impalement of antidromically identified motoneuron, their electrophysiological properties were collected (Chapter 2), and then RIPSPs were electrically evoked at 10Hz, 20Hz, and 30Hz in all cells. In some motoneurons, additional frequencies were also tested: 2Hz, 5Hz, 40Hz, and 100Hz. A total of 32 lumbar motoneurons from the 16 rats were included in this part of the current thesis. Motoneuron selection was based on the stability of recording, i.e. stable recording with minimal changes in Vm. this allowed reliable comparisons of RIPSPs amplitude (highly sensitive to Vm changes). Also, time course parameters (total duration, half decay time, and half width) were calculated from IPSPs recorded from the same cell but at different stimulus frequencies. This allowed for internal controls for data presented in this chapter, i.e. cell by cell basis. In each cell, RIPSP amplitudes and time course parameters were normalized to those obtained at 10 Hz.

In addition, firing behavior and frequency dynamics were analyzed in 7 Renshaw cell recorded intracellularly. Similar frequencies were used for antidromic stimulation (2Hz, 10Hz, 20Hz, and 30Hz).

IPSP Simulations

Amplitude and time course of two RIPSPs recorded from gastrocnemius α-MNs were simulated in somatic voltage produced by somatic current injection. The basis for selection was the distinct time course of these two RIPSPs (Figure 4.6), one RIPSP had a total duration of only ≈ 8 msec. while the other one had a longer duration of ≈20 msec. Both simulated IPSPs were injected via the glass micropipette into three lumbar α-MNs driven to fire by suprathreshold intracellular current injection into the soma via the glass micropipette. Again, each cell served as its own internal control and all other variables such as Vm and the amount of current injected were controlled for within each cell. The only variable remained was the duration of the simulated IPSPs.

Statistical analysis

Changes in RIPSP amplitude and time course were normalized to those obtained at 10 Hz in each cell. Independent Student t-test was used to compare parameters obtained at 30 Hz to those obtained at 10 Hz for time course, and those obtained at 20 Hz to those obtained at 10 Hz for amplitude. Statistical significance was set at $P < 0.05$.

Results

RIPSPs become shorter as the frequency of stimulation increases

Figure 4.1 shows the time course of RIPSPs obtained at different peripheral nerve stimulation frequencies in the same LGS α-MN. The total duration of the RIPSP decreased from 57 msec. at 2Hz stimulation to 26 msec. at 30 Hz stimulation, 54% shortening (Figure 4.1b). The same trend was seen for the half decay time and the half width of the RIPSP (Figures 4.1.c and 4.1d).

RIPSPs recorded in 29 α-MNs were analyzed by dividing the duration, half decay time, and half width obtained at 20 and 30 Hz over the one obtained at 10 Hz in each α-MN, normalized time course parameters to those obtained at 10Hz (Figure 4.2). The mean ± SD for normalized duration obtained at 30 Hz was 76% ± 22% ($P < 0.000001$), for half decay time was 69% ± 18% ($P < 0.000001$), and for half width was 72% ± 15% ($P < 0.000001$). The same applied for rise time of the RIPSPs and the normalized mean ± SD at 30 Hz was 88% ± 19% ($P < 0.005$) (data not shown).

Since time course parameters might look different because of differences in amplitude, rise rate and half decay rate were normalized for amplitude. For rise rate, amplitude was divided by rise time which gives a velocity measurement for the rise and thus control for any possible confound caused by differences in amplitude. The same was done for half decay rate but here the RIPSP amplitude was divided by 2 and the result was divided by

the half decay time (Figure 2.1). Both rise rate and half decay rate were faster for RIPSPs obtained at 30 Hz compared to those obtained at 10 Hz. For rise rate the normalized mean ± SD was 150% ± 50%, $P < 0.00001$ (n=29) and for half decay rate was 197% ± 80%, $P < 0.000001$ (n=29), data are not shown in the Figure.

RIPSP amplitude shows interesting frequency dynamics behavior

Here, the frequency dynamics of RIPSPs were examined. In Figure 4.3 (Panel a), three RIPSPs obtained under the same strength of peripheral nerve stimulation, and at the same resting membrane potential, -65 mV, the only variable was limited to the frequency of stimulation. Panel b compares amplitudes at the three frequencies tested, and as can be seen from the raw records and the plot, the maximum amplitude was largest at 20 Hz. This was in contrast to previous studies described above, also see discussion below. In panel (c), the mean ± SD of normalized amplitudes to those obtained at 10 Hz (in each cell) were measured in 17 motoneurons (selected because of stable Vm during all three frequencies tested). 10 Hz was selected for normalization because RIPSPs measured at this frequency had the smallest amplitude in most cases; however, occasionally, such as in (Figure 4.1), the amplitude measured at 30 Hz stimulation was the smallest. The mean RIPSP amplitude at 20 Hz was 134% ± 12% of the one recorded at 10 Hz, $P < 0.0000001$, n=17. While the mean ± SD at 30 Hz was 115% ± 21%, $P < 0.01$.

Figure 4.1**. *Distinct time course for RIPSPs antidromically evoked in the same cell at different peripheral stimulus frequency*.** Panel (a) shows four different records obtained from one LGS motoneuron (Rheobase = 4 nA; AP spike = 60 mV; Vm= -50 mV). Records were obtained following supra-maximal stimulation of the ABSM nerve. Panels (b), (c), and (d) shows numerical values for the time course parameters of the recorded RIPSPs (duration, half decay time, and half width). As can be seen, all time course parameters were shortened at higher frequencies.

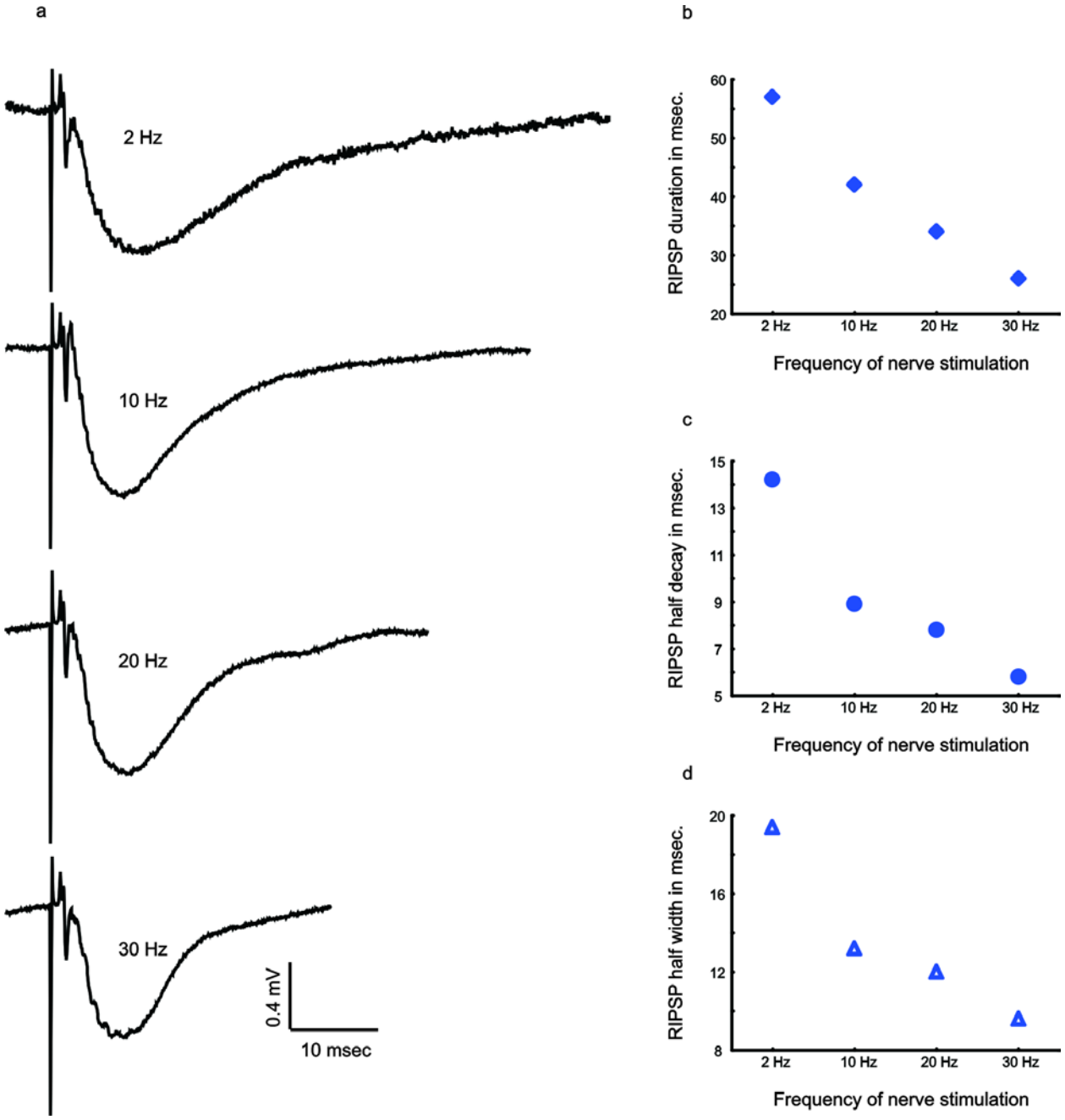
a
2 Hz
10 Hz
20 Hz
30 Hz
0.4 mV
10 msec
b
RIPSP duration in msec.
60
50
40
30
20
2 Hz
10 Hz
20 Hz
30 Hz
Frequency of nerve stimulation
c
RIPSP half decay in msec.
15
13
11
9
7
5
2 Hz
10 Hz
20 Hz
30 Hz
Frequency of nerve stimulation
d
RIPSP half width in msec.
20
16
12
8
2 Hz
10 Hz
20 Hz
30 Hz
Frequency of nerve stimulation

Figure 4.2**. *Population changes in time course parameters*.** Here, data from 29 motoneurons (MG, LGS and ABSM) were pooled together and Whisker box plots showing the mean ± SD and mean ± SE. The same trend observed in (Figure 4.1) was seen in most other motoneurons. The comparison was limited to 10, 20, and 30 Hz due to the physiological relevance of these firing frequencies to mammalian motoneurons, including those of the rat (Gorassini, Eken et al. 2000). Panels a, b, and c show normalized means (to those obtained at 10 Hz) for RIPSP duration, half width, and half decay time, respectively. The mean duration (a) decreased by 24% at 30 Hz stimulation, the mean half decay (b) shortened by 31%. And the mean half width (c) decreased by 28%. Independent Student t-test was used for statistical comparison of means obtained at 30 Hz or 20 Hz to those obtained at 10 Hz.

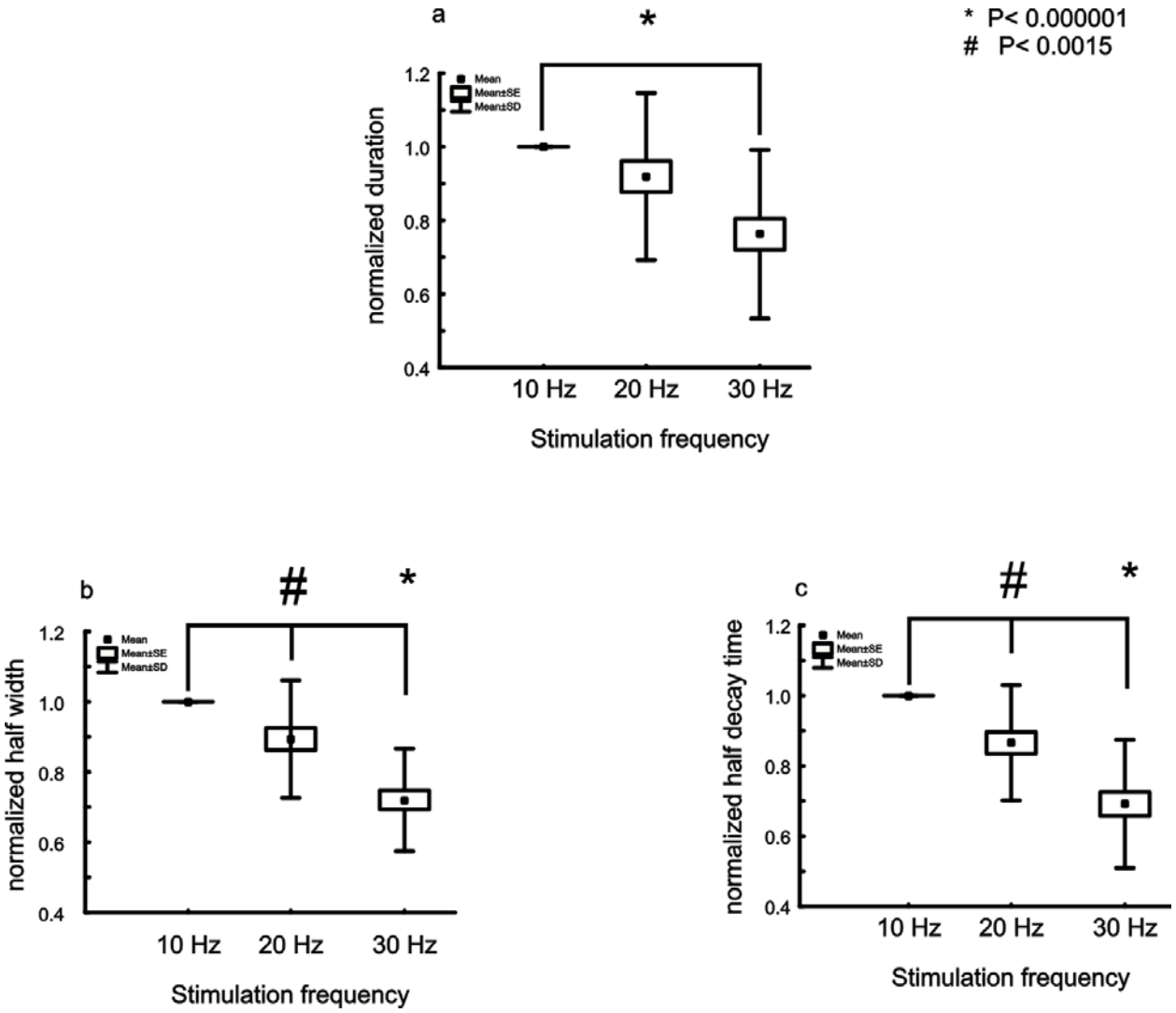
a
*
* P< 0.000001
# P< 0.0015
Mean
Mean±SE
Mean±SD
normalized duration
1.2
1.0
0.8
0.6
0.4
10 Hz
20 Hz
30 Hz
Stimulation frequency
b
#
*
normalized half width
c
#
*
normalized half decay time

Renshaw cell frequency dynamics

We recorded intracellularly from 7 Renshaw cells in control rats. One representative example (resting Vm = -60 mV) is shown (Figure 4.4). Renshaw cells decreased their firing response as the stimulation frequency increased. The number of action potential spikes and the duration of the firing train both decreased at higher frequencies. This is in agreement with Haase findings (Haase 1963). Figure 4.4b shows the relationship between the mean Renshaw cell firing durations and the RIPSP total duration from pooled data at the three stimulation frequencies tested.

In addition to changes in the firing duration of Renshaw cells, the initial frequency of Renshaw discharge was found to decrease as the antidromic stimulation frequency increases (Figure 4.5). The upper panel of Figure 4.5 shows Renshaw cell inter-spike-intervals (frequency = 1/ISI). The lower panel shows the actual measurement of Renshaw discharge rate for each of the ISIs at different stimulus frequency. The higher the stimulus frequency, the slower was the initial Renshaw cell discharge rate. This is in agreement with the work of Haase in 1963. Finally, the characteristic repetitive firing behavior of Renshaw cells expresses itself in the rising phase of the RIPSP as unique ripples (Figure 1.3). Those ripples express frequencies that resemble the frequency of Renshaw cell spike discharge. Interestingly, those ripples can still be seen at higher frequencies of motoneuron stimulation such as in records obtained at 30 Hz (Figure 4.1).

Figure 4.3***. RIPSP maximum amplitude peaks in records obtained following peripheral stimulation at 20 Hz.*** Three RIPSPs obtained from MG motoneuron in response to supra-maximal stimulation of the ABSM nerve. For this motoneuron (Rheobase was 9 nA; AP spike measured 70 mV; Vm= -65 mV). As shown in panels (a) and (b), the maximum amplitude was obtained at stimulation frequency = 20 Hz. This was also the case for all the 17 motoneurons analyzed (panel c). RIPSP amplitude was normalized in each cell to that obtained following 10 Hz stimulation, the reason being is that among the three frequencies reported, 10 Hz resulted in RIPSPs with the smallest amplitude in most cases, very few exceptions were encountered. Normalized values were used instead of the absolute value because RIPSP amplitude varied widely from one motoneuron to another (as small as tens of microvolts and as large as 5 or more millivolts).

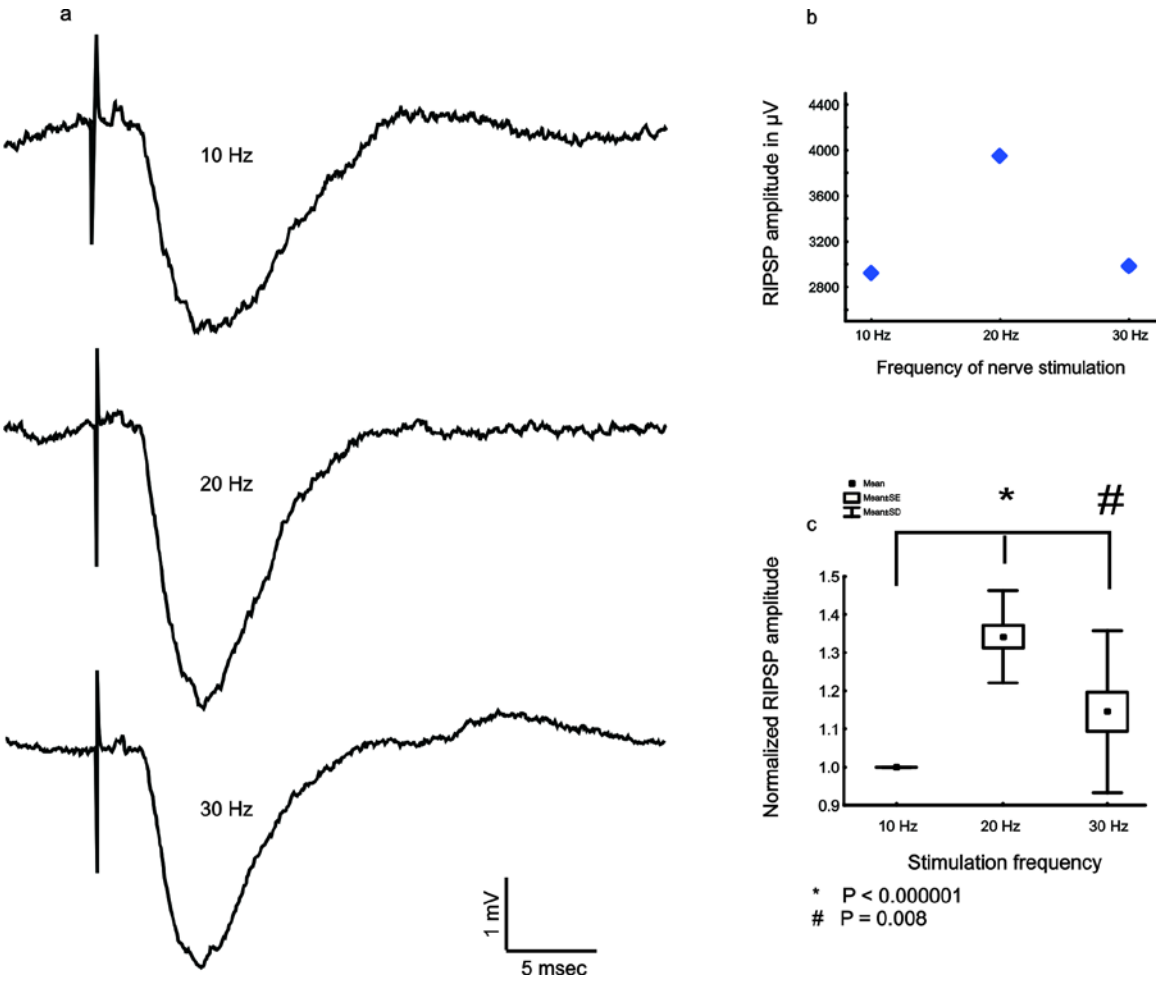
a
10 Hz
20 Hz
30 Hz
1 mV
5 msec
b
RIPSP amplitude in µV
4400
4000
3600
3200
2800
10 Hz
20 Hz
30 Hz
Frequency of nerve stimulation
c
Mean
Mean±SE
Mean±SD
*
#
Normalized RIPSP amplitude
1.5
1.4
1.3
1.2
1.1
1.0
0.9
10 Hz
20 Hz
30 Hz
Stimulation frequency
* P < 0.000001
# P = 0.008

Figure 4.4***. Frequency dynamics of the duration and number of action potential spikes in the Renshaw cell.*** The higher the stimulus rate, the fewer the action potentials fired by the Renshaw cell and the shorter was the duration of repetitive firing. The mean ± SD and ± SE for the number of action potential spikes and total duration of Renshaw cell firing is plotted for 78 sweeps recorded at 2 Hz, 58 sweeps at 10 Hz, 147 sweeps at 20 Hz, and 130 sweeps at 30 Hz. Random variation of stimulus frequency was done, i.e. switching between different frequencies randomly to avoid any possible contamination by activity dependent or time dependent synaptic modulation.

(Vm for this Renshaw cell was – 60 mV)

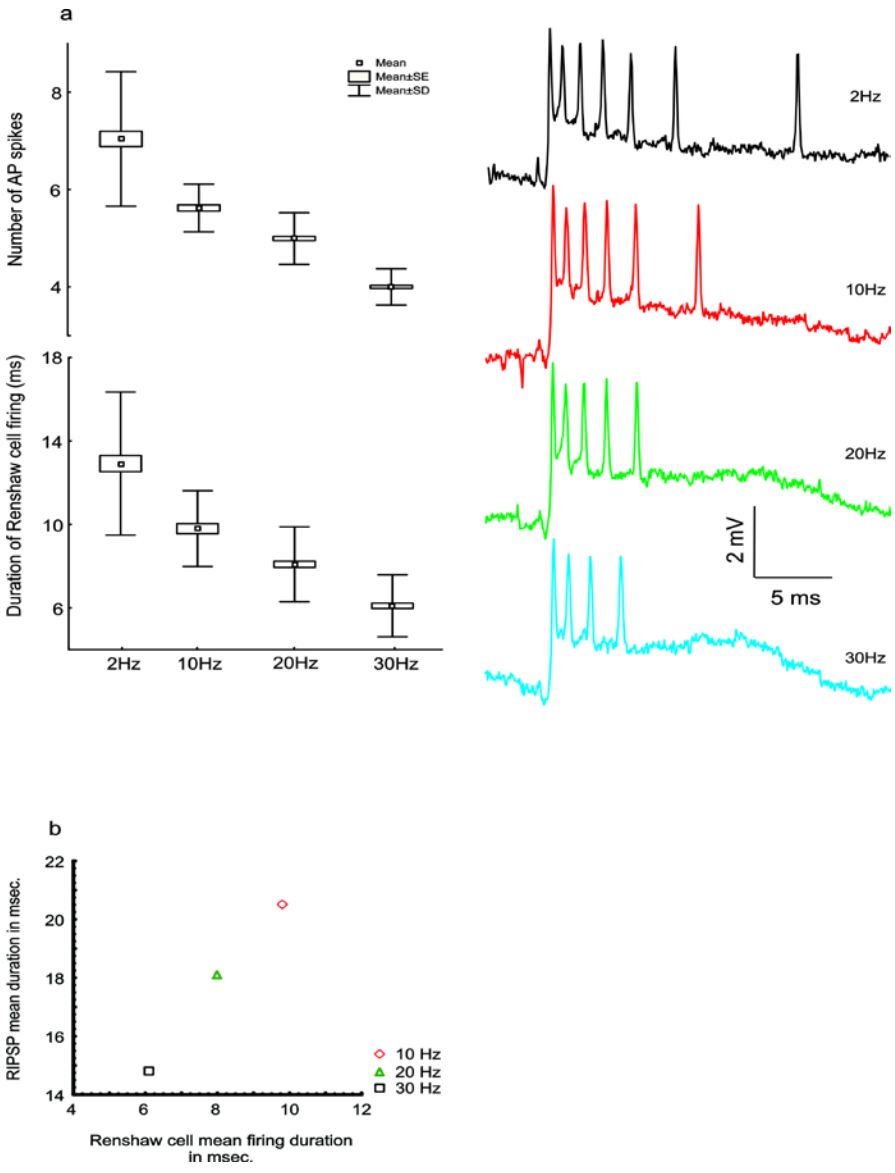
a
Mean
Mean±SE
Mean±SD
Number of AP spikes
8
6
4
Duration of Renshaw cell firing (ms)
18
14
10
6
2Hz
10Hz
20Hz
30Hz
2Hz
10Hz
20Hz
30Hz
2 mV
5 ms
b
RIPSP mean duration in msec.
22
20
18
16
14
4
6
8
10
12
10 Hz
20 Hz
30 Hz
Renshaw cell mean firing duration
in msec.

Figure 4.5***. Renshaw cell firing frequency in response to varying input frequency.*** For every single impulse arriving at the MN-Renshaw synapse, the latter responds by repetitive firing which typically starts at a very high frequency >1000 Hz and declines with time. Here, inter-spike intervals (ISI, see upper panel for illustration) for each response of Renshaw cell to antidromic stimulation (a total of 413 stimuli) were measured and their reciprocal (1/ISI, i.e. firing frequency) was calculated. This was done for Renshaw responses to different input frequencies (2, 10, 20, & 30 Hz). The mean ± SD, mean ± SE is reported for each ISI (up to a maximum of 8 in any one response). Again, less ISIs were seen at higher frequencies due to a smaller number of AP spikes. Faster decline in Renshaw firing frequency was always seen after the first ISI. More spacing between consecutive spikes was seen at higher frequencies compared to the Renshaw behavior at slow inputs such as 2 Hz. The frequency of Renshaw cell burst was inversely related to the input frequency.

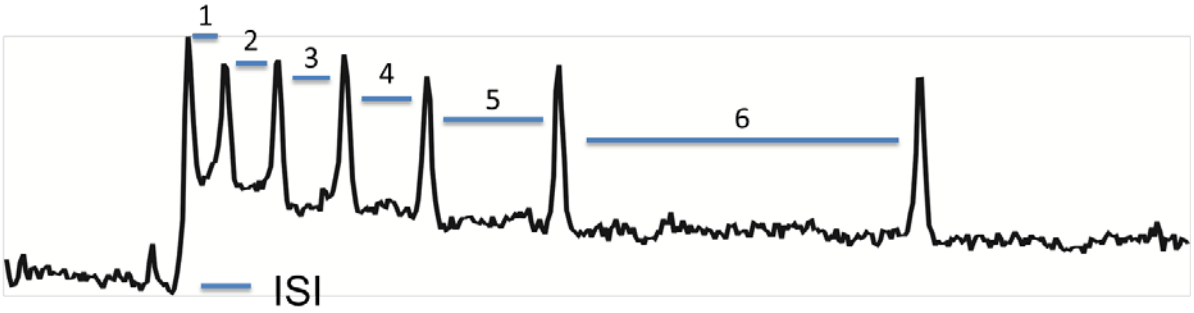
1
2
3
4
5
6
ISI

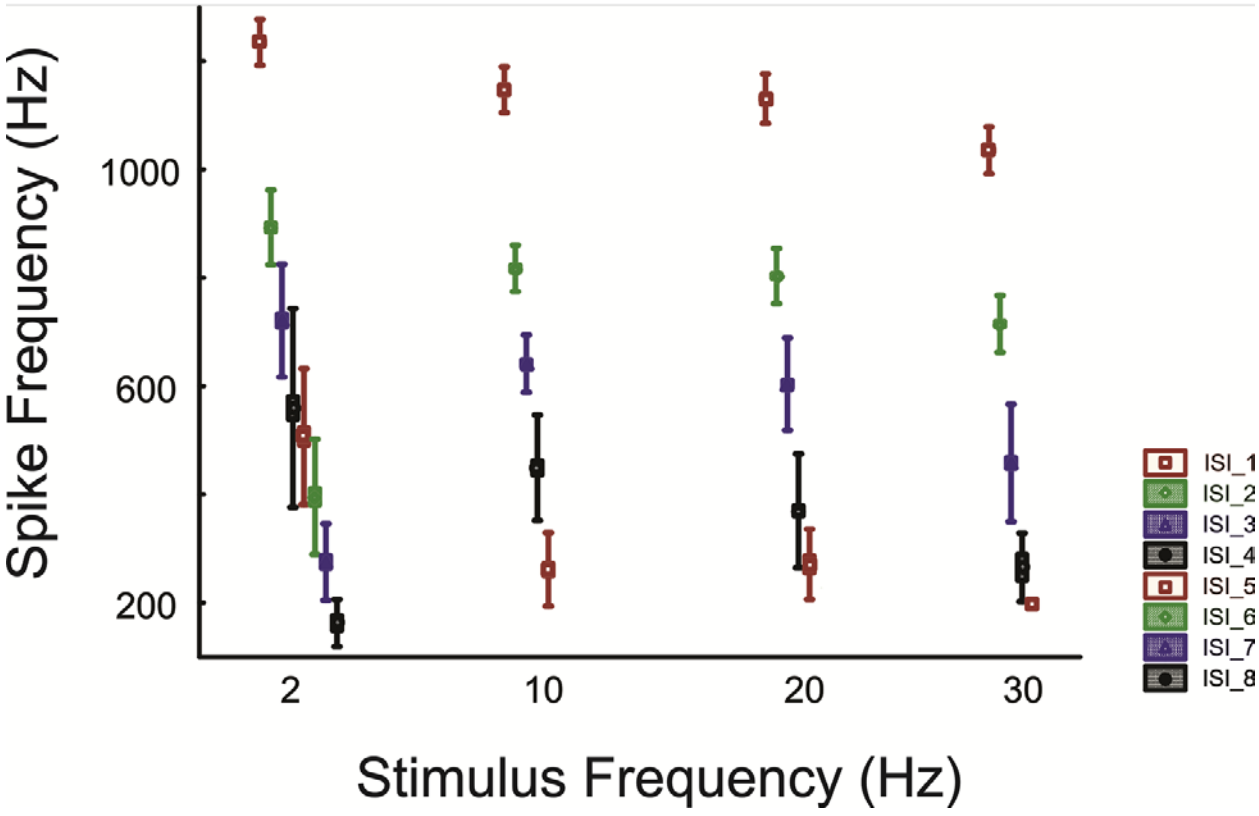
Spike Frequency (Hz)
1000
600
200
2
10
20
30
Stimulus Frequency (Hz)
ISI_1
ISI_2
ISI_3
ISI_4
ISI_5
ISI_6
ISI_7
ISI_8

Differential effect of short and long simulated IPSPs on motoneuron firing

The effect of varying the duration of hyperpolarization (simulating those of RIPSPs) on firing rate of motoneurons was examined. Two RIPSPs recorded in previous experiments and selected based on their distinct time course (durations: 8 versus 20 msec.) were scaled to 4 nA in amplitude to produce a simulated version in somatic voltage that can be injected directly into the soma of the motoneuron via the glass micropipette (Figure 4.6). This differs from the physiological condition where the RIPSP arrives to the soma after passing through the dendritic arbor. Despite this difference, simulated IPSPs can sufficiently serve the main goal of the current experiments, where all other variables were controlled. Although proposed as having local effect on dendrites (Fyffe 1991), their direct modulatory effect on firing rate shall be measured in the soma where the "effective synaptic current" is usually measured in motoneurons (Heckman and Binder 1988).

Each of the simulated IPSPs (short and long) was injected in separate trials in the same motoneuron during repetitive firing that was induced by suprathreshold intracellular current injection. After stable repetitive firing is attained, each motoneuron action potential was used to trigger a hyperpolarizing current injection to produce motoneuron membrane hyperpolarization with amplitude and duration representing one long and one short RIPSP sampled from motoneurons in this study (Figure 4.6).

Motoneuron firing rates were measured in all three cases (with long simulated IPSP, with short simulated IPSP and without any, i.e. control). The mean rates (measured over two

seconds of repetitive firing) where pooled from multiple trials in each cell and in each category. Results are reported here (Figure 4.7). In all motoneurons (a, b, and c), the short simulated IPSP augmented firing rate. On the other hand, the long simulated IPSP augmented the rate only if the control firing rate was slow (Figure 4.7c). In all motoneurons, firing rate was faster with the short versus the long simulated IPSPs. Interestingly, in all three motoneurons, the absolute difference: The mean firing with short IPSP minus the mean firing with long IPSP was equal to 13 spikes. This indicates that other variables were sufficiently controlled for, and the difference observed is only due to the time course difference between the two simulated IPSPs.

Figure 4.6. ***Simulated IPSPs used in firing rate studies.*** Hyperpolarizing current injection was used to simulate the time course of two actually recorded RIPSPs. One RIPSP had a total duration of 8 msec. (short) while the other had a total duration of more than 20 msec. (long). Both had different amplitude and time course naturally (see blue records), but simulations were calibrated to the same amplitude (4nA, see black traces). Both were designed to be injected through the glass micropipette to align with AHP of the action potential spike in motoneurons driven to fire repetitively by intracellular suprathreshold current injection.

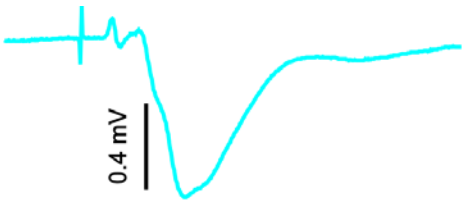

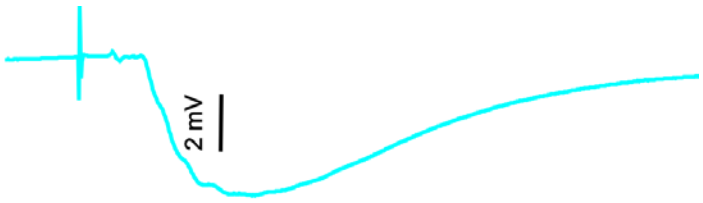

RIPSPs produced by disynaptic recurrent inhibition

IPSPs produced by hyperpolarizing current injection into motoneuron soma

Figure 4.7. ***Motoneurons fire faster when challenged with short simulated IPSPs than it does with longer ones*.** Simulated IPSPs shown in figure 4.6 were injected into three motoneurons driven to fire repetitively by intracellular current injection as described in chapter 3 above. Firing trials with and without simulated IPSPs were averaged for the mean firing rate. Each data point here represents the mean rate measured over 2 seconds of repetitive firing. Injected current in all reported trials was 24, 20, and 10 nA for motoneurons (a), (b) and (c), respectively. Statistical analysis: independent Student t-test.

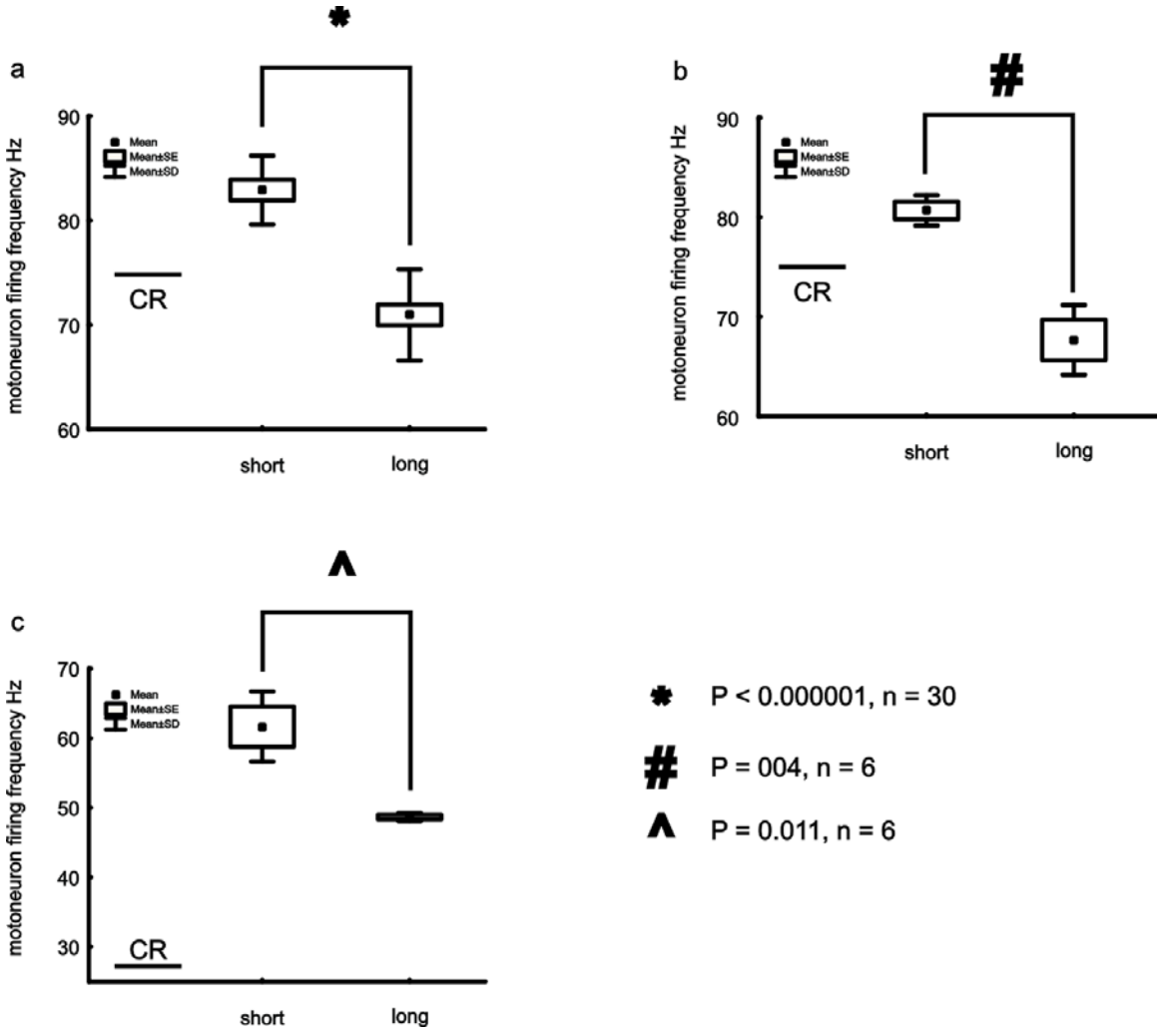
a
b
c
motoneuron firing frequency Hz
Mean
Mean±SE
Mean±SD
CR
short
long
90
80
70
60
50
40
30
P < 0.000001, n = 30
P = 004, n = 6
P = 0.011, n = 6

Discussion

The current work was designed to address an interesting question initially raised by Renshaw and later examined by many other investigators. A novel approach to answer Renshaw concerns was adopted in this study. The frequency dynamics of Renshaw cells (first described by Haase (extracellular recordings) and confirmed in this study (intracellular recording) were linked to RIPSP amplitude and time course, with more emphasis on the latter. However, not all observed frequency dynamics of RIPSPs are fully explained by Renshaw cell frequency dynamics. Although RIPSP time course dynamics intimately followed those of Renshaw cells (Figures 4.2 and 4.4), the amplitude dynamics of RIPSP did not.

Frequency dynamics of RIPSP time course

In response to different stimulation frequency, both Renshaw cells and RIPSPs showed interesting and correlated behavior. As the frequency of stimulation increased, RIPSP duration, half decay and half width all decreased i.e. shortened (Figures 4.1 and 4.2). For Renshaw cells, the number of action potential spikes and the duration of firing decreased with increasing stimulus frequency (Figure 4.4). The latter potentially explains the changes observed in RIPSPs time course. This type of “built in” adaptation is important, the reason being is that time course is not easily modifiable within each motoneuron, e.g. in response to membrane potential fluctuations. This necessitates a pre-synaptic site of modulation, which is shown by this study to be the Renshaw cell itself. If time course is

not as malleable as described in this work, then motoneurons are faced with an inevitable long inhibition that can limit their firing behavior (for simplicity we ignore descending inputs to Renshaw cells). If long and fixed, RIPSP can impede motoneuron firing rate (Fetz and Gustafsson 1983) which is mainly regulated via the afterhyperpolarizing potential AHP (Chapter 1 and Chapter 3). It is essential that RIPSPs accommodate motoneuron firing rates by appropriately changing their time course.

The current findings leave us with the following conclusion: Recurrent inhibition has the capacity to efficiently accommodate changes in motoneuron firing rates.

Frequency dynamics of RIPSP maximum amplitude

In partial agreement with a previous report (Boorman, Windhorst et al. 1994), RIPSP maximum amplitude decreased at higher frequency of inputs to Renshaw cells (40 Hz and 100 Hz, data not shown). However, optimal amplitude was obtained at a frequency of 20 Hz in the rat (Figure 4.3). One could observe a similar trend that peaks around 10 Hz in the cat, figures 2, 3, 4 and 6 in (Boorman, Windhorst et al. 1994). The current study found that RIPSPs recorded at 30 Hz have smaller amplitudes than those recorded at a slower frequency 20 Hz. However, the latter were larger than those recorded at 10 Hz. The initial increase in RIPSP amplitude observed at 20 Hz was in contrast with earlier conclusions stating that RIPSP amplitude inversely follows the frequency of stimulation (Boorman, Windhorst et al. 1994). Our findings, however, cannot be fully explained by the number and duration of Renshaw cell discharge observed at those frequencies. If the

latter were the only players in determining RIPSP amplitude, then one would expect to see smaller RIPSPs at 20 Hz when compared to those obtained at 10 Hz in the same cell and under the same conditions (e.g. same Vm). One interesting observation, in agreement with a previous report (Haase 1963), is that the initial firing frequency of the Renshaw cell shown in (Figure 4.4) tended to decrease as the input frequency increased. In addition, the spacing between successive spikes (ISI) tended to increase as antidromic frequency increases (Figure 4.5). This might suggest that Renshaw cells become more efficient in their firing behavior at higher frequencies, i.e. while they fire less spikes for each impulse they receive, the degree of spacing is increased between the initial burst of spikes perhaps to maximize their influence on the target motoneuron, i.e. to result in the maximum possible RIPSP. This might serve to explain the discrepancy observed between the duration of Renshaw firing and the RIPSP amplitude; in addition it might provide an opportunity for speculations. For example, what if the increased spacing in Renshaw discharge observed at higher frequencies is adaptive, i.e. it might allow more time for the synaptic machinery (at the Renshaw – MN synapse) to replenish itself, i.e. synaptic re-uptake and release. This might result in more efficient effects on the post synaptic cell (i.e. motoneuron), and perhaps more receptor (GABA and Glycine) activation and hence stronger inward anionic current. The current findings suggest that the relationship between the frequency dynamics of Renshaw cells and those of RIPSPs are more complex, especially for amplitude dynamics. Although we show that the time course of the RIPSP decreases at higher frequencies of stimulation (potentially explained by

Renshaw cell firing transformation), the peak of amplitude at 20 Hz is not fully explained by the current data. Therefore, investigations at the molecular level might be required to further explore the mechanisms responsible for the latter effect.

Short versus long IPSP: effect on motoneuron firing rate

After characterizing the frequency dynamics of RIPSPs and Renshaw cells, one would like to see direct and relevant applications. Two RIPSPs were simulated in somatic voltage and calibrated to the same amplitude. The only difference between the two was time course. One had a short time course, i.e. ≈ 8 msec. while the other had a relatively long time course, i.e. ≈20 msec. the direct question to be answered here was: if all other conditions are the same, what is the effect of IPSP time course on motoneuron firing rate?

Three motoneurons were recorded from three rats. In each motoneuron, stable membrane potential was maintained, the same amount of current was injected in each trial, and the same resting period was left between consecutive trials. Simulated IPSP were triggered to be injected through the glass micropipette by action potential spikes in the repetitively firing motoneuron. In all motoneurons, the short simulated IPSP increased firing rate from the control baseline (Figure 4.7a-c). On the other hand, the long IPSP usually decreased firing rate from control values (Figure 4.7a, b) unless control firing rate was very low (Figure 4.7c). Interestingly, in all three motoneurons, the mean rate of firing with the short IPSP superimposed on the AHP was 13 spikes more than the one obtained with superimposed long IPSP. This is quite fascinating and suggests that the time course

of the IPSP can be an independent factor in determining motoneuron firing rate. Also, this speaks to the reliability of the test used and reproducibility of the results across different motoneurons. These findings are in-line with what was presented in chapter 3 and further support the notion that Renshaw "inhibition" might actually increase motoneuron discharge rate under certain conditions. Moreover, the frequency dynamics described in this chapter together with earlier literature suggest that Renshaw inhibition doesn't restrict *the degree of firing freedom* of α-motoneurons.

I would like to end this chapter by referring back to the question raised by Renshaw himself: "What is the functional significance for the repetitive firing seen in this internuncial system?"

My answer would be: without repetitive responses to start with, Renshaw cells will not have the capacity to adapt to motoneuron varying input (typically across wide range of frequencies). Therefore, Renshaw cells themselves are able to fine-tune their own output to match the best interest of the target cell, i.e. the motoneuron. Moreover, this distinctive behavior that became a classical feature of these interneurons is not an artifact of slower experimental stimulation rates as suggested before (Granit and Renkin 1961). In summary, the work in the current thesis has confirmed earlier observations of transformation of Renshaw cell firing. In addition, a novel finding that RIPSP duration and other time course parameters shorten at higher frequencies which allow α-MNs to fire at faster rates was reported. Moreover, RIPSP maximum amplitude did not decrease linearly with increasing stimulus frequency but rather showed a maximum peak at 20 Hz.

The latter finding calls for future studies to uncover the molecular basis behind the observed findings, *in vivo.*

Chapter 5: Plasticity of Renshaw inhibition after nerve injury and regeneration

Introduction

Havton and Kellerth demonstrated that the recurrent inhibitory circuit responds to injury with structural degeneration and functional adaptation (Havton and Kellerth 1984; Havton and Kellerth 1990a; Havton and Kellerth 1990b). These findings were obtained when the nerve was severed and prevented from regeneration. The current thesis aimed at examining the extent of which successful peripheral nerve regeneration can restore the structure (in collaborative work) and function of the recurrent inhibitory system.

Motor axons, unlike sensory axons are highly successful at reinnervating their appropriate target. We ask here whether this advantage enables the centrally projecting collateral axons and their spinal circuits to recover better than centrally projecting sensory neurons (Alvarez, Titus-Mitchell et al. 2011; Bullinger, Nardelli et al. 2011) whose axons have greater difficulty achieving appropriate reinnervation.

Collaborative experiments done in the Cope and Alvarez labs, demonstrated that the centrally projecting collateral axons retain permanent anatomical deficits (unpublished observations). These deficits together with the striking dissociation of structural and functional recovery seen before under conditions of peripheral nerve ligation (Havton and Kellerth 1990b) led us to further investigate the function of Renshaw inhibition after nerve injury and regeneration.

In pervious studies, permanent elimination of axon collaterals of α-MNs (up to 40% elimination) was accompanied by full recovery of the function of the circuit at 12 weeks post injury, i.e. functional adaptation of the circuit overcame physical degeneration (Havton and Kellerth 1990a; Havton and Kellerth 1990b). In order to explain the observed paradox, the authors proposed that surviving synapses made by axon collaterals with Renshaw cells increased their efficacy (Havton and Kellerth 1990b).

In their work, Havton and Kellerth examined the maximum amplitude of RIPSPs at different time points after nerve injury and ligation. They reported full recovery of the function at 12 weeks post injury. Despite their findings, several issues remain unresolved. First, the extent by which nerve regeneration might affect circuit recovery is still unknown. Second, the extent by which connectivity itself is affected by the injury was not addressed. Third, there is a known strong relationship between RIPSP amplitude and the membrane potential of the motoneuron (Figure 5.1). However, this relationship was not taken into account during the comparison of RIPSP amplitudes across treatment groups in the previous work. Finally, in addition to RIPSP maximum amplitude, several other electrophysiological parameters can be of functional significance. For example, the functional importance of the RIPSP time course has been examined earlier in this thesis, see simulation studies (Figure 4.7). Therefore, one might wonder about the extent by which time course of the RIPSP is affected by the injury and whether it recovers after nerve regeneration. In fact, Figure 2 in (Havton and Kellerth 1990b) showed one example of a RIPSP elicited by antidromic stimulation of the injured MG nerve and recorded from

uninjured Soleus motoneuron 12 weeks postoperatively. This RIPSP appears to have a very long durtation (>80 msec.) compared to what is typically reported for cat α-MNs, around 40 – 50 msec. (Eccles, Fatt et al. 1954). The possibility of prolonged time course of these synaptic events after regeneration could have important functional consequences and therefore, requires further examination.

Another important issue is that for any α-MN, the degree of proximity to the active motor pool supplying recurrent inhibition is key for RIPSP amplitude, or even the presence of RIPSP (McCurdy and Hamm 1994). This issue can be controlled for by measuring the intracellular motoneuron field potential (Figures 2.1 and 5.2).

To summarize, this part of the thesis was designed to study the extent by which the function of recurrent inhibition is restored after nerve regeneration. Functional recovery was examined in terms of: 1. Recovery of the connectivity of the circuit, 2. Recovery of the RIPSP maximum amplitude (Vm and proximity were taken into account), and 3. Recovery of RIPSP time course if affected.

All experiments were done in the anesthetized adult rat, either control or treated by MG nerve cut and immediate surgical repair 6 -13 months before terminal electrophysiological recordings.

Figure 5.1. ***the RIPSP is highly sensitive to membrane potential changes.*** Here, in one motoneuron, the RIPSP maximum amplitude increased in response to Vm depolarization. (Range of Vm tested: -52 mV to -99 mV). Five fold change in RIPSP amplitude over 10 mV change in Vm. this steep relationship has to be considered when RIPSP amplitudes are compared across motoneurons. Notice, the reversal potential was approximately = -76 mV, in accord with data available from the adult cat (Eccles, Fatt et al. 1954; Coombs, Eccles et al. 1955). Each point on the curve (right panel) corresponds to one of the original records (left panel), the upper most point on the curve corresponds to the lower most RIPSP record on the left. RIPSP amplitudes had a negative sign to distinguish from reversed ones.

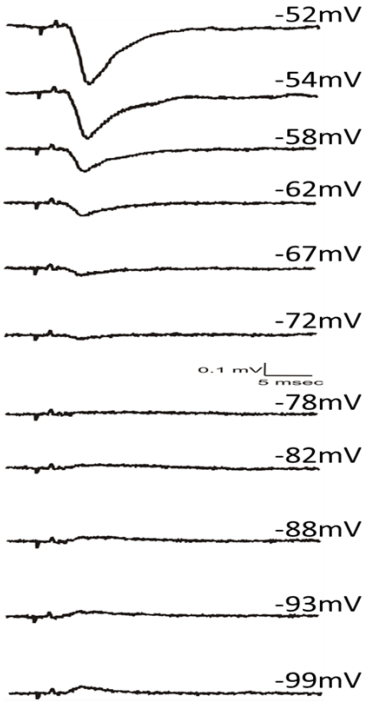
-52mV
-54mV
-58mV
-62mV
-67mV
-72mV
0.1 mV
5 msec
-78mV
-82mV
-88mV
-93mV
-99mV

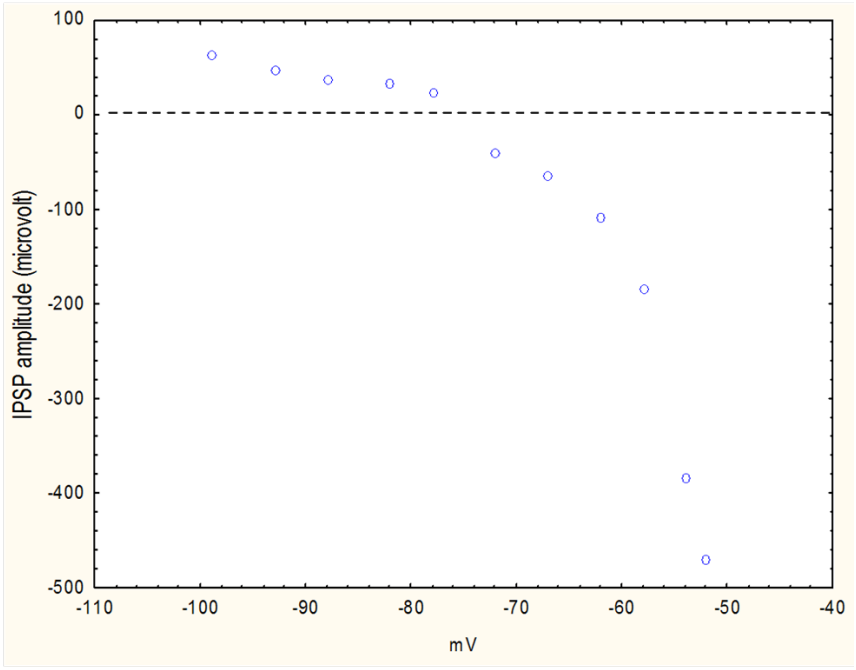
IPSP amplitude (microvolt)
100
0
-100
-200
-300
-400
-500
-110
-100
-90
-80
-70
-60
-50
-40
mV

Methods

Animals

Adult female wistar rats were randomly placed into either control (n=22) or treated (n=13) groups. The treated group was subjected to to MG nerve section followed by immediate surgical repair (survival surgeries). Rats in both groups were studied in terminal experiments and electrophysiological measures were obtained.

Survival surgeries

A total of 13 rats were subjected to MG nerve cut and immediate surgical repair. Isoflurane (4.0-5.0 % in 100% Oxygen) was used to induce and maintain anesthesia (1-3 % in 100% Oxygen, through nose cone). The skin over the left popliteal fossa was cut and open to gain access to the MG nerve. the nerve was surgically cut and immediately repaired by suturing both ends through the epineurium using 10-0 ethilon sutures. This was followed by wound irrigation using 0.9 saline. Then, all covering layers (fat, fascia, and skin) were sutured back and closed. Analgesia (NSAID) was subcutaneously given before the anesthesia was discontinued and for the next 48 hours. Then, rats were returned back to their cages and all were monitored during recovery for signs of stress or infection which were treated as appropriate. Regular care was given from the time of surgery until their transfer to the lab for terminal experiments. Terminal experiments took place 6 – 13 months after the survival surgery.

Terminal experiments

Similar in control and treated rats. After anesthesia was induced, the ABSM, MG, and LGS nerves were isolated in the left hindlimb. Standard surgical procedures were used to dissect the spinal cord for prepartion for recording motoneruon bioelectric signals (Seburn and Cope 1998). In brief, the lumbar spinal cord (T10-S1) was exposed dorsally by dissecting the layers including laminectomy (for bone removal) and removal of meningeal layers (dura and arachinoid). Then. the rat was fixed in a recording frame for continuous stability. Skin flaps were used to form pouches that were filled with warm mineral oil. The aim was to cover the exposed tissues and prevent their drying. All ipsilateral dorsal roots were acutely severed and reflected away from the cord before starting the recording session.

Recording Preparation

All three muscle nerves were placed on monopolar stimulating hook electrodes for antidromic identification of impaled motoneurons. Peripheral nerve stimulation strength was set at 2.5 times the threshold for visible muscle contraction for heteronymous nerves and submaximal for the antidromic action potential for homonymous nerves.

Data collection

Motoneurons were impaled with glass microelecrodes filled with 2M potassium acetate (1.2 mm OD, 6-11 MΩ resistance, World Precision Instruments) advanced through the

spinal cord using a micromanipulator. Motoneurons were identified as either MG, LGS or ABSM when the stimulation of one of the mentioned peripheral nerves resulted in antidromic action potential spike. Upon identification, the antidromic action potential was recorded, and its amplitude was measured. Only those cells whose membrane potential was stable and action potential amplitude was meaured at +60 mV or larger were included for further analysis. The motoneuron's intrinsic electrical properties (rheobase current, afterhyperpolarization (AHP) half decay time and peak amplitude) were recorded. In addition, homonymous (submaximal peripheral stimulation) and/or heteronymous (supramaximal peripheral nerve stimulation) recurrent inhibitory post synaptic potentials (RIPSPs) were recorded from one or up to three sources depending on the stability of the recorded cell. RIPSPs were evoked by antidromic stimulation of individual nerves at 20 Hz, the reason for using this frequency was described (Chapter 4).

Data analysis

In all α-MNs recorded, the presence or absence of a recurrent synaptic potential in response to homonymous and/or heteronymous motor pool stimulation was tested. For intracelluar records not showing a synaptic potenial, a measurable field potenial has to be present in order to accept the record for further analysis. Figure 5.2 shows two cases obtained from the same ABSM α-MN. Record (a) shows neither a synaptic potential nor a field potential, therefore, the record was excluded from further analysis. In record (b), a field potential but not a synaptic potential was detected, therefore, the record was

considered and counted as a lack of connectivity, see Table 5.1 in the result section. The presence of a motoneuron field potential provides evidence that the α-MN of interest is located in close anatomical proximity to the motor pool being antidromically stimulated. A factor that has been shown to have significant effect on RIPSP connectivity and peak amplitude (McCurdy and Hamm 1994). This serves to assure that the absence of a RIPSP from any particular source in an α-MN is not confounded by the anatomical location. i.e. its remote location from motor pools actively supplying recurrent inhibition.

Statistical analysis

Percentages were compared using the two-tailed Fisher Exact test. Factorial 2-way ANOVA was used to compare the means of RIPSP time course and amplitude because dependent variables were continuous while independent variables were categorical. Least squares means (LSmeans) adjusted for unbalanced design were used and compared. In addition the Mean ± SD was reported. Statistical help was obtained through the Wright State Statistical center, specifically (Bev Grunden).

Figure 5.2. ***Motoneuron field potential has to be present for successful inclusion of the record***. Intracelluarly recorded ABSM motoneuron showing the effect of antidromic activation of the LGS pool (a) and MG pool (b). Both of which didn't result in a detectable synaptic potential, however, a field potential was detected in (b). therefore, (b) and not (a) was included in the connectivity analysis.

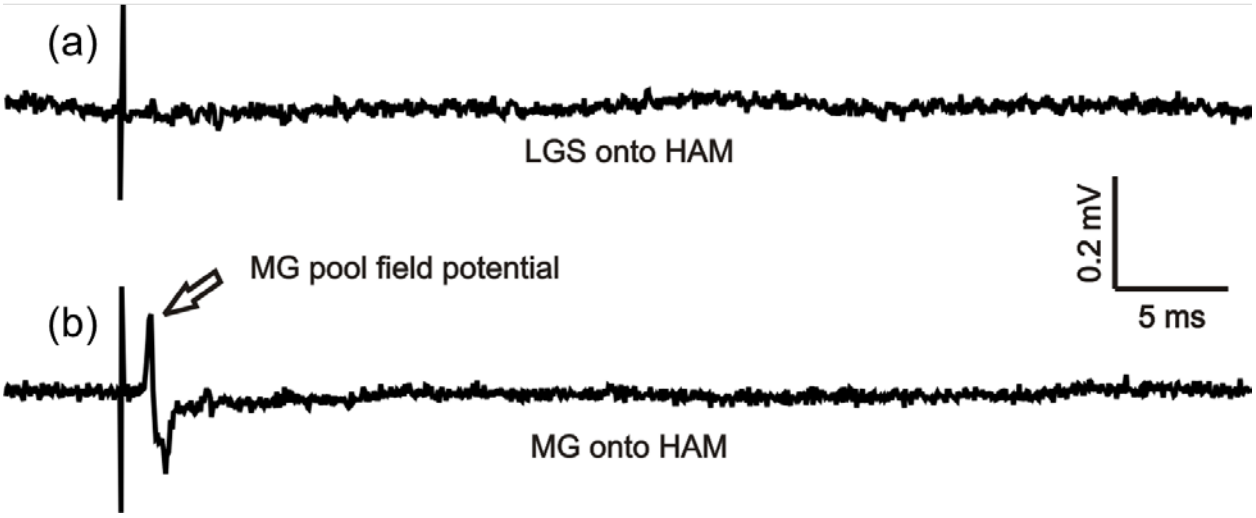
(a)
LGS onto HAM
0.2 mV
5 ms
MG pool field potential
(b)
MG onto HAM

Results

Our preliminary findings (in collaboration with Dr. Francisco Alvarez research group) that peripheral nerve regeneration fails to restore central axon collaterals after post injury loss led to the current work which is pursued to directly examine the consequences on the function of this unique and important spinal circuit. Connectivity and efficacy are the two primary determinants of circuit function and both were examined in detail in the current work.

Connectivity

This is defined as the presence of a measured recurrent synaptic potential in the motoneuron following the antidromic activation of other motoneurons in the same pool or in functionally synergist pools. In this thesis, motor pools were limited to MG, LGS, and ABSM (Figure 5.3). In control motoneurons, recurrent synaptic potentials were detected in 94% of the records exhibiting a field potential (n=273). On the other hand, recurrent synaptic potential were detected in only 78% of records obtained from MG regenerated rats and exhibiting a field potential (n=291, $P < 0.000001$, Chi-square, fisher exact test).

Connectivity for recurrent inhibition initiated by the regenerated motor pool and its close synergist (LGS)

As shown in (Figure 5.4), recurrent inhibition among synergists following peripheral nerve injury and regeneration did not fully recover despite successful peripheral

regeneration of the MG nerve. Regenerated MG neurons failed to re-establish normal connections in homonymous and heteronymous recurrent inhibitory circuits. Deficits were mainly detected in connections established with the relatively distant ABSM motor pool. Interestingly, LGS motor pool (LGS nerve wasn't surgically severed) also showed significant attenuations in homonymous connections and in connections established with the ABSM motor pool. This was accompanied by relative recovery of the functional connections established with the injured MG motor pool.

Figure 5.4 and Table 5.1 show the percent change in connectivity in MG regenerated rats. Successful connectivity refers to the presence of any detectable recurrent synaptic potential. The current results demonstrated that recurrent inhibition initiated by the regenerated motor pool or its closest synergist (LGS) were compromised.

Connectivity for recurrent inhibition initiated by remote synergist (ABSM)

Recurrent inhibition connections initiated by the ABSM pool (Table 5.2) and (Figure 5.5) showed no detectable or significant changes from controls regardless of the identity of the recipient motor pool. These observations ruled out the contribution of post synaptic factors to the observed decrease in connectivity observed in (Figure 5.4).

Recurrent synaptic potentials

Types of recurrent synaptic potentials

Figure 5.6 shows the three examples of recurrent synaptic potentials encountered during the current study, one typical example of a RIPSP (Figure 5.6a), one example of recurrent facilitation (Figure 5.6b) and a mixed recurrent synaptic potential, i.e. recurrent inhibition followed by recurrent facilitation (Figure 5.6c). The latter 2 types (b and c) were less frequently observed in our study. As shown in the figure, the onset of recurrent facilitation is typically longer (≈ 8 msec.) than recurrent inhibition (typically ≈ 2.5-3 msec.). The mixed type was more frequently observed than the pure recurrent facilitation; see also (Turkin et al 1998).

The prevalence of each of the events was expressed as a percent of all observations (recurrent inhibition, recurrent facilitation, and mixed potentials). Results are shown and compared across treatment groups in figure 5.7. The occurrence of recurrent inhibition tended to decrease in animals recovering from isolated peripheral nerve lesions as shown for all pathways tested (a – i). On the other hand, recurrent facilitation tended to appear more frequently in some pathways in the treated group (Figure 5.7, panels c, d, f, g, h, and i), and was mostly of the mixed type. The observed change in the prevalence of recurrent facilitation might indicate circuit re-organization (see discussion).

To summarize, the occurrence of recurrent inhibition initiated by the regenerated motor pool and its closest synergist was decreased while the occurrence for recurrent facilitation was relatively increased.

RIPSP time course after nerve regeneration

The time course of RIPSPs initiated by the MG motor pool or received by the MG motoneurons were compared in MG regenerated rats to control values. A generalized prolongation of the mean for RIPSP time course parameters (duration, half decay, and rise time) was seen in records obtained from MG regenerated rats in comparison to those recorded in controls. Figures 5.8 and 5.9 provide numerical values across different pathways tested. Interestingly, in rats with regenerated MG nerve, multiphasic RIPSPs were highly observed in contrast to records from controls (Figure 5.10 and Table 5.3). This type of RIPSP was more prolonged and might reflect changes in the firing behavior of Renshaw cells (Figure 5.14). Table 5.3 compares the prevalence of multiphasic RIPSPs in control and MG regenerated rats. Multiphasic RIPSPs were rarely observed in records obtained from controls. On the other hand, their prevalence in MG regenerated rats was much higher. Synaptic delay represented by RIPSP onset did not change is any of the pathways tested (Table 5.4).

In chapter 4 in this thesis, it was shown that RIPSP duration is important in determining the effect on motoneuron firing rate. Therefore, longer and multiphasic RIPSPs are expected to adversely affect motoneuron firing rate.

Figure 5.3. ***The three motor pools Labeled in the spinal cord***. Motor neurons were retrograde labeled with CTB (Cholera toxin). (a) Illustrates the location of the motor neurons in relationship to the regions and each other 4x. (b) & (c) illustrates 10x magnification of the MG, LG and ABSM motor neurons, the LG muscle was injected with 0.5% 488 conjugated CTB, the MG muscle was injected with 0.5% 647 conjugated CTB and the ABSM nerve was injected with 1% 555 conjugated CTB. 1 week after injections the rat was perfused with 4% paraformaldehyde and cut into 100 um thick longitudinal sections. The images were taken using the 4x on the RT-Spot epi-fluorescent scope and the 10x images were acquired on the Olympus FV1000 confocal microscope, Histology provided by Lori Goss and Jackie Sisco.

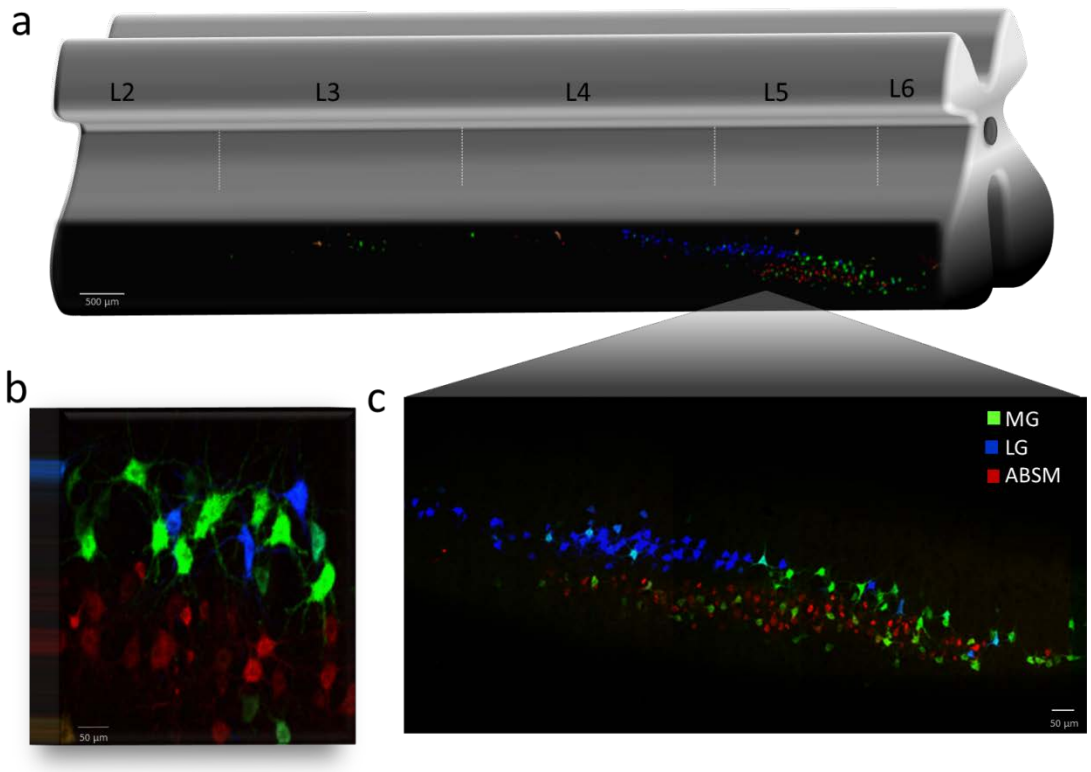
a
L2
L3
L4
L5
L6
500 µm
b
50 µm
c
MG
LG
ABSM
50 µm

Table 5.1. ***Connectivity initiated by the regenerated motor pool and its closest synergist is attenuated.*** Data comparing the recurrent inhibition connectivity observed in control and MG regenerated rats. Absolute numbers and percentages are shown. Statistical analysis: (2x2 tables, two-tailed Fisher exact test, G-statistics), significance $P < 0.05$.

Circuit Connectivity

Connection	Control	Regenerated	%Change	P-value
MG→ MG	45/46 (98%)	25/33 (76%)	-22%	0.0033
MG → LGS	22/22 (100%)	17/20 (85%)	-13%	0.099
MG → ABSM	33/37 (89%)	30/48 (63%)	-37%	0.006
LGS → LGS	22/22 (100%)	7/10 (70%)	-30%	0.024
LGS → MG	25/25 (100%)	21/24 (88%)	-15%	0.11
LGS → ABSM	36/39 (92%)	28/45 (62%)	-33%	0.0017

Figure 5.4. ***Connectivity initiated by the injured motor pool and its closest functional synergist (LGS).*** Diamonds represent motor neurons in the spinal cord; circles represent different Renshaw cell populations. Homonymous projections for triceps surae and heteronymous projections to ABSM showed significant decline of connectivity. Less dramatic decrease was seen in heteronymous projections between the close synergists (MG and LGS). Lower panel illustrates one example of synaptic occlusion frequently observed between MG and LGS but not between triceps surae and ABSM. This is why shared Renshaw pools are illustrated in the upper panel (brown pool)

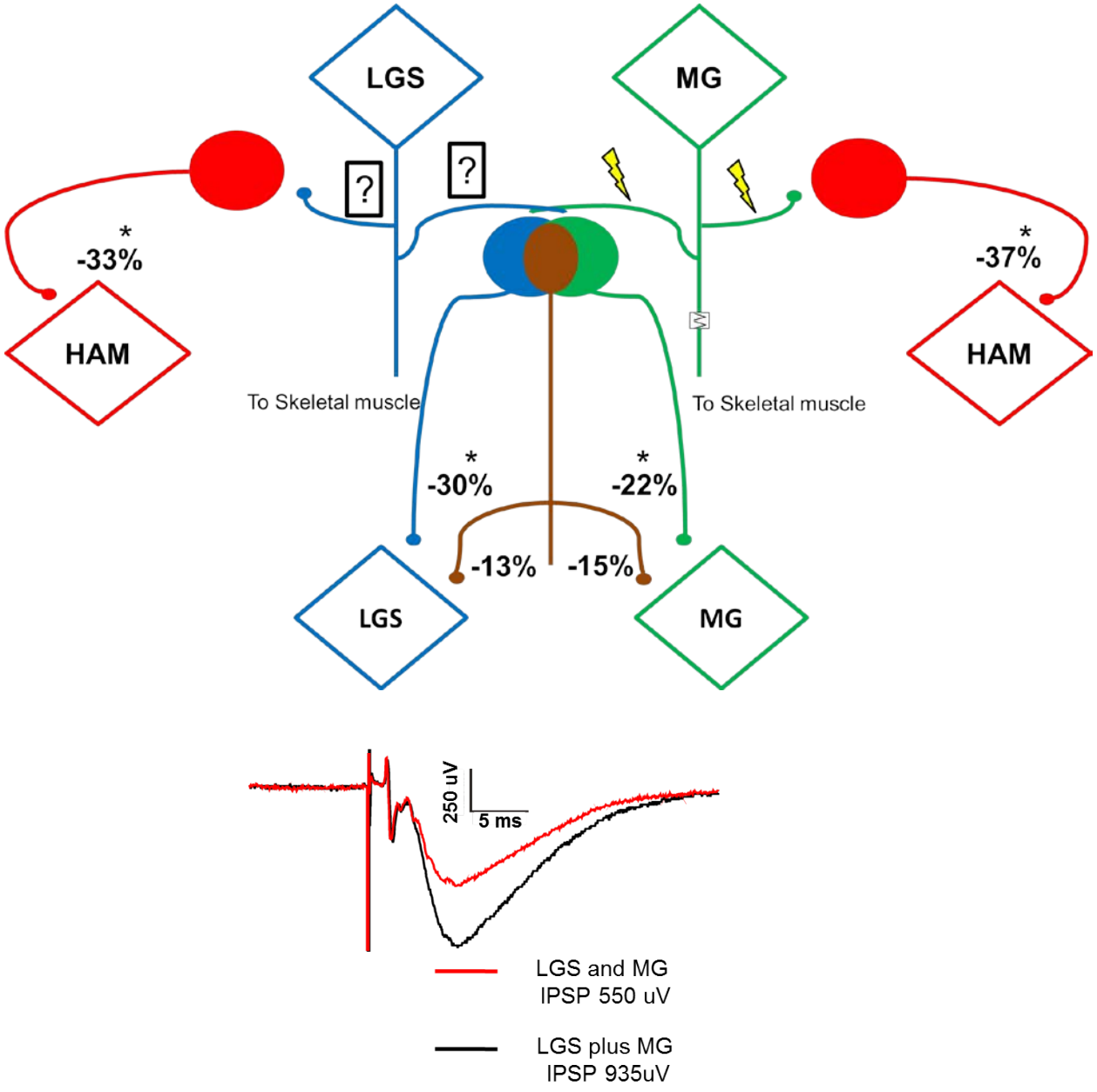

Note: MG and LGS frequently showed synaptic occlusion. This was not the case between ABSM and both Gastrocs. Earlier findings in the cat are in agreement

Figure 5.5. ***Connectivity initiated by the uninjured ABSM motor pool***. All connections initiated by the ABSM motor pool were not significantly different from those obtained in controls (Fishers exact G-statistics, $P>0.05$). Diamonds corresponds to α-motoneurons. Black circle illustrates Renshaw cell pool that receives input from ABSM and projects to MG and LGS.

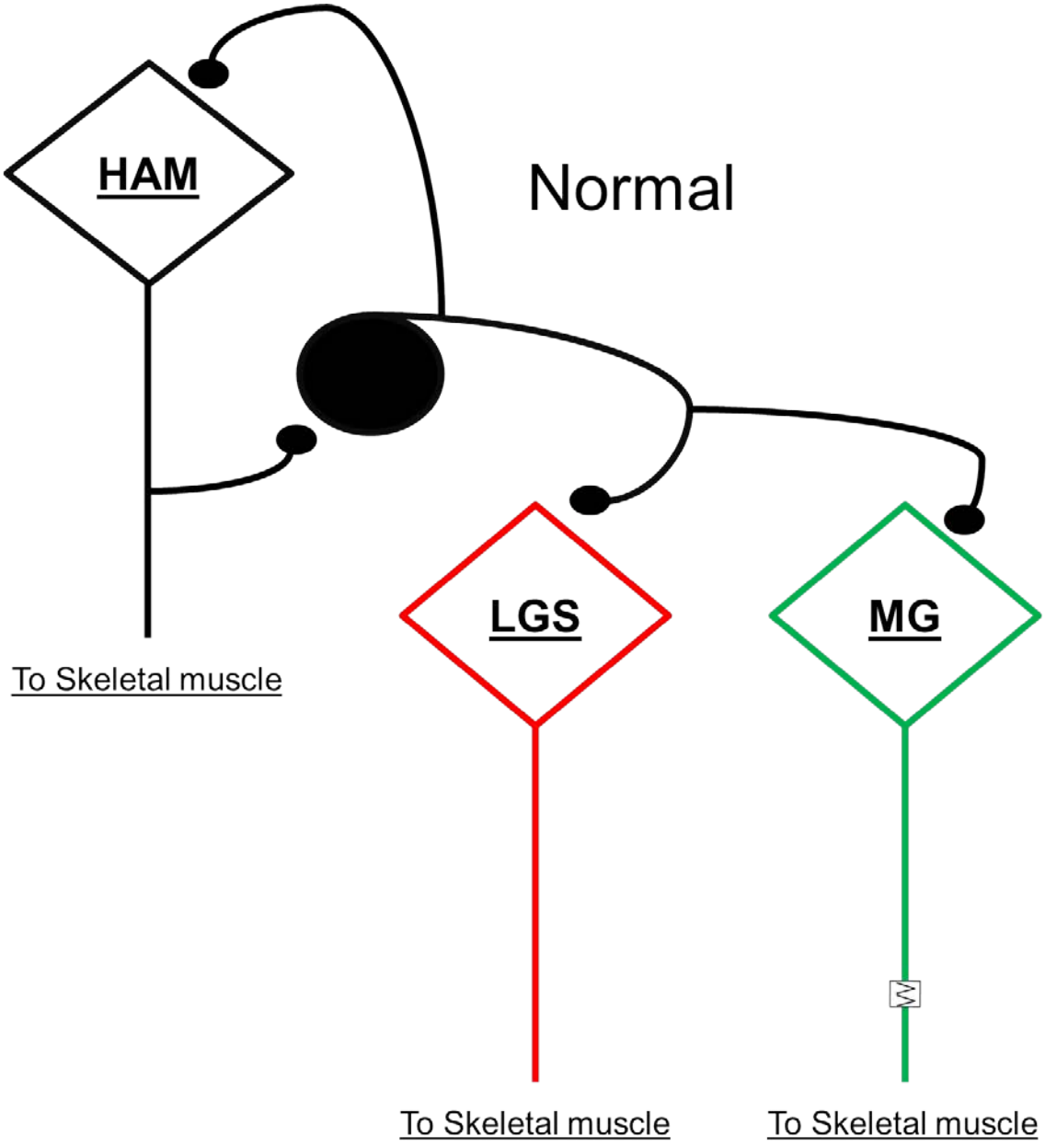
HAM
Normal
LGS
MG
To Skeletal muscle
To Skeletal muscle
To Skeletal muscle

Table 5.2. ***Homonymous and heteronymous connectivity initiated by the hamstrings motor pool in control and regenerated rats*.** Each row presents the proportion of cells that showed a detectable recurrent synaptic potential, percent, percent change, and statistical analysis (2x2 tables, two-tailed Fisher exact test, G-statistics), significance $P < 0.05$.

Circuit Connectivity

Connection	Control	Regenerated	%Change	P-value
ABSM→ MG	17/19 (89%)	25/28 (89%)	0%	1
ABSM → LGS	23/23 (100%)	25/25 (100%)	0%	1
ABSM → ABSM	32/40 (80%)	50/58 (86%)	+7.5%	0.42

Figure 5.6***. Recurrent synaptic potentials*.** Three types of recurrent synaptic potentials were encountered during data collection; recurrent inhibition (a), recurrent facilitation (b) or inhibition followed by facilitation (mixed) (c). Recurrent facilitation and the mixed type were observed more in rats with regenerated MG nerve. For more details, see text and Figure 5.7. Note the delayed onset for recurrent facilitation, open arrow heads, compared to recurrent inhibition (filled arrow heads); (I) inhibition, (F) facilitation.

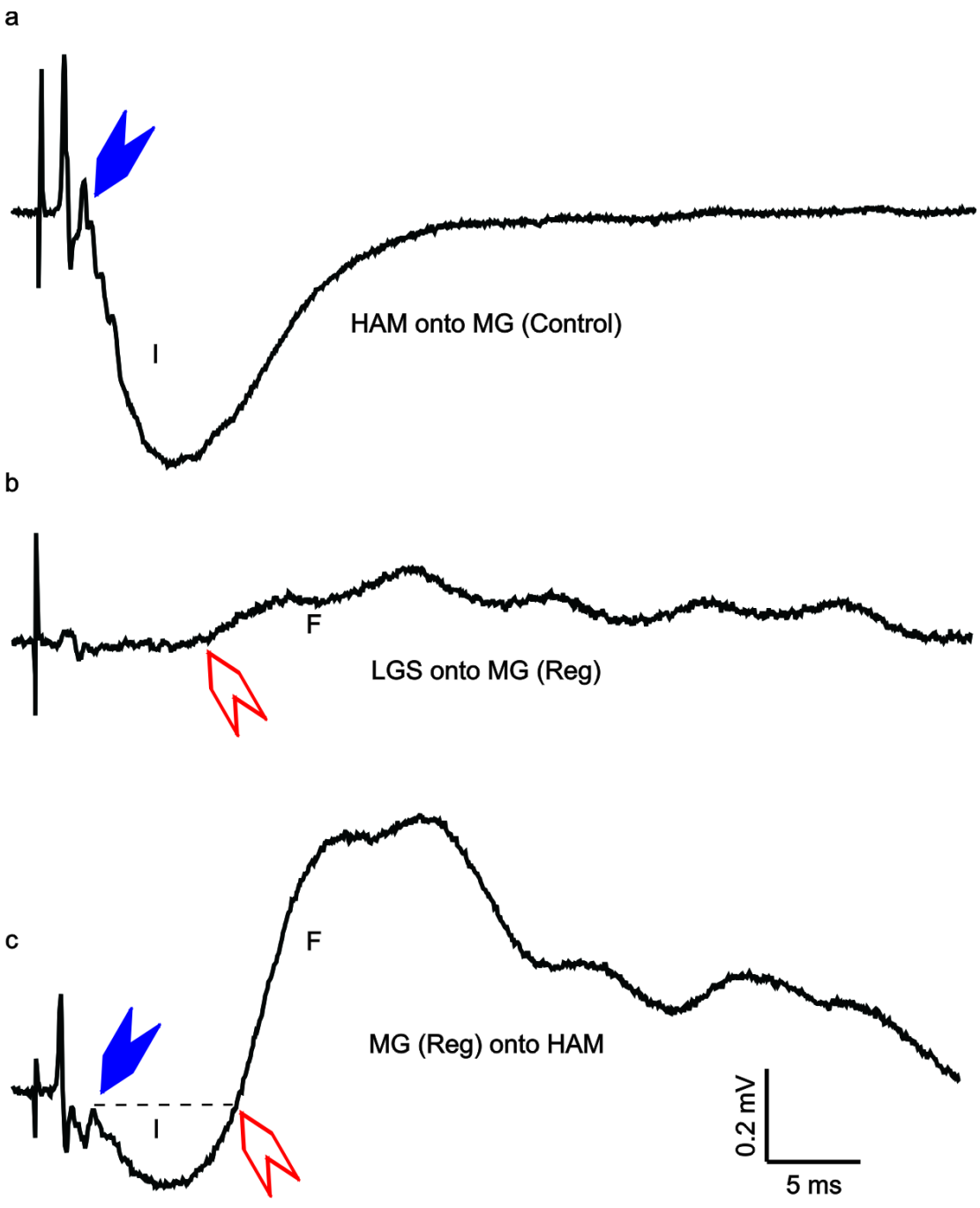
a
I
HAM onto MG (Control)
b
F
LGS onto MG (Reg)
c
F
I
MG (Reg) onto HAM
0.2 mV
5 ms

Figure 5.7. ***Recurrent synaptic potentials recorded in control and MG regenerated rats*.** Each panel shows the percentages of each of the four possibilities (recurrent inhibition, recurrent facilitation, mixed, or absence of any recurrent synaptic potential). Controls and in MG regenerated animals are compared. (a – c), (d – f) and (g – i) correspond to outcomes measured in different pools of motoneurons after antidromic stimulation of the MG, LGS, and ABSM nerves, respectively. Statistical analysis: (2x2 tables, two-tailed Fisher exact test, G-statistics), significance $P < 0.05$.

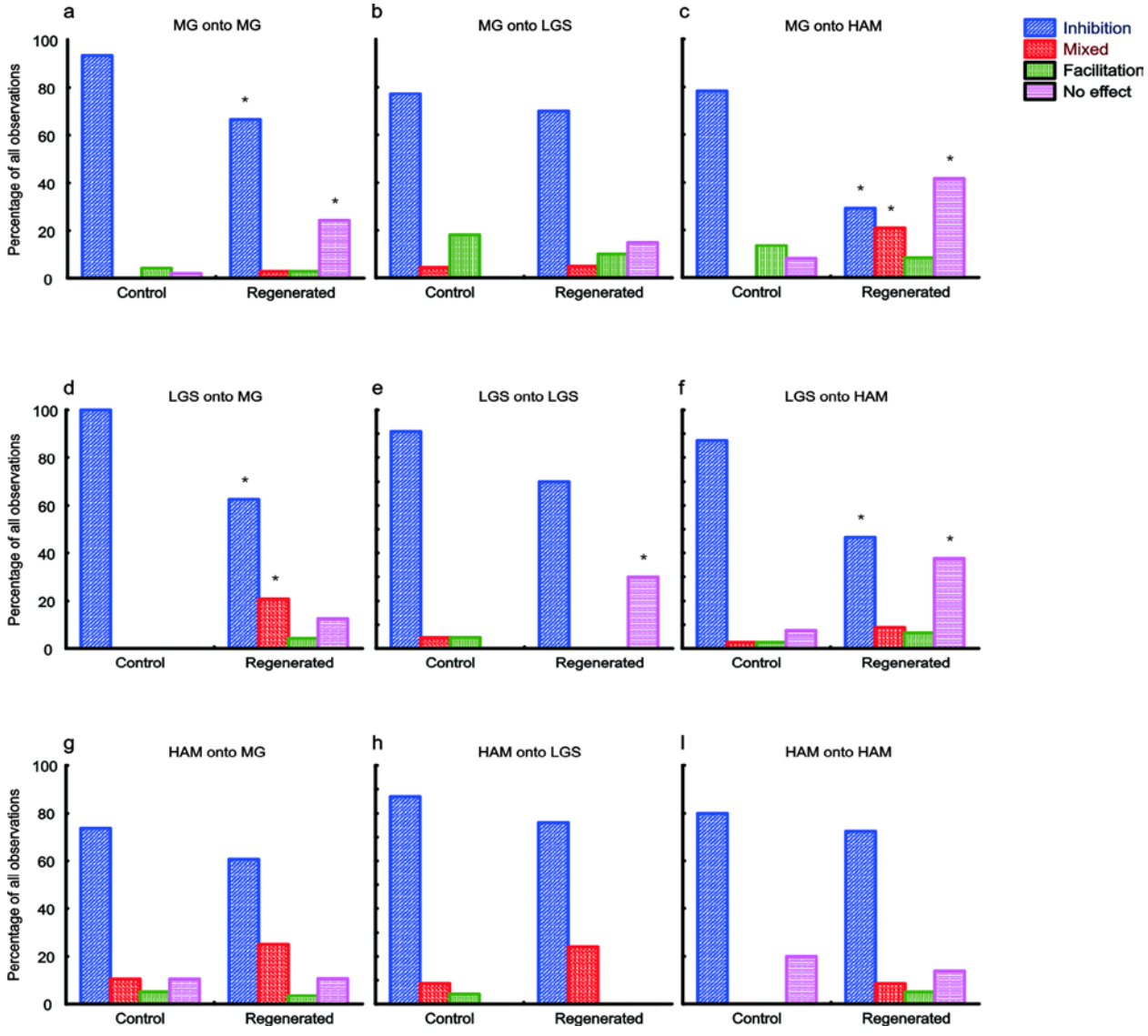
a
MG onto MG
b
MG onto LGS
c
MG onto HAM
d
LGS onto MG
e
LGS onto LGS
f
LGS onto HAM
g
HAM onto MG
h
HAM onto LGS
i
HAM onto HAM
Percentage of all observations
100
80
60
40
20
0
Control
Regenerated
Inhibition
Mixed
Facilitation
No effect

Figure 5.8***. Time course parameters for RIPSPs initiated by the regenerated motor pool and recorded from uninjured LGS or ABSM motoneurons.*** All durations are expressed in milliseconds. Significant prolongation of RIPSP duration and rise time was observed in this pathway. Half decay time also increased but did not achieve statistical significance. Statistics: Factorial 2-way ANOVA.

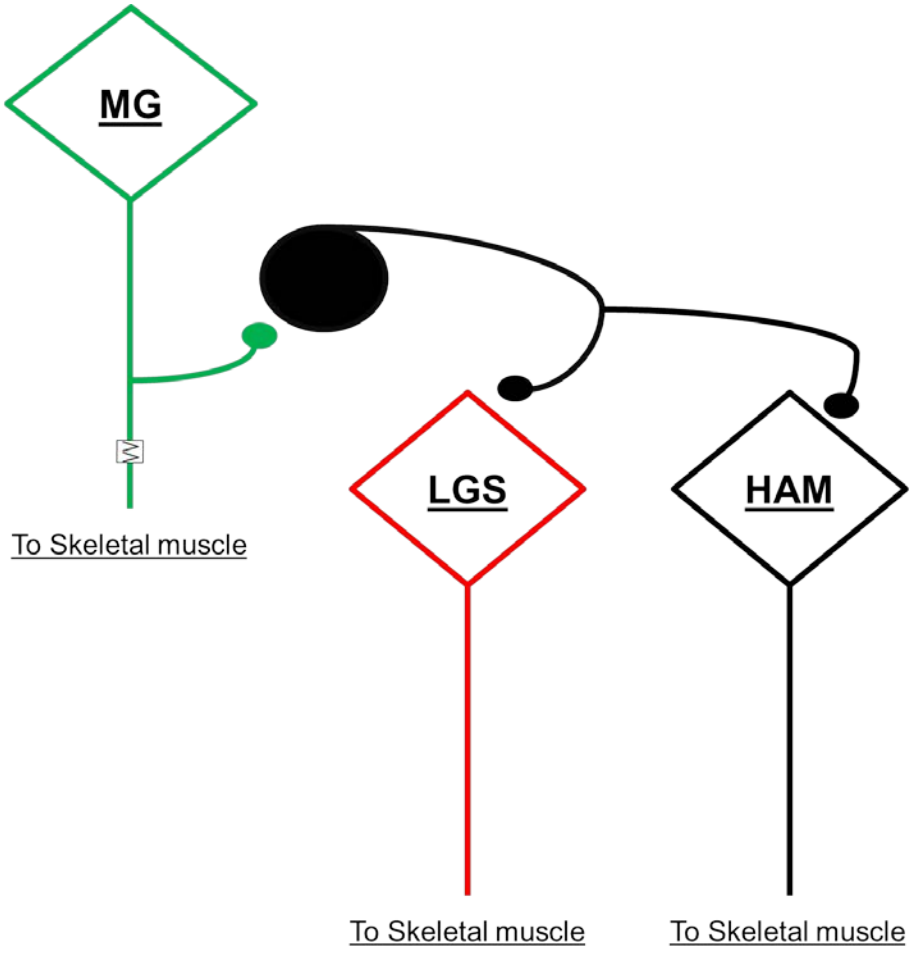

	(control)	(regenerated)	% change	P-Value
Duration (Mean ± SD)(n)	26.3±6.7 (21)	32.2±7.6 (15)	+22.4%	0.0163
Rise time (Mean ± SD)(n)	4.5±0.9(21)	6.4±2.5(14)	+42.2%	0.0067
Half decay time (Mean ± SD)(n)	7.5±1.6 (21)	8±3.8 (15)	+6.7%	0.55

Figure 5.9. ***Time course parameters for RIPSPs initiated by uninjured LGS or ABSM motor pool and recorded in injured MG motoneurons***. All durations are expressed in milliseconds. RIPSPs initiated by uninjured motor pools and recorded in regenerated MG motoneurons also showed a generalized and significant prolongation in all time course parameters. Statistics: Factorial 2-way ANOVA.

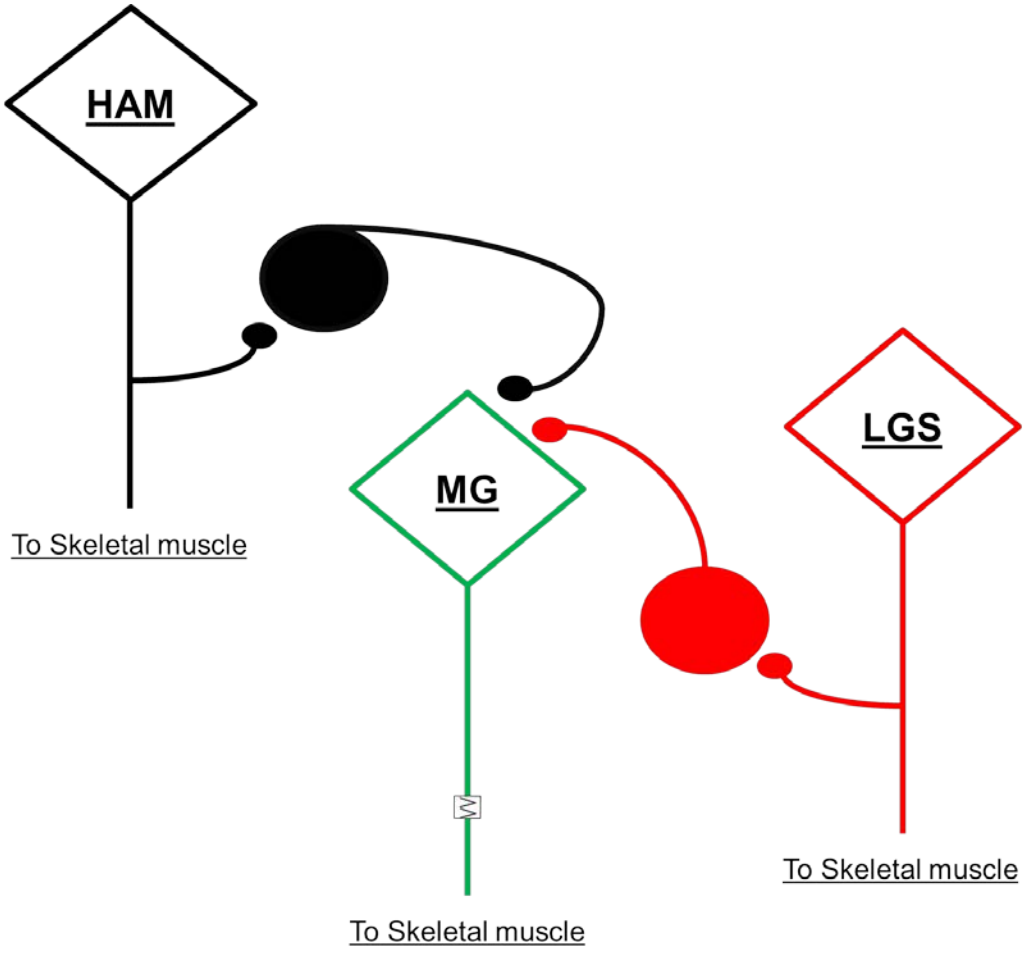

	(control)	(regenerated)	% change	P-Value
Duration (Mean ± SD)(n)	23.4±2.2 (28)	29.3±5.2 (28)	+25%	0.0164
Rise time (Mean ± SD)(n)	4.9±1.3(28)	6.8±4.1(27)	+39%	0.0067
Half decay time (Mean ± SD)(n)	6±1.4 (28)	8±4 (28)	+33%	0.0064

Figure 5.10***. RIPSPs show different time courses.*** An illustration of two examples of RIPSPs in control (a) and MG regenerated (b) rats. Both were recorded from a ABSM motoneuron and were initiated by antidromic stimulation of the MG nerve. Both resulted in a hyperpolarization of the cell resting potential, but qualitatively faster with the RIPSP in (a) compared to the one in (b) which showed a second phase of hyperpolarization starting ≈ 10 milliseconds following the beginning of the RIPSP decay (multiphasic RIPSPs), see Table 5.3 and text for more details.

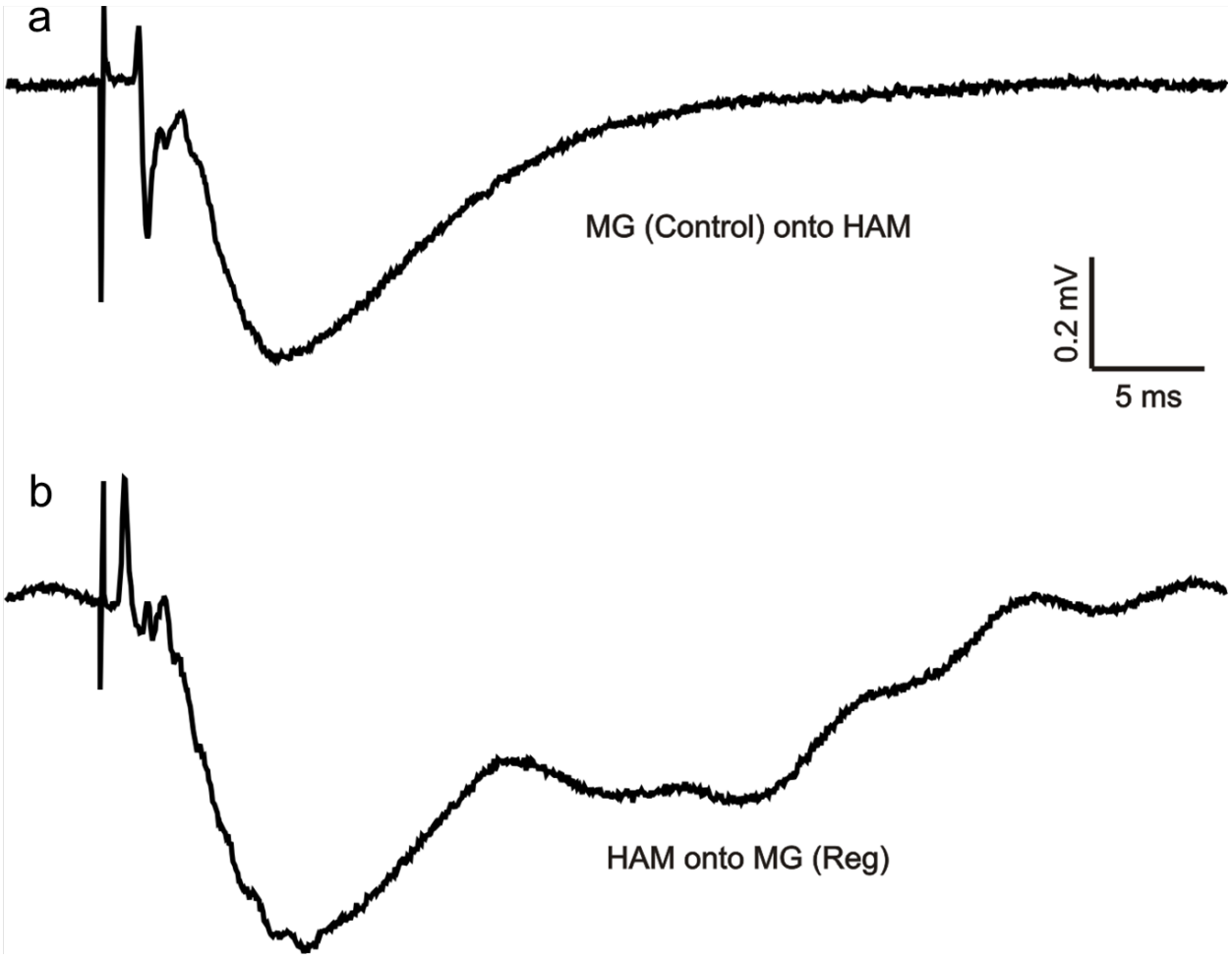
a
MG (Control) onto HAM
0.2 mV
5 ms
b
HAM onto MG (Reg)

Table 5.3***. Percent of multiphasic RIPSPs in regenerated rats compared to controls.*** In almost all pathways from and to regenerated motoneurons except (LGS → MG), the prevalence of multiphasic RIPSPs in MG regenerated rats was significantly higher than in controls. Statistical analysis: (2x2 tables, two-tailed Fisher exact test, G-statistics), significance $P < 0.05$.

% of multiphasic RIPSP

	Control	Regenerated	P-Value
MG → MG	7/43 (16.3%)	11/22 (50%)	0.0074
MG → LGS	1/17 (6%)	9/14 (64%)	0.0012
MG → ABSM	0/27 (0%)	8/16 (50%)	0.0001
LGS → MG	5/25 (20%)	3/15 (20%)	1
ABSM → MG	1/14 (7%)	10/17 (59%)	0.0068

Table 5.4. ***RIPSP onset showed no significant changes after nerve regeneration***. In all pathways tested, no significant differences were detected in RIPSP onset measured in millisecond delay after the peripheral electrical shock; others refer to LGS and ABSM.

	Control (Mean ± SD)(n)	Regenerated (Mean ± SD)(n)	P- Value
MG → MG	3.1 ± 0.5 (27)	2.9 ± 0.3 (5)	0.16
MG → Others	3.1 ± 0.34 (21)	2.9 ± 0.22 (10)	0.28
Others → MG	2.6 ± 0.38 (28)	2.7 ± 0.36 (19)	0.08
Others → Others	2.7 ± 0.4 (56)	2.6 ± 0.33 (43)	0.26

Maximum amplitude of RIPSPs and nerve regeneration

The peak amplitudes of RIPSPs either initiated by the MG motor pool or recorded in MG motoneurons were measured and the means were compared across treatment groups. Measures of RIPSP amplitude are dependent on uncontrolled variables, resting Vm (Figure 5.1) and field potential magnitude (FP), i.e. proximity to the active motor pool supplying Renshaw inhibition and an observation that within the same cell, if the strength of the electrical stimulus is changed, RIPSP amplitude will follow this change. These are strong dependencies and were taken into account here. Only RIPSPs recorded at resting potentials of $\leq$ -55 mV were included in all subsequent numerical comparative analysis and the Mean ± SD for Vm in both treatment groups was calculated and compared for any statistical differences (Figures 5.11 and 5.12).

RIPSPs were grouped as follow: initiated by MG motor pool (regenerated) and recorded in either LGS or ABSM motoneurons (uninjured) (Figure 5.11) or initiated by either LGS or ABSM motor pools (uninjured) and recorded in MG motoneurons (regenerated), (Figure 5.12).

RIPSPs initiated by regenerated MG motor pool and recorded from uninjured motoneurons tended to have smaller amplitude (-65%). However, when correction for FP was made, no significant differences were observed, $P>0.05$ (Figure 5.11).

On the other hand, RIPSPs initiated by uninjured motor pools and recorded from regenerated motoneurons, (Figure 5.12) showed no significant differences from control values, in fact, a tendency for larger amplitudes was observed in regenerated animals.

In Figure 5.13, the ratio RIPSP amplitude / FP of records initiated by the injured motor pool and recorded from uninjured synergists was plotted against Vm. The green triangles represent records obtained in MG regenerated rats. Red diamonds represent controls. RIPSP amp /FP ratio tended to cluster at lower values, mostly <1, but didn't achieve statistical significance.

Renshaw cells after nerve regeneration

Intracellular recording from Renshaw cells revealed a change in their firing behavior. One representative example is shown in (Figure 5.14). In comparison with the control record, upper panel in (Figure 5.14), the duration of Renshaw cell firing was longer and more action potential spikes were fired in response to each impulse, lower panel in (Figure 5.14). This finding help explain changes in RIPSP time course parameters in rats with MG nerve regeneration.

Figure 5.11. ***Recurrent inhibition initiated by regenerated motor pool***. Maximum amplitude and membrane potential for RIPSPs initiated by the MG motor pool and recorded in either LGS or ABSM motoneurons in control and MG regenerated rats. FP: Field potential (Figure 5.2), the Amp/FP ratio controls for the proximity of the recorded motoneuron to the active motor pool supplying recurrent inhibition.

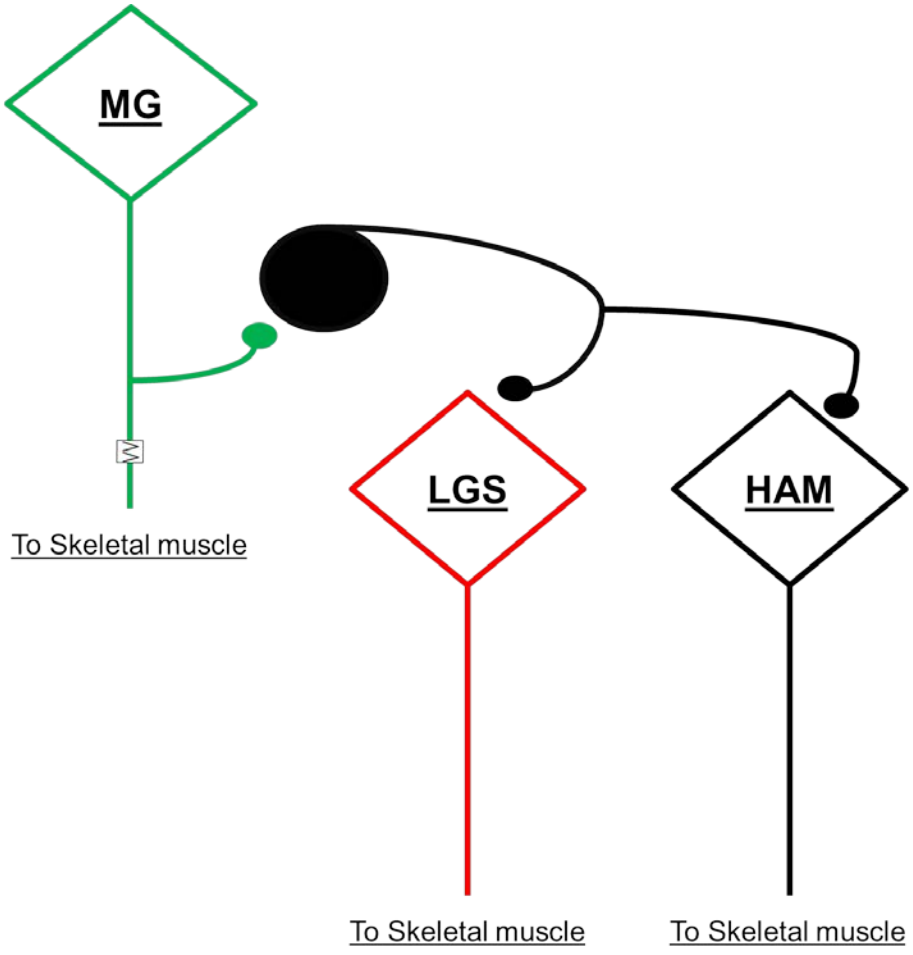

	Control	Regenerated	% change
Amplitude, µV (Mean ± SD)(n)	185±177 (20)	65±43 (13)	-65%
Vm, mV (Mean ± SD)(n)	-66±7 (20)	-64±5 (12)	+3%
Amp/FP (Mean ± SD)(n)	1.6±1.4 (18)	0.8±1.4 (12)	-50%

Figure 5.12. ***Recurrent inhibition received by the regenerated motoneurons***. Maximum amplitude and membrane potential for RIPSPs initiated by either LGS or ABSM motor pools and recorded in MG motoneurons in control and MG regenerated rats. FP: Field potential, the Amp/FP ratio controls for the proximity of the recorded motoneuron to the active motor pool supplying recurrent inhibition.

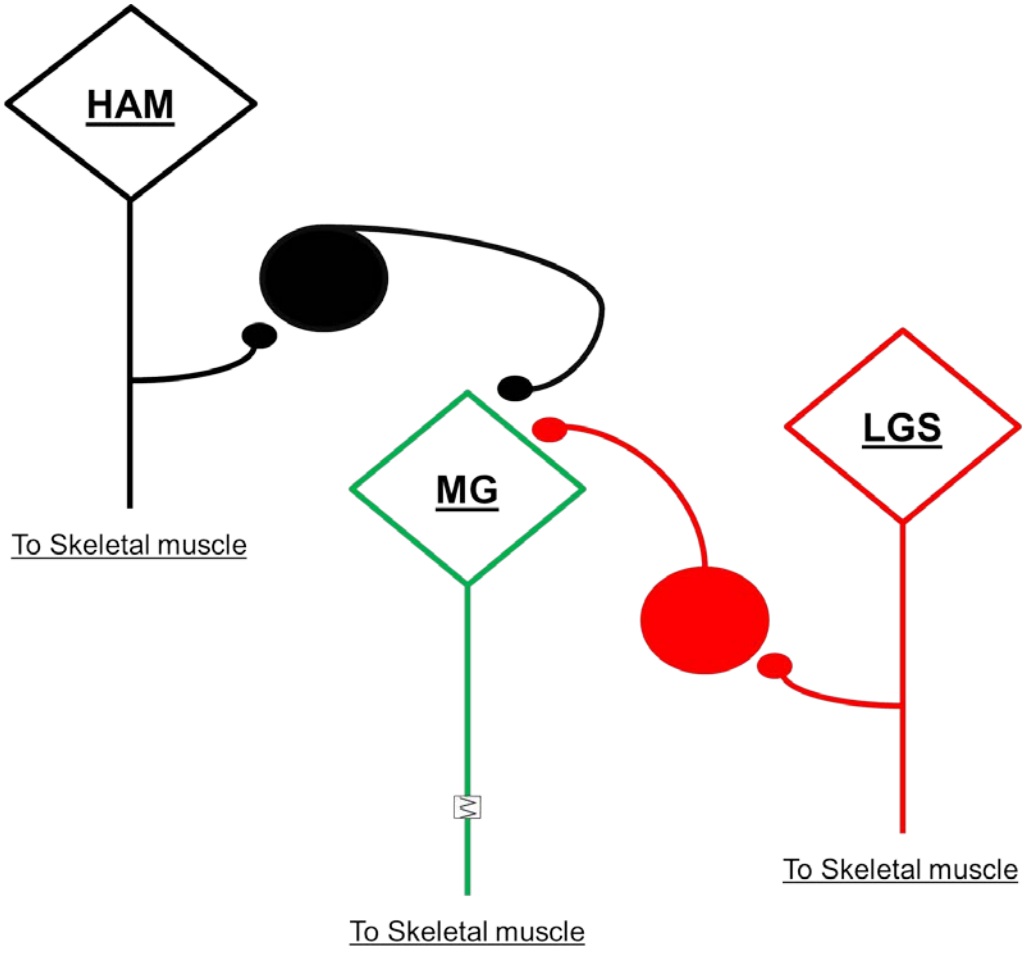

	Control	Regenerated	% change
Amplitude, µV (Mean ± SD)(n)	172±190 (20)	283±333 (23)	+65%
Vm, mV (Mean ± SD)(n)	-66±8(20)	-66±6(23)	0%
Amp/FP (Mean ± SD)(n)	1.3±1.1(20)	1.6±1.2(23)	+23%

Figure 5.13. ***Resting membrane potential and RIPSP amp/FP in control and MG regenerated rats.*** The plot represents RIPSP amp / FP for 32 RIPSPs initiated by the regenerated motor pool. Abscissa: resting Vm; Ordinate: RIPSP amplitude / field potential, correction for proximity.

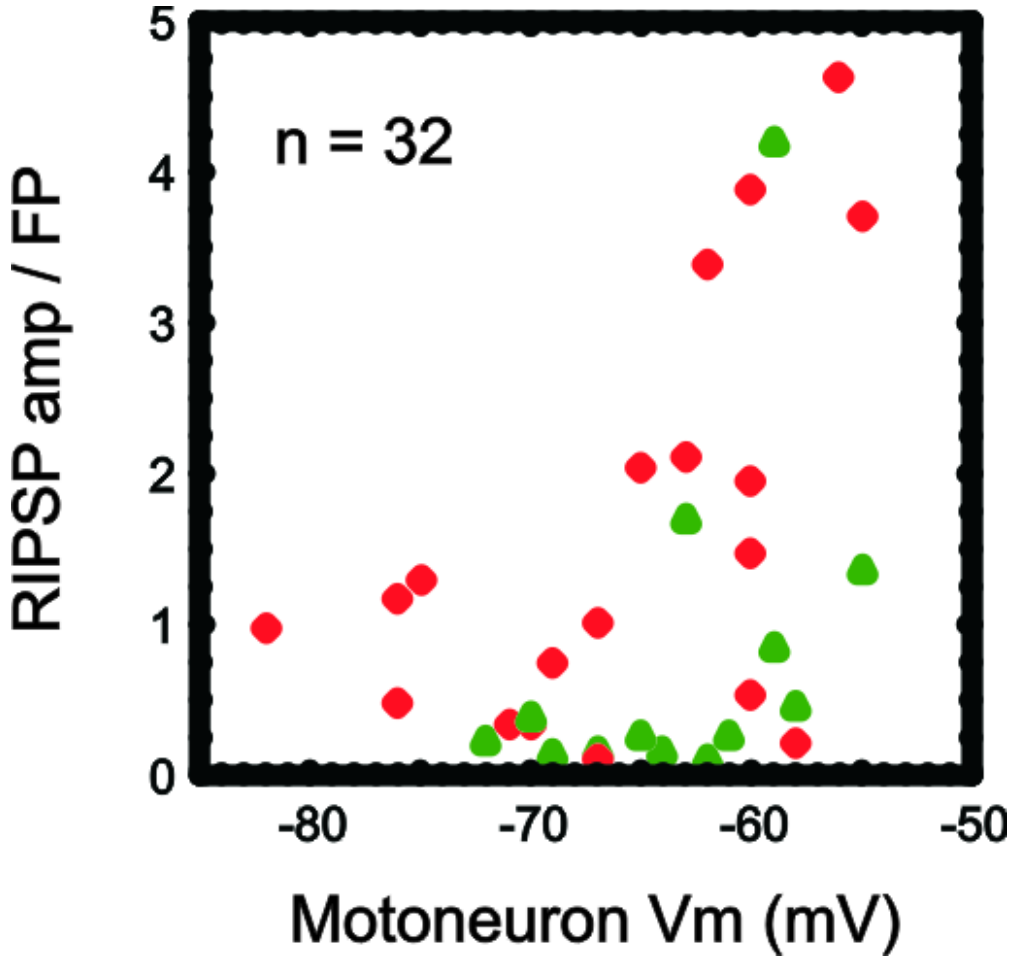
n = 32
RIPSP amp / FP
Motoneuron Vm (mV)
0
1
2
3
4
5
-80
-70
-60
-50

Figure 5.14***. Renshaw cell firing response to single antidromic impulses in control and regenerated rats.*** This shows a dramatic prolongation of firing, both records were obtained at resting Vm of -60 mV. Upper panel (control), lower panel (regenerated)

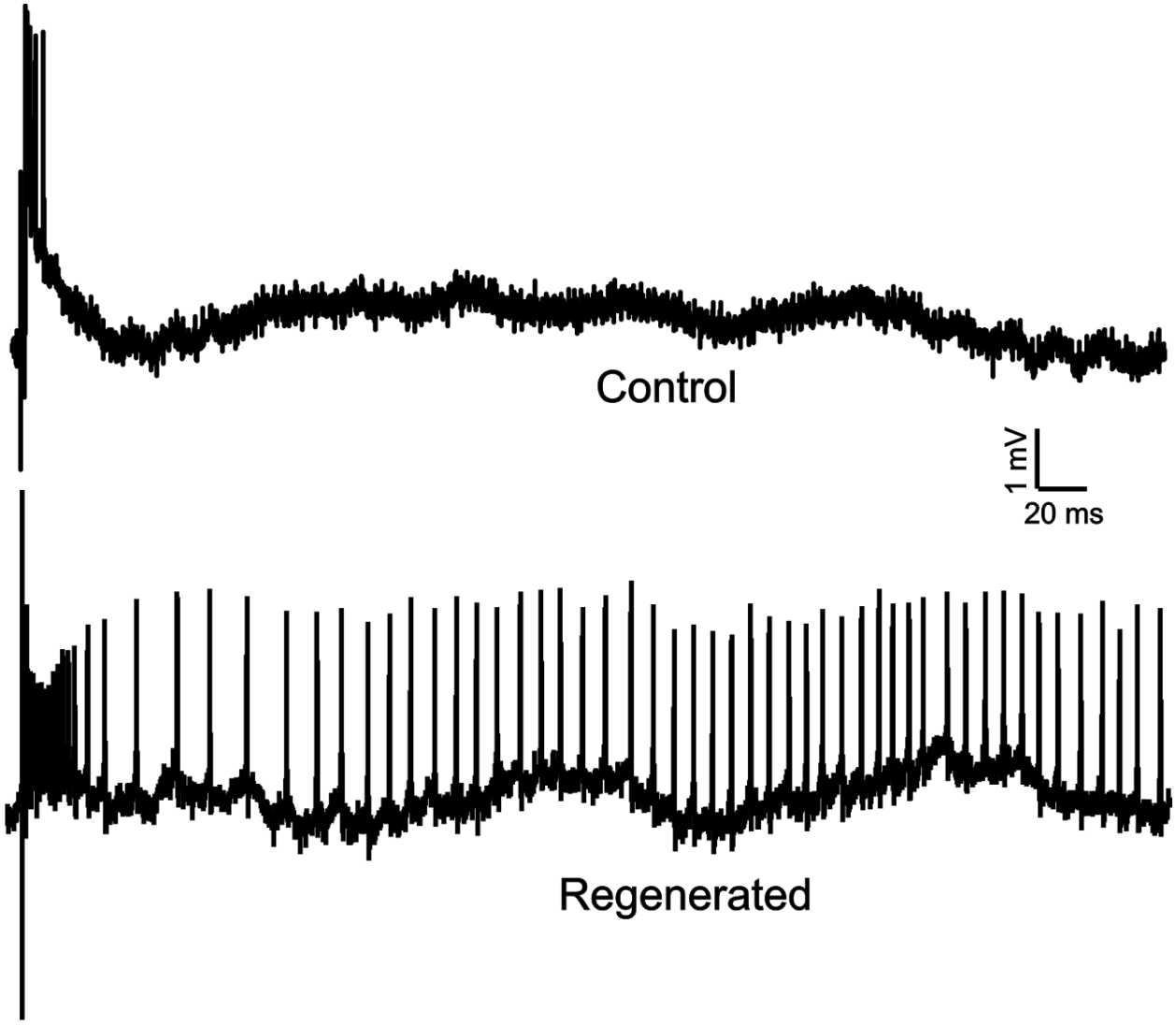
Control
1 mV
20 ms
Regenerated

Discussion

The current work has examined the plasticity of a central spinal cord circuit in response to an isolated and peripherally located nerve injury. Earlier studies reported what can be referred to as dissociation between structure and function (Havton and Kellerth 1990a; Havton and Kellerth 1990b). Despite permanent loss of recurrent axon collaterals, the function of Renshaw inhibition was fully recovered at 12 weeks post injury and ligation. The present study was designed to answer the following main questions: Can peripheral nerve regeneration help central axon collaterals to regenerate? And can it also restore normal function? This was based on the fact that previous work did not allow nerve regeneration and used nerve ligation instead. Also, most injured peripheral nerves will undergo some degree of regeneration, whether assisted or natural re-growth of the peripheral axons. So, the current model is expected to provide novel and clinically relevant information.

To answer the important question of whether nerve regeneration can rescue axon collaterals, several α-MNs in control and MG regenerated rats were intracellularly filled *in vivo* with neurobiotin (in our lab), and their axon collaterals were quantitatively analyzed in Dr. Francisco Alvarez laboratory (data not shown). Unforeseen results were obtained and nerve regeneration failed to restore central axon collaterals (unpublished observations). Permanent reduction of recurrent collaterals was seen despite successful nerve regeneration.

The striking full functional recovery despite permanent structural abnormalities following nerve ligation (Havton and Kellerth 1984; Havton and Kellerth 1990a; Havton and Kellerth 1990b) raised some questions that were addressed by the current work. First, Renshaw inhibition is known to be distributed unevenly across motor pools and α-MNs of different types within the same pool (Wilson, Talbot et al. 1960; Eccles, Eccles et al. 1961; Friedman, Sypert et al. 1981; Hultborn, Lipski et al. 1988; McCurdy and Hamm 1994). Therefore, in any experiment, whether a control or a treated animal, it is expected to find no evidence for recurrent inhibition in some α-MNs. This is especially important in experiments where one or few motor nerves are electrically stimulated, i.e. one or few motor pools are antidromically active and are supplying Renshaw inhibition. Work that has been done before did not take this into consideration, i.e. did not examine the possibility of loss of connectivity. Therefore, it was examined in the current work.

It is of great importance to correlate connectivity with anatomical findings in the work of both groups (ours and Havton and Kellerth). The observed permanent reduction in recurrent collaterals might not only affect RIPSP maximum amplitude but rather can affect connectivity. This indeed was the case as shown in this study. In fact Renshaw inhibition initiated by the regenerated motoneurons showed less connectivity with all motor pools. This is highly consistent with anatomical findings observed in all the work that has been done to date.

Surprisingly, Renshaw inhibition initiated by the uninjured LGS motor pool, the closest synergist to MG, showed significant reductions in connectivity even when supplying

Renshaw inhibition to the uninjured ABSM pool (Figure 5.4). This observation leads to speculations about possible mechanisms of this loss. First, MG and LGS are very close synergists and are known to share pools of Renshaw cells, see synaptic occlusion studies (Figure 5.4) and (Eccles, Eccles et al. 1961a). Shared Renshaw cells have suffered from partial denervation as a result of permanent reduction of MG axon collaterals (Havton and Kellerth 1990a; Havton and Kellerth 1990b). Their partial denervation might induce secondary changes in LGS axon collaterals, i.e. the injury signal might extend and cause secondary reduction in LGS axon collaterals. This possibility is currently under investigation in collaboration with Dr. Francisco Alvarez at Emory University. Results are expected to appear in future reports.

On the other hand, the ABSM motor pool showed no detectable attenuation of connections projecting to all examined motor pools (ABSM, MG and LGS). This is consistent with the smaller degree of synaptic occlusion seen between the ABSM motor pools and the triceps surae pools, and thus, Renshaw cells receiving input from ABSM are not expected to be involved directly in the injury process and are not expected to suffer from partial de-innervation (Eccles, Eccles et al. 1961a).

Based on the above connectivity studies, one could conclude that selective and remote insult to one motor pool can result in generalized functional deficits that extend to Renshaw inhibition initiated by the closest motor pools (LGS) but not to (ABSM). The current work provided the first evidence that connectivity of this circuit is altered following peripheral nerve injury.

Recurrent inhibition was the most prevalent type of recurrent synaptic potential encountered in this study, and reported by previous studies (Wilson, Talbot et al. 1960; McCurdy and Hamm 1994a). Recurrent facilitation with or without preceding inhibition was also recorded but to a lesser extent. An interesting and sometimes significant increase in the prevalence of recurrent facilitation was seen in many pathways in MG regenerated rats (Figure 5.7). Several mechanisms were suggested to explain recurrent facilitation. In their Figure 6, McCurdy and Hamm proposed three mechanisms for recurrent facilitation. One being mutual inhibition among Renshaw cells first described in (Ryall, Piercey et al. 1971). Another possibility was proposed for the mixed type where the excited motoneuron inhibits other motoneurons via Renshaw cells that also inhibit other Renshaw cells and therefore results in a mixed synaptic potential. The third proposed mechanism was the direct excitation between motoneurons (for short latency facilitation which was not seen in the current work).

So, all proposed mechanism for recurrent facilitation requires strong recurrent inhibition to start with, i.e. the stronger the mutual inhibition between Renshaw cells, the stronger the recurrent facilitation. The current study showed that recurrent inhibition strength was not significantly increased. Therefore, one would not expect to see an increase in the expression of recurrent facilitation. However, recurrent facilitation actually increased in occurrence and in amplitude after nerve regeneration (data not shown). Another way of looking at mutual inhibition might be through examining the behavior of Renshaw cells after nerve regeneration. Here a few cells were recorded from and one representative

example was shown (Figure 5.14). The prolongation of Renshaw firing might in fact explain the increase in recurrent facilitation observed after nerve injury, i.e. prolonged firing of some Renshaw cells might increase mutual inhibition, and thus recurrent facilitation.

On the other hand, one might actually wonder if recurrent facilitation is an independent spinal cord circuit that is unmasked by the reduction in recurrent inhibition. One possibility might be through the interneuron of Machacek and Hochman (Machacek and Hochman 2006). In their study in the neonatal rodent, these authors have unmasked a novel recurrent excitatory circuit with the drug Noradrenalin. Ventral root evoked reflexes through this circuit were 5 msec. longer than the monosynaptic reflex in the same preparation. This is in good agreement with our latency measurements for recurrent facilitation that were 5 msec. longer than the latency for recurrent inhibition (Figure 5.6). So, this suggests that similar or may be the same circuit exists in the adult rat and might be unmasked in MG regenerated rats.

Next, the possibility of plastic changes in RIPSP time course was addressed. Figure 2 in (Havton and Kellerth 1990b) illustrates one example of a RIPSP initiated by the injured motor pool and recorded from uninjured synergist (soleus), from their illustration, one might wonder about the possibility of a prolonged time course since the total duration of that RIPSP was more than 80 milliseconds in contrast to normal values reported from the cat work that are usually ≈ 40 – 50 msec. (Eccles, Fatt et al. 1954)

Renshaw cells fire in brief repetitive trains in response to single impulses arriving at the α-MN - Renshaw synapse, site 1 in (Figure 1.2). Also, as shown in chapter 4, the duration of Renshaw cell firing can affect the time course of the RIPSP. Therefore, Renshaw cells might increase their firing duration in response to the denervation caused by recurrent collateral loss. If this effect was global, then one would expect longer RIPSPs in regenerated α-MNs and even in uninjured synergistic α-MNs that share part of a common Renshaw pool. Also, if Renshaw cells are coupled by gap junctions as suggested recently (Lamotte d'Incamps, Krejci et al. 2012), one might expect a generalized prolongation in RIPSP durations after nerve regeneration.

Indeed this was the case; we observed a generalized prolongation of the time course of RIPSPs recorded from MG regenerated rats. This prolongation was not restricted to RIPSPs recorded from regenerated α-MNs. In addition, direct intracellular recordings from Renshaw cells revealed a "transformation" in Renshaw cell responses to single impulses arriving at the α-MN-Renshaw synapse; instead of brief repetitive firing as seen normally in the rat, Renshaw cells responded with a dramatically prolonged and sustained repetitive firing behavior (Figure 5.14).

Finally, RIPSP maximum amplitudes were examined after nerve regeneration and compared to controls. Previous work has reported at least full recovery of RIPSPs measured by maximum amplitude and by total area (Vm × ms) (Havton and Kellerth 1990b). Several points shall be addressed here: For example, one important feature of RIPSP maximum amplitude is that it is highly sensitive to motoneuron membrane

potential changes (Eccles, Eccles et al. 1961; McCurdy and Hamm 1994) and (Figure 5.1). Therefore, whenever amplitudes are compared, Vm has to be accounted for. Those accounts were lacking in the described cat work. The current study included RIPSPs that were recorded at Vm ≤ -55 mV and the mean ± SD for Vm for each of the compared groups was reported and tested for any significant differences. Therefore, Vm differences cannot account for the observed decrease in RIPSP amplitude observed in some pathways in this study.

In addition, intracellular motoneuron field potential magnitude was measured and considered in RIPSP amplitude analysis. This is of significant importance since proximity to the active motor pool supplying Renshaw inhibition can influence the maximum amplitude of the RIPSP (McCurdy and Hamm 1994). Interestingly, the ratio between RIPSP amplitude and field potential amplitude tended to decrease in α-MNs recorded from MG regenerated rats; however, no significant differences were detected.

In summary, the current work demonstrated that permanent functional deficits are observed despite peripheral nerve regeneration in contrast to (Havton and Kellerth 1990b). First, significant reductions in connectivity of recurrent inhibition initiated by the regenerated motor pool and its closest synergist (LGS) were shown. This was accompanied by a significant increase in recurrent facilitation. Second, RIPSPs recorded from α-MNs in regenerated rats showed significant increase in duration and / or other time course parameters. Finally, Renshaw cells fired larger number of spikes and for longer durations in MG regenerated rats. Therefore, it appears that Renshaw cells are one

site of compensation for the permanent loss of axon collaterals; however, the compensation might actually be counterproductive since it results in longer RIPSPs that might adversely affect α-MN firing behavior (Chapter 4).

In conclusion, the current work provided another example that successful peripheral nerve regeneration failed to restore the structure (in collaborative studies) and function of important spinal cord circuits, see (Cope, Bonasera et al. 1994; Alvarez, Titus-Mitchell et al. 2011; Bullinger, Nardelli et al. 2011). The current work showing permanent dysfunctions in Renshaw inhibition function after nerve injury and successful regeneration might help to identify potential targets for pharmacological treatment to improve motor function in victims living with regenerated nerves.

Chapter 6: General discussion

The work presented in this thesis was designed to advance the current knowledge about a spinal cord circuit that was first described more than 70 years ago (Renshaw 1941). Despite decades of elegant investigations done in many species (Windhorst 1996; Alvarez and Fyffe 2007), we still have no answers about many aspects of this simple, yet intricate circuit.

Here a novel preparation (the adult rat) was used to study this circuit in vivo to complement earlier work done before in the adult cat. Several properties of this circuit in the adult rat were confirmed to be similar to the adult cat, e.g. dependency on Vm, dependency on proximity, distribution across motor pools, synaptic occlusion, reversal potential, central latency of the RIPSPs, and presence of "ripples" on the rising phase of the RIPSP, range of maximal amplitudes for RIPSPs, and Renshaw cell firing behavior. The total duration for rat RIPSPs was shorter ≈ 23 msec. (our data) than cat RIPSPs ≈ 40 – 50 msec. (Eccles 1954). This is not surprising since many other electrophysiological measures were shown to be shorter in the adult rat in comparison with the adult cat. For example, many of the motor unit properties were shown to be shorter in the adult rat (Krutki, Celichowski et al. 2006). Moreover, the afterhyperpolarizing potential for action potential spikes in the rat was shown to be shorter than in the adult cat (Gardiner and Kernell 1990).

Several advantages were gained by moving to the adult rat. First, we were able to study

the effect of peripheral nerve injury and regeneration in the same species that was used for recent published work from our labs analyzing central plasticity after nerve regeneration (Bichler, Carrasco et al. 2007; Alvarez, Titus-Mitchell et al. 2011; Bullinger, Nardelli et al. 2011). Second, information about this circuit from the adult rat can help in providing comparative data across species and finally, given the large number of reports studying Renshaw inhibition in the neonatal rodent, for review see (Alvarez and Fyffe 2007), it is legitimate to provide descriptions of the circuit in the adult, so one can directly follow the development of this circuit from early embryonic life up to late adulthood.

Three main concepts were examined by the current work, summarized in (Figure 6.1). First, the effect of Renshaw inhibition on motoneuron firing (Chapter 3) was approached in a novel way trying to maximize relevance for available reports coming from studies done in human subjects where timing of inhibition is shown to be important. The following novel findings were reported: 1. Renshaw inhibition had robust effects on spike timing and firing rhythm production. 2. Renshaw inhibition failed to decrease motoneuron discharge rate and actually frequently increased firing rates. 3. Renshaw inhibition and simulated IPSPs successfully delayed spike frequency adaption. The latter finding suggests, especially in slow motor units (known to receive strong Renshaw inhibition), that this inhibitory circuit might explain, at least in part, the reversal of SFA observed during fictive locomotion (Brownstone, Jordan et al. 1992; Brownstone, Krawitz et al. 2011)

Then we went on to examine the frequency dynamics of Renshaw inhibition (Chapter 4). Here, some earlier observations from the cat work were confirmed, e.g. the ability of Renshaw cells to follow frequency dynamics and the transformation behavior of Renshaw cell firing seen at higher frequencies (Haase 1963). In addition, the frequency dynamics of RIPSP duration, half width and half decay were studied for the first time and consistent findings were reported. Interestingly, the dynamics of the time course parameters of the RIPSP correlated with the dynamics observed in the Renshaw cell and were actually sufficiently explained by Renshaw cell behavior. Moreover, the effect of RIPSP frequency dynamics on motoneuron discharge rate was tested and obtained results suggested that this transformation might be highly adaptive to the motoneuron function, i.e. shortening of the RIPSP at higher frequency allows for higher degree of motoneuron firing freedom and reflect what can be seen as an automatic adjustment of function. In addition, the frequency dynamics of RIPSP amplitude were examined. Here, although hard to explain, an interesting optimal frequency was shown at 20 Hz, i.e. the largest RIPSP in each of the motoneurons tested was recorded after stimulating the circuit at 20 Hz. This was in partial disagreement with previous conclusions stating that RIPSP amplitudes exponentially decrease as the frequency of stimulation increases. It is worth mentioning that in their illustrations (Boorman, Windhorst et al. 1994), RIPSPs did not immediately decrease in size but rather showed an initial increase (peak around 10 Hz) that was followed by exponential decrease. So it seems that even in the cat, the same trend exists.

Finally, we examined the structure and function of recurrent inhibition long after nerve injury and regeneration (Chapter 5). A surprising failure of nerve regeneration to restore circuit function was demonstrated. Although RIPSP maximal amplitudes seemed to recover, permanent reductions in circuit connectivity were observed and prolonged, multiphasic RIPSPs were commonly recorded. In addition, the prevalence of recurrent facilitation was increased in sampled records from regenerated rats compared to controls. In general, those permanent changes are expected to affect normal function of this circuit and might result in permanent effects on motoneuron firing behavior and thus motor dysfunction.

Figure 6.1. S***ummary of the main points discussed in this thesis.***

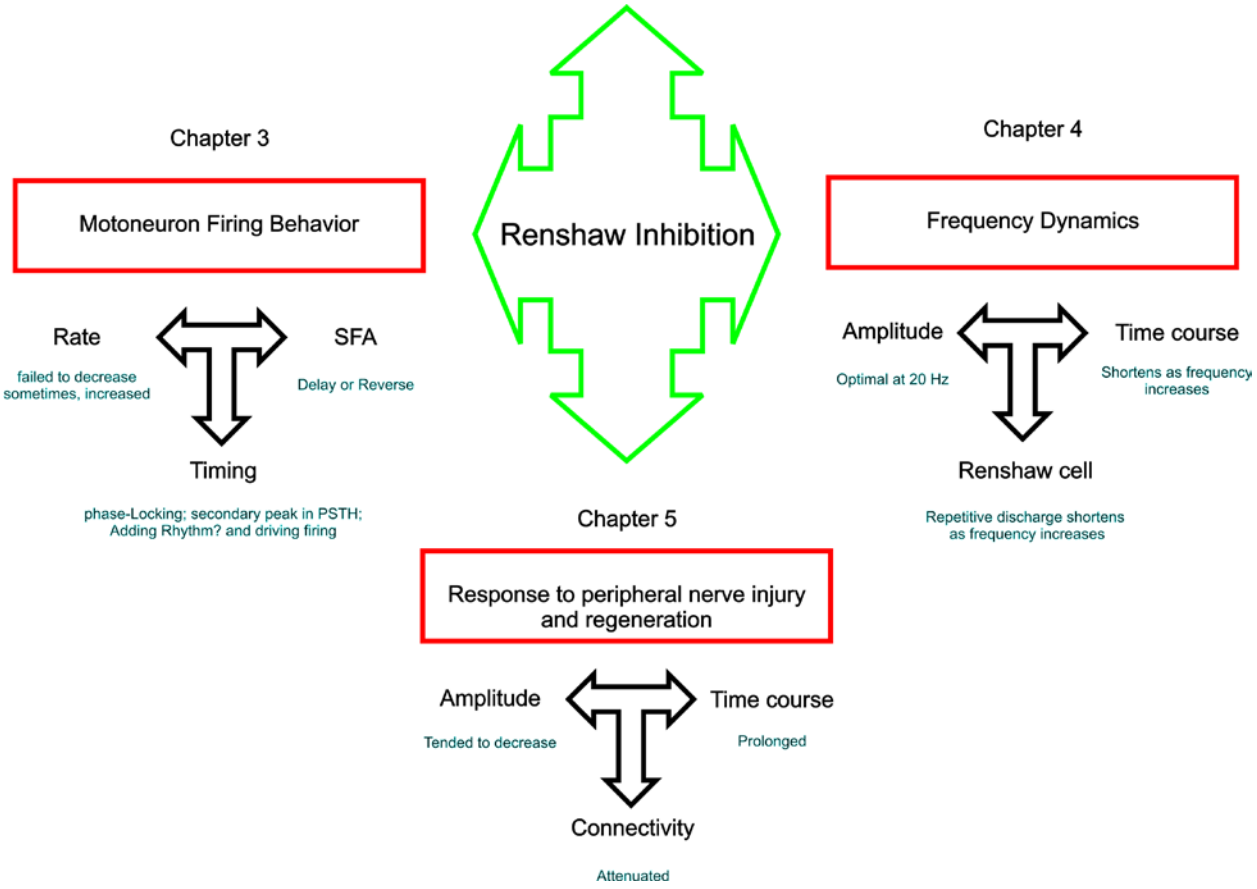
Chapter 3
Motoneuron Firing Behavior
Rate
failed to decrease sometimes, increased
SFA
Delay or Reverse
Timing
phase-Locking; secondary peak in PSTH; Adding Rhythm? and driving firing
Renshaw Inhibition
Chapter 4
Frequency Dynamics
Amplitude
Optimal at 20 Hz
Time course
Shortens as frequency increases
Renshaw cell
Repetitive discharge shortens as frequency increases
Chapter 5
Response to peripheral nerve injury and regeneration
Amplitude
Tended to decrease
Time course
Prolonged
Connectivity
Attenuated

Appendix A: Commonly used abbreviations

ABSM	Anterior biceps –semimembranosus
AHP	Afterhyperpolarization
AP	Action Potential
α-MN	α-motoneuron
ISI	Inter spike interval
LGS	Lateral gastrocnemius- soleus
MG	Medial gastrocnemius
msec.	Millisecond
mV	Millivolt
µV	Microvolt
PSF	Peristimulus frequencygram
PSTH	Peristimulus time histogram
Vm	Membrane potential

Alvarez, F. J., H. E. Titus-Mitchell, et al. (2011). "Permanent central synaptic disconnection of proprioceptors after nerve injury and regeneration. I. Loss of VGLUT1/IA synapses on motoneurons." J Neurophysiol **106**(5): 2450-70.

Bakels, R. and D. Kernell (1993). "Matching between motoneurone and muscle unit properties in rat medial gastrocnemius." J Physiol **463**: 307-24.

Bengtsson, F., C. F. Ekerot, et al. (2011). "In vivo analysis of inhibitory synaptic inputs and rebounds in deep cerebellar nuclear neurons." PLoS One **6**(4): e18822.

Bichler, E. K., D. I. Carrasco, et al. (2007). "Rat motoneuron properties recover following reinnervation in the absence of muscle activity and evoked acetylcholine release." J Physiol **585**(Pt 1): 47-56.

Bigland-Ritchie, B., R. Johansson, et al. (1983). "Changes in motoneurone firing rates during sustained maximal voluntary contractions." J Physiol **340**: 335-46.

Boorman, G., U. Windhorst, et al. (1994). "Waveform parameters of recurrent inhibitory postsynaptic potentials in cat motoneurons during time-varying activation patterns." Neuroscience **63**(3): 747-56.

Brownstone, R. M. (2006). "Beginning at the end: repetitive firing properties in the final common pathway." Prog Neurobiol **78**(3-5): 156-72.

Brownstone, R. M. (2012). ""“Spike frequency adaptation in motoneurons:is it an artefact?”" Abstracts of Conference Motoneurons and Beyond, 25.

Brownstone, R. M., L. M. Jordan, et al. (1992). "On the regulation of repetitive firing in lumbar motoneurones during fictive locomotion in the cat." Exp Brain Res **90**(3): 441-55.

Brownstone, R. M., S. Krawitz, et al. (2011). "Reversal of the late phase of spike frequency adaptation in cat spinal motoneurons during fictive locomotion." J Neurophysiol **105**(3): 1045-50.

Bullinger, K. L., P. Nardelli, et al. (2011). "Permanent central synaptic disconnection of proprioceptors after nerve injury and regeneration. II. Loss of functional connectivity with motoneurons." J Neurophysiol **106**(5): 2471-85.

Burke, R. E. (2007). "Sir Charles Sherrington's the integrative action of the nervous system: a centenary appreciation." Brain **130**(Pt 4): 887-94.

Button, D. C., J. M. Kalmar, et al. (2007). "Spike frequency adaptation of rat hindlimb motoneurons." J Appl Physiol **102**(3): 1041-50.

Christakos, C. N., U. Windhorst, et al. (1987). "Frequency response of spinal Renshaw cells activated by stochastic motor axon stimulation." Neuroscience **23**(2): 613-23.

Clarac , F. (2005). "The History of Reflexes Part 2: From Sherrington to 2004." IBRO History of Neuroscience.

Cleveland, S., A. Kuschmierz, et al. (1981). "Static input-output relations in the spinal recurrent inhibitory pathway." Biol Cybern **40**(3): 223-31.

Cleveland, S. and H. G. Ross (1977). "Dynamic properties of Renshaw cells: frequency response characteristics." Biol Cybern **27**(3): 175-84.

Cobb, S. R., E. H. Buhl, et al. (1995). "Synchronization of neuronal activity in hippocampus by individual GABAergic interneurons." Nature **378**(6552): 75-8.

Coombs, J. S., J. C. Eccles, et al. (1955). "The inhibitory suppression of reflex discharges from motoneurones." J Physiol **130**(2): 396-413.

Cope, T. C., S. J. Bonasera, et al. (1994). "Reinnervated muscles fail to produce stretch reflexes." J Neurophysiol **71**(2): 817-20.

Cope, T. C. and B. D. Clark (1993). "Motor-unit recruitment in self-reinnervated muscle." J Neurophysiol **70**(5): 1787-96.

Cope, T. C., E. E. Fetz, et al. (1987). "Cross-correlation assessment of synaptic strength of single Ia fibre connections with triceps surae motoneurones in cats." J Physiol (Lond) **390**: 161-88.

Cullheim, S. and J. O. Kellerth (1981). "Two kinds of recurrent inhibition of cat spinal alpha-motoneurones as differentiated pharmacologically." J Physiol **312**: 209-24.

Davey, N. J., P. H. Ellaway, et al. (1993). "Rhythmicity associated with a high degree of short-term synchrony of motor unit discharge in man." Exp Physiol **78**(5): 649-61.

Desmaisons, D., J. D. Vincent, et al. (1999). "Control of action potential timing by intrinsic subthreshold oscillations in olfactory bulb output neurons." J Neurosci **19**(24): 10727-37.

Du, W., J. F. Bautista, et al. (2005). "Calcium-sensitive potassium channelopathy in human epilepsy and paroxysmal movement disorder." Nat Genet **37**(7): 733-8.

Eccles, J. C., R. M. Eccles, et al. (1961). "Distribution of recurrent inhibition among motoneurones." J Physiol **159**: 479-99.

Eccles, J. C., R. M. Eccles, et al. (1961a). "Electrophysiological investigations on Renshaw cells." J Physiol **159**: 461-78.

Eccles, J. C., R. M. Eccles, et al. (1958). "The action potentials of the alpha motoneurones supplying fast and slow muscles." J Physiol **142**(2): 275-91.

Eccles, J. C., P. Fatt, et al. (1954). "Cholinergic and inhibitory synapses in a pathway from motor-axon collaterals to motoneurones." J. Physiol. **126**: 524-562.

Fetz, E. E. and B. Gustafsson (1983). "Relation between shapes of post-synaptic potentials and changes in firing probability of cat motoneurones." J. Physiol. Lond. **341**: 387-410.

Friedman, W. A., G. W. Sypert, et al. (1981). "Recurrent inhibition in type-identified motoneurons." J Neurophysiol **46**(6): 1349-59.

Fulton, J. F. (1926). Muscular Contraction and the Reflex Control of Movement, Williams & Wilkins, Baltimore.

Fyffe, R. E. (1991). "Spatial distribution of recurrent inhibitory synapses on spinal motoneurons in the cat." J Neurophysiol **65**(5): 1134-49.

Gardiner, P. F. and D. Kernell (1990). "The "fastness" of rat motoneurones: time-course of afterhyperpolarization in relation to axonal conduction velocity and muscle unit contractile speed." Pflugers Arch **415**(6): 762-6.

Gorassini, M., T. Eken, et al. (2000). "Activity of hindlimb motor units during locomotion in the conscious rat." J Neurophysiol **83**(4): 2002-11.

Granit, R., J. Haase, et al. (1960). "Recurrent inhibition in relation to frequency of firing and limitation of discharge rate of extensor motoneurones." J Physiol **154**(2): 308-28.

Granit, R., D. Kernell, et al. (1963a). "Quantitative Aspects of Repetitive Firing of Mammalian Motoneurones, Caused by Injected Currents." J Physiol **168**: 911-31.

Granit, R., D. Kernell, et al. (1963b). "The Behaviour of Mammalian Motoneurones During Long-Lasting Orthodromic, Antidromic and Trans-Membrane Stimulation." J Physiol **169**: 743-54.

Granit, R. and B. Renkin (1961). "Net depolarization and discharge rate of motoneurones, as measured by recurrent inhibition." J Physiol **158**: 461-75.

Granit, R. and L. T. Rutledge (1960). "Surplus excitation in reflex action of motoneurones as measured by recurrent inhibition." J Physiol **154**: 288-307.

Guertin, P. A. and J. Hounsgaard (1999). "Non-volatile general anaesthetics reduce spinal activity by suppressing plateau potentials." Neuroscience **88**(2): 353-8.

Haase, J. (1963). "[The transformation of the discharge pattern in Renshaw cells in tetanic antidromic irritation]." Pflugers Arch Gesamte Physiol Menschen Tiere **276**: 471-80.

Hamm, T. M. (1990). "Recurrent inhibition to and from motoneurons innervating the flexor digitorum and flexor hallucis longus muscles of the cat." J Neurophysiol **63**(3): 395-403.

Havton, L. and J. O. Kellerth (1984). "Retrograde effects of axotomy on the intramedullary axon collateral systems and recurrent inhibitory reflexes of cat spinal motoneurones." Neurosci Lett **52**(1-2): 13-7.

Havton, L. and J. O. Kellerth (1990a). "Elimination of intramedullary axon collaterals of cat spinal alpha-motoneurons following peripheral nerve injury." Exp Brain Res **79**(1): 65-74.

Havton, L. and J. O. Kellerth (1990b). "Plasticity of recurrent inhibitory reflexes in cat spinal motoneurons following peripheral nerve injury." Exp Brain Res **79**(1): 75-82.

Heckman, C. J. and M. D. Binder (1988). "Analysis of effective synaptic currents generated by homonymous Ia afferent fibers in motoneurons of the cat." J Neurophysiol **60**(6): 1946-66.

Holmgren, B. and P. A. Merton (1954). "Local feedback control of motoneurones." J Physiol **123**(2): 47-8P.

Hultborn, H., M. E. Denton, et al. (2003). "Variable amplification of synaptic input to cat spinal motoneurones by dendritic persistent inward current." J Physiol **552**(Pt 3): 945-52.

Hultborn, H., J. Lipski, et al. (1988). "Distribution of recurrent inhibition within a motor nucleus. I. Contribution from slow and fast motor units to the excitation of Renshaw cells." Acta Physiol Scand **134**(3): 347-61.

Iles, J. (2008). "Seeking functions for spinal recurrent inhibition." J Physiol **586**(Pt 24): 5843-4.

Katz, R. and E. Pierrot-Deseilligny (1999). "Recurrent inhibition in humans." Prog Neurobiol **57**(3): 325-55.

Kernell, D. (1965). "Synaptic Influence on the Repetitive Activity Elicited in Cat Lumbosacral Motoneurones by Long-Lasting Injected Currents." Acta Physiol Scand **63**: 409-10.

Kernell, D. and A. W. Monster (1982). "Motoneurone properties and motor fatigue. An intracellular study of gastrocnemius motoneurones of the cat." Exp Brain Res **46**(2): 197-204.

Krutki, P., J. Celichowski, et al. (2006). "Interspecies differences of motor units properties in the medial gastrocnemius muscle of cat and rat." Arch Ital Biol **144**(1): 11-23.

Kudina, L. P. and N. L. Alexeeva (1992). "After-potentials and control of repetitive firing in human motoneurones." Electroencephalogr Clin Neurophysiol **85**(5): 345-53.

Kudina, L. P. and R. E. Pantseva (1988). "Recurrent inhibition of firing motoneurones in man." Electroencephalogr Clin Neurophysiol **69**(2): 179-85.

Lamotte d'Incamps, B. and P. Ascher (2008). "Four excitatory postsynaptic ionotropic receptors coactivated at the motoneuron-Renshaw cell synapse." J Neurosci **28**(52): 14121-31.

Lamotte d'Incamps, B., E. Krejci, et al. (2012). "Mechanisms shaping the slow nicotinic synaptic current at the motoneuron-renshaw cell synapse." J Neurosci **32**(24): 8413-23.

Lamy, J. C., C. Iglesias, et al. (2008). "Modulation of recurrent inhibition from knee extensors to ankle motoneurones during human walking." J Physiol **586**(Pt 24): 5931-46.

Liddell, E. G. (1952). "Sir Charles Sherrington 1857-1952." Br Med Bull **8**(4): 379.

Lindsay, A. D. and M. D. Binder (1991). "Distribution of effective synaptic currents underlying recurrent inhibition in cat triceps surae motoneurons." J Neurophysiol **65**(2): 168-77.

Liu, T. T., B. A. Bannatyne, et al. (2009). "Cholinergic terminals in the ventral horn of adult rat and cat: evidence that glutamate is a cotransmitter at putative interneuron synapses but not at central synapses of motoneurons." Neuroscience **161**(1): 111-22.

Machacek, D. W. and S. Hochman (2006). "Noradrenaline unmasks novel self-reinforcing motor circuits within the mammalian spinal cord." J Neurosci **26**(22): 5920-8.

Mattei, B., A. Schmied, et al. (2003). "Pharmacologically induced enhancement of recurrent inhibition in humans: effects on motoneurone discharge patterns." J Physiol **548**(Pt 2): 615-29.

Mattei, B., A. Schmied, et al. (2003). "Recurrent inhibition of wrist extensor motoneurones: a single unit study on a deafferented patient." J Physiol **549**(Pt 3): 975-84.

McCrea, D. A., C. A. Pratt, et al. (1980). "Renshaw cell activity and recurrent effects on motoneurons during fictive locomotion." J Neurophysiol **44**(3): 475-88.

McCurdy, M. L. and T. M. Hamm (1994). "Topography of recurrent inhibitory postsynaptic potentials between individual motoneurons in the cat." J Neurophysiol **72**(1): 214-26.

McCurdy, M. L. and T. M. Hamm (1994a). "Spatial and temporal features of recurrent facilitation among motoneurons innervating synergistic muscles of the cat." J Neurophysiol **72**(1): 227-34.

Mentis, G. Z., F. J. Alvarez, et al. (2005). "Noncholinergic excitatory actions of motoneurons in the neonatal mammalian spinal cord." Proc Natl Acad Sci U S A **102**(20): 7344-9.

Miles, T. S., T. H. Le, et al. (1989). "Biphasic inhibitory responses and their IPSPs evoked by tibial nerve stimulation in human soleus motor neurones." Exp Brain Res **77**(3): 637-45.

Navarro, X., M. Vivo, et al. (2007). "Neural plasticity after peripheral nerve injury and regeneration." Prog Neurobiol **82**(4): 163-201.

Nishimaru, H., C. E. Restrepo, et al. (2005). "Mammalian motor neurons corelease glutamate and acetylcholine at central synapses." Proc Natl Acad Sci U S A **102**(14): 5245-9.

Noga, B. R., S. J. Shefchyk, et al. (1987). "The role of Renshaw cells in locomotion: antagonism of their excitation from motor axon collaterals with intravenous mecamylamine." Exp Brain Res **66**(1): 99-105.

Person, A. L. and I. M. Raman (2011). "Purkinje neuron synchrony elicits time-locked spiking in the cerebellar nuclei." Nature **481**(7382): 502-5.

Person, R. S. and L. P. Kudina (1972). "Discharge frequency and discharge pattern of human motor units during voluntary contraction of muscle." Electroencephalogr Clin Neurophysiol **32**(5): 471-83.

Piotrkiewicz, M., L. Kudina, et al. (2004). "Recurrent inhibition of human firing motoneurons (experimental and modeling study)." Biol Cybern **91**(4): 243-57.

Pratt, C. A. and L. M. Jordan (1987). "Ia inhibitory interneurons and Renshaw cells as contributors to the spinal mechanisms of fictive locomotion." J Neurophysiol **57**(1): 56-71.

Renshaw, B. (1941). "Influence of discharge of motoneurons upon excitation of neighboring motoneurons." J. Neurophysiol. **4**: 167-183.

Renshaw, B. (1946). "Interaction of nerve impulses in the gray matter as a mechanism in central inhibition." Fed Proc **5**(1 Pt 2): 86.

Robinson, L. R. (2000). "Traumatic injury to peripheral nerves." Muscle Nerve **23**(6): 863-73.

Ross, H. G., S. Cleveland, et al. (1976). "Quantitative relation between discharge frequencies of a Renshaw cell and an intracellularly depolarized motoneuron." Neurosci Lett **3**(3): 129-32.

Ross, H. G., S. Cleveland, et al. (1982). "Dynamic properties of Renshaw cells: equivalence of responses to step changes in recruitment and discharge frequency of motor axons." Pflugers Arch **394**(3): 239-42.

Ross, H. G., S. Cleveland, et al. (1973). "Changes in the excitability of Renshaw cells due to orthodromic tetanic stimuli." Pflugers Arch **344**(4): 299-307.

Ryall, R. W., M. F. Piercey, et al. (1971). "Intersegmental and intrasegmental distribution of mutual inhibition of Renshaw cells." J Neurophysiol **34**(4): 700-7.

Sears, T. A. and D. Stagg (1976). "Short-term synchronization of intercostal motoneurone activity." J Physiol **263**(3): 357-81.

Seburn, K. L. and T. C. Cope (1998). "Short-term afferent axotomy increases both strength and depression at Ia-motoneuron synapses in rat." J. Neurosci. **18**: 1142-1147.

Spielmann, J. M., Y. Laouris, et al. (1993). "Adaptation of cat motoneurons to sustained and intermittent extracellular activation." J Physiol **464**: 75-120.

Stauffer, E. K., J. C. McDonagh, et al. (2007). "Historical reflections on the afterhyperpolarization--firing rate relation of vertebrate spinal neurons." J Comp Physiol A Neuroethol Sens Neural Behav Physiol **193**(2): 145-58.

Uchiyama, T. and U. Windhorst (2007). "Effects of spinal recurrent inhibition on motoneuron short-term synchronization." Biol Cybern **96**(6): 561-75.

Van Keulen, L. (1981). "Autogenetic recurrent inhibition of individual spinal motoneurones of the cat." Neurosci Lett **21**(3): 297-300.

Wehr, M. and A. M. Zador (2003). "Balanced inhibition underlies tuning and sharpens spike timing in auditory cortex." Nature **426**(6965): 442-6.

Whelan, P. J. (1996). "Control of locomotion in the decerebrate cat." Prog Neurobiol **49**(5): 481-515.

Wilanowski, G. and M. Piotrkiewicz (2012). "Is spike frequency adaptation an artefact? Insight from human studies." Front Cell Neurosci **6**: 50.

Wilson, V. J., W. H. Talbot, et al. (1960). "Distribution of recurrent facilitation and inhibition in cat spinal cord." J Neurophysiol **23**: 144-53.

Windhorst, U. (1996). "On the role of recurrent inhibitory feedback in motor control." Prog Neurobiol **49**(6): 517-87.

Windhorst, U., G. Boorman, et al. (1995). "Renshaw cells and recurrent inhibition: comparison of responses to cyclic inputs." Neuroscience **67**(1): 225-33.